“Sapienza”
Università di Roma

Giuseppe Rocco Casale

PhD Thesis in Biophysics
XIX Cycle (2004-2006)

"ASSESSMENT OF SOLAR UV EXPOSURE IN THE ITALIAN POPULATION"

Supervisors:
Dr. Anna Maria Siani
Prof. Sabino Palmieri

PhD Coordinator:
Prof. Alfredo Colosimo

To Paola

To Carlotta

To my mother and father

Acknowledgments

This work was carried out at the G-Met, Dept. of Physics, University of Rome "Sapienza". I wish to express my sincere gratitude to:

My two Supervisors, **Dr. Anna Maria Siani** and **Prof. Sabino Palmieri** (Dept. of Physics, Univ. of Rome "Sapienza"), for their teaching and attitude towards science and life. This study originated especially from encouraging discussions with **Anna Maria** and was possible thank to her enthusiastic involvement in the experiments. Thank to her for having meticulously checked my manuscripts, too.

My PhD Coordinator, **Prof. Alfredo Colosimo** (Dept. of Human Physiology and Pharmacology, Univ. of Rome "Sapienza"), for his open-minded scientific vision. I was really impressed by his ability in suggesting the right direction even when it was harder.

Dr. Michael Kimlin (School of Public Health, Queensland University of Technology, Australia), who initiated me in the "art of polysulphone". His visit to Rome in 2004 was the beginning of everything.

Prof. Carlo Coluzza (Dept. of Physics, Univ. of Rome "Sapienza") for the possibility of using the spectrophotometer in his laboratory and the time he spent with me in fruitful discussions.

Dr. Renata Sisto, **Dr. Massimo Borra** and **Dr. Andrea Militello** (ISPESL DIL, Monteporzio Catone). **Renata** gave me a fundamental help in the interpretation of the results by means of her background as a theoretical physicist. **Massimo** and **Andrea** were enthusiastic and creative collaborators in many field campaigns.

Dr. Giovanni Agnesod (ARPA VdA Aosta), who readily supported the skiers experiment. The collaboration with him, started in that date, is still ongoing.

Dr. Giovanni Leone (Phototherapy Laboratory, IFO San Gallicano Institute of Rome), who suggested the study on photodermatoses as an example of scientific collaboration between dermatologists and physicists on a theme of actuality.

Dr. Antonella Lisi (INMM-CNR Rome), for providing the data of free radicals and suggesting possible interpretations.

My school colleague **Francesca Scarnecchia** who, as English mother-tongue, spent time in carefully reading my PhD Thesis.

Aldo, **Iolanda**, **Valerio, Romina** and **Chiara**, who created a friendly and nice atmosphere to work in the Department. **Nicola**, who collaborated with me in the former part of the PhD.

Abbreviations

BCC	Basal Cell Carcinoma
BHT	Butylated Hydroxytoluene
CFCs	Chlorofluorocarbons
ER	Exposure Ratio
FR	Free Radicals
IU	International Units (of vitamin D amount)
MED	Minimal Erythemal Dose
MSC	Melanoma Skin Cancer
NMSC	Non-Melanoma Skin Cancer
PCA	Principal Component Analysis
PS	Polysulphone
PSF	Polysulphone Film
SCC	Squamous Cell Carcinoma
SED	Standard Erythemal Dose
SZA	Solar Zenith Angle
UT	Universal Time
UV	Ultraviolet
UVA	Ultraviolet Radiation A (400-320 nm)
UVB	Ultraviolet Radiation B (320-290 nm)
UVC	Ultraviolet Radiation C (290-200 nm)
UVI	Ultraviolet Index
UVR	Ultraviolet Radiation

Format description

Chapter: **number. TITLE**
(Example: **4. RESULTS**)

Section: ***number. Title***
(Example: ***4.1 Variability among polysulphone calibration curves***)

Sub-section: *number. Title*
(Example: *4.1.1 Calibration curves of polysulphone films*)

Figure quotation: Figure chapter.number
(Example: Figure 4.1)

Table quotation: Table chapter.number
(Example: Table 4.1)

Equation quotation: Equation (number.chapter)
(Example: Equation (1.4))

Reference quotation: [number.year] or Author [number.year]
(Example: [3.2004]) or (Example: Diffey [3.2004])

ABSTRACT

Solar ultraviolet radiation (UVR) has influenced the evolution of life on earth and likely caused the development of different skin pigmentation in humans: those inhabiting low latitudes, with high UVR intensity, have darker skin pigmentation for protection from the deleterious effects of UVR, while those in higher latitudes have developed fair skin to maximize vitamin D production from much lower ambient UVR.

In the last centuries, however, there has been an increase in human migration from its original areas and human skin pigmentation is no longer necessarily suited to the environment where it lives. Dark-skinned populations at low latitudes have very low incidence of melanoma skin cancer (MSC) and non melanoma skin cancer (NMSC, such as squamous cell carcinoma, SCC, and basal cell carcinoma, BCC) but their migration to high latitudes has seen an increase in the incidence of rickets and osteomalacia; meanwhile, fair-skinned populations who have migrated to low latitudes have experienced a rapid rise in the incidence of MSC and NMSC. Furthermore, changes in habits and attitudes have meant that many people all over the globe are now exposed to more, or less, UVR than ever before.

In addition, the documented stratospheric ozone downward trend due to chlorofluorocarbons (CFCs) has been associated with an increase of solar ultraviolet radiation B (UVB) at the earth's surface, even though UVR changes are also associated with fluctuations in cloud cover and atmospheric pollution. If ambient UVR increases, in the absence of changes in personal attitudes and sun protection, there will be an increase in health diseases due to excessive UVR exposure.

The only positive human benefit from a moderate degree of solar UVR exposure is the production of vitamin D required for skeletal health. Recently, there has been a debate within the scientific community regarding the health duality of UVR. Various articles have suggested that low vitamin D can be considered a risk factor for breast, prostate and colon cancers.

Kimlin's research group (Australia) is currently focusing on the positive and negative effects of UVR on human health in order to quantify the correct exposure of populations. For such reasons, evaluation of the personal solar UVR doses on different body parts and the search for related easy to measure biological indicators can be helpful in the study of the best levels of exposure and the understanding of what is still unknown.

The purpose of this study was to suggest and test a methodology for the measuring of personal solar UVR doses and search for possible biological indicators of its effects. We chose polysulphone (PS) dosimetry as the main investigative methodology. Several field experiments were performed, five of them with groups of volunteers (*in vivo*) selected among the Italian population (schoolchildren, sun bathers, vineyard growers, skiers and hikers), presented and discussed here.

The main result was the data collection of personal UVR exposures, added to the global dataset as Exposure Ratio (ER) between the erythemally weighed dose measured by the PS dosimeter and the corresponding ambient dose on a horizontal plane measured by a radiometer.

Mean (median) values of ER on the chest for schoolchildren, sun bathers and hikers were respectively 0.07 (0.07), 0.19 (0.19) and 0.11 (0.07). Since the schoolchildren ER turned out to be the lowest, we asked whether the dose allowed a sufficient production of vitamin D, discovering that some children of the sample showed inadequate modalities of exposure (probably recovered during the summer months). The study on sun bathers, decided so as to supply indications on the relationship between the absorbed doses and the development of the photodermatoses, evidenced that the latter were not linked to high values of Exposure Ratio but they rather depended on the genetic characteristics of the individuals, which probably reacted to the exposure not through the production of melanin but with an increase in the dilation of blood vessels, leading to skin reddening.

ER on the forehead for skiers and hikers showed an average value of 1.01 (1.03) and 0.27 (0.24) respectively, with the

difference due to snow albedo. The study on vineyard growers, carried out in three different seasons (spring, summer and autumn), supplied an average value of 0.71 (0.69) for the nape and of 0.46 (0.42) for the arm, with an elevated variability due to the different atmospheric conditions and to the different duties between one season and another.

The study also proposed a methodology combining the use of colorimetric parameters, skin temperature and additional information (such as the amount of free radicals in the skin) that were collected during the experiments. All data were analyzed by means of well known statistical multivariate approaches, namely PCA (Principal Component Analysis) and Cluster Analysis, useful when variables are not only correlated but also numerous. Finally, to interpret the results, an empirical model for the estimation of short and long term doses was proposed.

Keywords: solar ultraviolet radiation (UVR), personal exposure, polysulphone (PS), personal dosimetry, colorimetry, skin temperature

CONTENTS

1. BACKGROUND

1.1 Introduction

Living organisms on earth have evolved over millions of years with the changing planet and its atmosphere. The stress due to solar ultraviolet radiation (UVR) is likely to be responsible for the development of different skin pigmentation in humans who migrated from areas of high ambient UVR to areas of lower ambient UVR. The inhabitants at low latitudes, with high UVR intensity, have darker skin pigmentation to protect themselves from the deleterious effects of UVR, while those in higher latitudes have developed fair skin to maximize vitamin D production from much lower ambient ultraviolet radiation.

In the last few hundred years, however, there has been an increase in human migration from its original areas and so skin pigmentation is no longer necessarily suited to the environment where we live. At low latitudes, dark-skinned populations have very low incidence of melanoma and skin cancers while their migration to high latitudes has led to an increase in the incidence of rickets and osteomalacia. The incidence of skin cancers (melanoma, MSC, and non-melanoma skin cancers, NMSC, such as squamous cell carcinoma, SCC, and basal cell carcinoma, BCC) in fair-skinned populations has increased over the recent decades as travel to lower latitudes, fashion and leisure time have contributed to changing habits and patterns towards cumulative sunlight exposure.

In Figure 1.1 we may find a summary of the major causative factors in several short and long term health diseases derived from ultraviolet radiation [19.2006].

Following the discovery of the Antarctic ozone hole in 1985 and the significant decrease in total ozone at middle latitudes observed since the 1970s, solar ultraviolet (UV) radiation became an important environmental, ecological and atmospheric parameter to be measured and studied. Increasing interest has been shown by the scientific community in human health risks deriving from overexposure to solar UV radiation.

Figure 1.1 Health impacts due to solar ultraviolet radiation [19.2006]

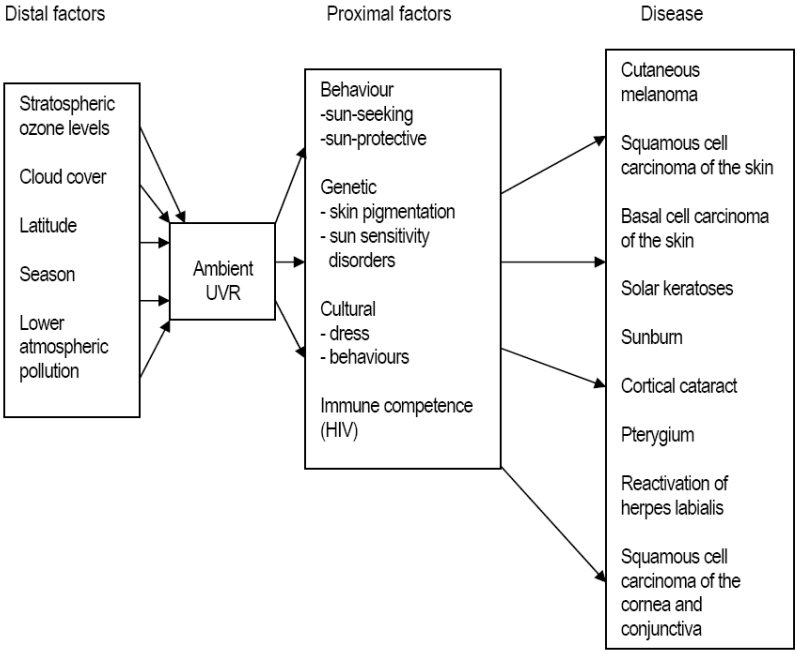

The assessment of surface UVR changes is a difficult task. UV radiation is mainly controlled by the absorptive power of ozone and molecular oxygen but other atmospheric factors, having time dependent behaviour characterized by trends or long period fluctuations, in turn may control UVR levels. In fact in highly polluted areas absorption of solar UV radiation by urban anthropogenic aerosols causes a reduction of UV levels masking their likely increase due to low total ozone events. In addition, slightly increased levels of UVR were observed in the northern hemisphere in unpolluted sites (such as the Alps where the atmosphere is relatively clear), while in Australia increased levels of UVR were monitored in months when cloud cover had been particularly low.

If ambient UVR increases, in the absence of behaviour modification and adequate sun protection strategies, health diseases due to overexposure to UVR increase.

Recent researches have highlighted the beneficial effects to health of adequate UVR exposure due to UVR-induced vitamin D synthesis. There has been increasing debate within the scientific community regarding the health duality of UV radiation. Various articles have suggested that low vitamin D can be considered a risk factor for breast, prostate and colon cancers. Kimlin's research group (Australia) is currently focusing on the positive and negative effects of UV radiation on human health in order to quantify the correct UV exposure of populations. The net health budget of ambient UVR will thus depend on the interaction of increased ambient UVR levels, skin type and behavioural changes influencing personal exposure.

For such reasons, evaluation of personal UVR doses on different body parts and the search for related, easy to measure biological markers can be helpful in the study of the best levels of exposure and the understanding of what is still unknown. The purpose of this study is to suggest and test a methodology for the measure of personal UVR doses and look for possible biological indicators of its effects.

This initial chapter covers the background topics of solar UV radiation and its effects.

1.2 Solar ultraviolet radiation

Ultraviolet radiation is produced either by heating a body to an incandescent temperature, as is the case with solar UVR, or by the passage of an electric current through a gas (usually vaporized mercury) [3.1992]. Radiometric terms and units are reported in Appendix I.

The spectrum of extraterrestrial solar radiation can be approximated by that of a black body of about 5800 K. The irradiance of solar radiation outside the atmosphere, at the earth's mean distance from the sun, is termed the solar constant and is 1370 W m^{-2}. About 9% is in the ultraviolet ($200<\lambda<400$ nm).

Solar ultraviolet radiation is arbitrarily divided into three bands of different wavelength. Environmental and dermatological photobiologists commonly use slightly different divisions, more closely associated with the biological effect of the different wavelengths [1.2002]. That is:

UVA 400-320 nm
UVB 320-290 nm
UVC 290-200 nm

UVC is totally absorbed by atmospheric ozone, has minimal penetration to the surface of the earth and consequently has little effect on human health. More than 90% of UVB is absorbed by atmospheric ozone, while UVA passes through the atmosphere with little change. Thus, the solar UVR radiation of importance to human health consists of UVA and UVB.

The solar output is not constant but varies with a 27-day apparent solar rotation and an 11-year cycle of sunspot activity. This variability affects mostly those wavelengths that are absorbed in the upper atmosphere (λ <290 nm) while the effect on terrestrial UVB and UVA is minimal. Because of the elliptical orbit of the sun, the sun-earth distance varies by about 3.4% from a minimum on the perihelion (about 3 January) to a maximum on the aphelion (about 5 July). This causes a variation in intensity of about 7% and slightly higher UV levels in southern hemisphere summers than in the northern hemisphere [16.2006]. An example of spectrum of clear sky, terrestrial summer sunlight measured at latitude of about 42°N is shown in Fig. 1.2.

Solar radiation effect on human health depends on the amount and type of radiation impinging on the body. This in turn depends on [9.2003]:

- solar zenith angle SZA (angle between the sun and the local vertical);
- atmospheric attenuation (firstly the atmospheric total ozone able to absorb ultraviolet radiation, particularly UVB);

- clouds (since pure water is a very weak absorber of UV radiation, clouds, which are composed of either liquid or ice droplets, attenuate ultraviolet primarily by scattering);
- surface albedo (reflection of solar UV radiation from most ground surfaces is normally less than 10%. The main exceptions are gypsum sand, which reflects about 15–30%, and snow, which can reflect up to 90%) [9.2002; 10.2003];
- altitude.

Figure 1.2 The effect of the atmosphere on solar ultraviolet radiation. BREWER and SUSIM are, respectively, the measured terrestrial and extra-terrestrial irradiance while STAR is the modelled value at the earth's surface

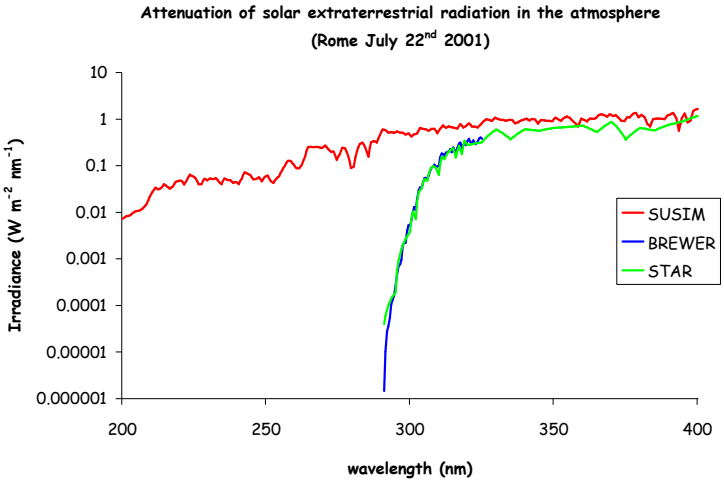

The amount and spectral structure of radiation reaching the body is mainly dependent on the geometry of radiation (the angle at which the sun's rays pass through the atmosphere) and the atmosphere composition. For example, at low latitudes there is more intense solar UVR with a greater proportion of shorter wavelengths, related to the low angle of incidence of the incoming radiation. This strongly influences biological activity. Increasing altitude increases UVR intensity by decreasing the air mass through which solar radiation must pass. Similarly, time of day and season, as well as clouds, dust, haze and various organic

compounds, can alter the intensity of incident solar radiation [2.2001]. Variations in cloud cover usually reduce ground level UVR, although this effect is highly variable, depending on the characteristics of the cloud itself. Indeed, cloud cover can result in increased ground level UVR if both direct sunlight and light scattered from clouds reach the earth's surface [3.2001].

Figure 1.3 Monthly average annual ambient erythemally weighed UVR, 1997-2003 [19.2006]

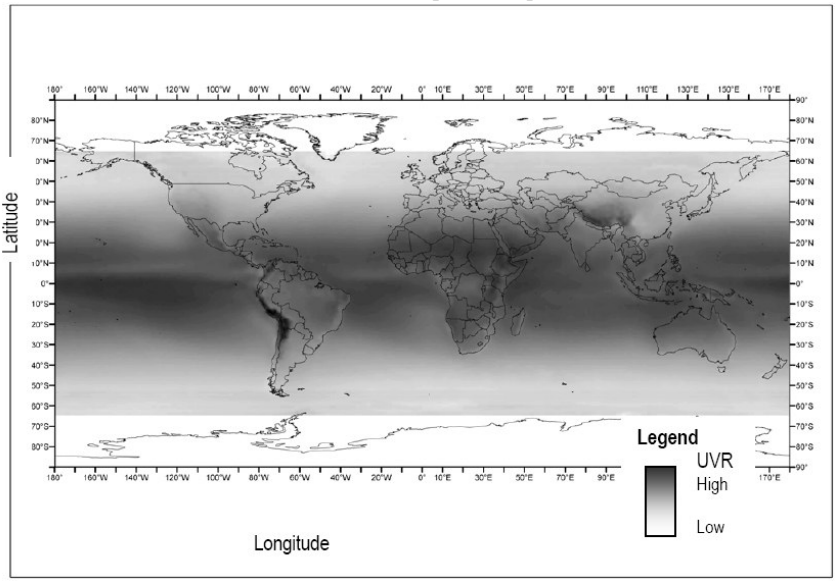

Latitude provides only a rough approximation to global variation of UVR (Figure 1.3). However, because of the elliptical nature of the earth's orbit around the sun there is a 7% difference in intensity between the hemispheres of any level of latitude, with the southern hemisphere having a greater intensity. In addition, clearer skies in the southern hemisphere can increase this difference in ambient UVR to 10-15%.

Ambient solar UVR is measured continuously by ground-level monitors, with publication of current values for particular locations [2.2002]. Extensive UV monitoring by means of spectroradiometers and broad-band radiometers started during the

1990s, although a homogeneous network for UV measurements does not yet exist. Recently, UV measurements by multi-channel (moderate- and narrow-band) radiometers have also become available.

The Solar Radiometry Observatory, University of Rome "Sapienza" (41.9° N, 12.5° E, 75 m asl) is one of the stations that regularly measures UV irradiance in Italy. It has a Brewer spectrophotometer (operational since 1992) for measurements of UV spectral irradiance and a Yes UVB-1 radiometer (working reliably since 2000). Both instruments are calibrated on a regular basis and their uncertainty ranges from 5 to 10%.

1.3 The skin and its interaction with solar UVR

The skin is the largest organ of the body. Human skin has two major components, separated by the basement membrane: sitting on this membrane is the outer cellular epidermis (approximately 100–150 μm) and beneath it the inner largely non-cellular dermis (approximately 2–4 mm), collagen and elastin (extra-cellular structural proteins). Keratinocytes are the main cell type of the epidermis. They proliferate by division in the basal layer sitting on the basement membrane. Non-melanoma skin cancers (NMSC), which represent the vast majority of skin cancers, derive from keratinocytes [1.1991]. Nonproliferating keratinocytes mature in transit through a series of well defined layers till they reach the outer non-living epidermis (stratum corneum, approximately 10 μm). By that time they are little more than keratin flakes and are termed corneocytes. Normal, epidermal turnover is under tight homeostatic control in which desquamation (corneocyte loss) is balanced with cell division. The stratum corneum is composed of 10–20 layers of corneocytes and it is a major component of the skin's physical barrier function. Melanocytes and Langerhans cells (having an antigen-presenting function and part of the systemic immune system) form two distinct (though much smaller) populations of dendritic cells within the epidermis. Melanins, synthesized by melanocytes, are transferred, as large particles called melanosomes, to adjacent keratinocytes in which

they are degraded into smaller particles (melanin dust). These particles are discarded with desquamation. Abnormal cell division of melanocytes may give rise to malignant melanoma which accounts for more than 90% of skin cancer deaths but is much less common than non-melanoma cancers (SCC and BCC).

The epidermis contains several chromophores which have absorption spectra (i.e. a plot of the effectiveness to absorb radiation of different wavelengths) within the UVR range [16.1997]. These include nucleic acids, urocanic acid, aromatic amino acids (proteins), melanins and their precursors. Several of these molecules, e.g. DNA and urocanic acid, show maximum absorbance at 260–270 nm in the UVC range. However, it is their absorbance between 295 and 400 nm which is of relevance when considering the photobiological consequences they initiate [1.1991].

Optical radiation incident on the skin may be:

- reflected at the skin surface due to a change in refractive index between air and stratum corneum;
- absorbed by chromophores in the epidermis or dermis;
- scattered by cell organelles in the epidermis or collagen in the dermis;
- transmitted to deeper tissues.

The reflection of light from the surface of the skin is between 4% and 7% for both black and white skin. Ultraviolet radiation and visible light that enters the skin is scattered mainly in a forward direction in the epidermis due to Mie scattering by cell organelles (e.g. melanosomes), which have dimensions of the order of the wavelength of light. In the dermis, however, scattering is much more isotropic and light reemitted from skin in vivo comes largely from the dermis. Moreover, dermal scattering increases rapidly with decreasing wavelength, approximately as predicted by Rayleigh scattering (probability of scattering inversely proportional with the fourth power of the wavelength). Consequently, dermal scattering determines principally the depth to which different wavelengths of optical radiation penetrate the dermis. In Table 1.1 the major chromophores that determine the

depth of penetration in the difference spectral regions are summarized [1.2002].

Table 1.1 Cutaneous chromophores for optical radiation [1.2002]

Spectral region	Wavelength interval (nm)	Major chromophores	
		Epidermis	Dermis
UVC	200-290	Nucleic Acids Aromatic Amino Acids	
UVB	290-320	Melanin	
UVA	320-400	Melanin	
Blue light	400-500	Melanin	Haemoglobin Bilirubin
Green light	500-570	Melanin	β-carotene
Red light	570-760	Melanin	Haemoglobin

Radiative transfer theory helped to attempt to model the propagation of UV radiation in the skin [10.2004]. Results show large differences from *ex vivo* and *in vivo* data: transmissions of 300 nm radiation to the basal layer of the epidermis differ from about 3–10% and 90% respectively. The reason for this difference has not been explained, and further experiments are indicated to gain a clearer insight into the penetration of UV radiation into the epidermis [16.1997].

The skin surface properties can be altered by the application of topical agents, that can selectively increase or decrease radiation to critical targets in the epidermis. UVA penetrates the human skin more deeply than UVB. Action spectra for biological responses indicate that DNA absorbs radiation in the UVB range and its damage seems to be a key factor in the initiation of the carcinogenic process in skin [1.1991].

Skin pigmentation alters the exposure-disease relationship for all UVR-induced skin diseases: deeply pigmented skin provides important sun protection, with quantitative estimates varying. Intermediate skin types have intermediate values of protection [19.2006].

The most common classification of skin types for UVR sensitivity is given by the Fitzpatrick scale (Table 1.2).

Table 1.2 Fitzpatrick skin pigmentation scale [19.2006]

Type	Description
I	Fair skinned Caucasians who burn very easily and never tan
II	Fair skinned Caucasians who burn easily and tan slowly and with difficulty
III	Medium skinned Caucasians who burn rarely and tan relatively easily
IV	Darker skinned Caucasians who virtually never burn and tan readily, e.g. some individuals with Mediterranean ancestry.
V	Asian or Indian skin
VI	Afro-Caribbean or Black skin

From entering the skin to causing biological and clinical effects, optical radiation has to initiate photochemical processes. Some of the important laws governing them are summarized below [1.2002]:

- Grotthus-Draper law: Only radiation that is absorbed is capable of initiating a photochemical process.
- Bunsen-Roscoe law (reciprocity law): Photochemical effect depends on dose (intensity by time) and not dose rate (intensity).
- Stark-Einstein law: Each photon absorbed by a molecule activates one molecule in the primary step of a photochemical process.
- Planck's law: The energy (E) of a photon is related to its wavelength (λ in nm) by
  $E = hc/[\lambda \cdot 10^{-9}]$ (E in J)
  where h is Planck's constant ($6.63 \cdot 10^{-34}$ Js), c is the velocity of light ($3 \cdot 10^{8}$ m/s).
- Lambert-Beer law: When a beam of monochromatic photons of incident intensity I_0 passes through an absorbing medium of thickness d, its intensity is reduced to $I_0\ 10^{-ecd}$, where e and c are the extinction coefficient and concentration of the absorbing substance, respectively. The product ecd is equal to the absorbance A; hence absorbance is equal to $log_{10}[1/transmittance]$. This definition is commonly used for measures with laboratory spectrophotometers, as explained further on.

1.4 Personal exposure to solar UVR

If total annual ultraviolet radiation varies approximately four-fold across the globe (see Figure 1.3), in any area there is likely to be at least a ten-fold difference in personal UVR exposure which is related to behavioural and cultural factors. This means that even in areas of relatively low ambient UVR it is possible to have high personal exposure. For most subjects, previous studies have shown that UVR exposure varies from between 5% to 15% of total ambient UVR, with the exception of outdoor workers whose exposures can reach 20-30% of ambient UVR [3.2005; 4.2005]. Groups of similar age subjects tend to receive a similar proportion of ambient UVR in different locations, with males consistently having higher UVR exposure than females [4.2005]. However, individual exposure within population groups may vary from one tenth to ten times the mean exposure in a particular location. In some people or sub-populations, much of the annual exposure to UVR may be concentrated in a brief annual summer holiday [4.2005].

Ambient UVR may be measured in purely physical units or weighed using an erythemal response function called action spectrum, a plot of the effectiveness of UV radiation of different wavelengths to induce a given biological effect [6.1988]. The biologically effective UVR is expressed as joules per square metre (J m^{-2}), minimal erythemal dose (MED), standard erythemal dose (SED) or the solar UV index (UVI). The MED is the dose of erythemally weighed UVR required to produce a barely perceptible erythema in people with skin type I (200 J m^{-2} of biologically effective UVR). The SED is the erythemally weighed UVR equivalent to 100 J m^{-2}. The UVI is the time weighed average effective UV irradiance in W m^{-2} multiplied by 40. Figure 1.4 reports the climatological UVI values from 1992 to 2004 in Rome (middle latitudes urban site). Maximum values tend to occur during summer and do not usually exceed 8 [32.1999; 12.2002; 20.2003; 21.2003].

Figure 1.4 Climatological UVI in Rome (1992-2004)

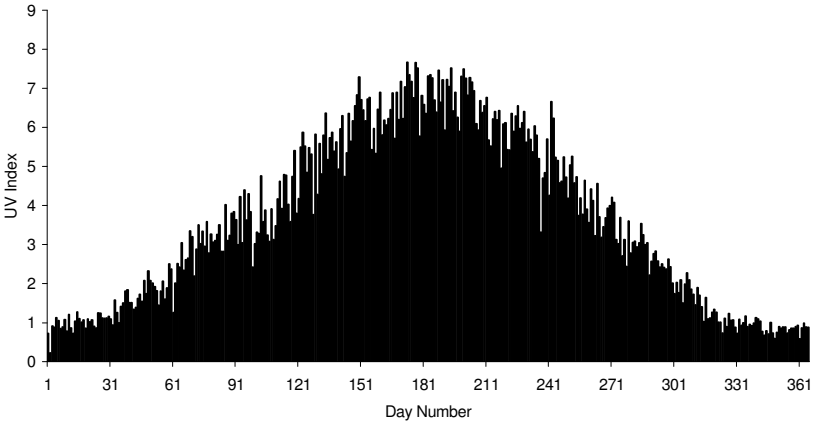

The MED is unfortunately sometimes used in populations of different skin types, thus the dose of UVR may not be 200 J m^{-2} but must be defined for the skin type under study. The SED has been developed as a fixed erythemally weighed measure of radiant exposure but it has the disadvantage of being independent from skin type. A particular exposure dose in SED may cause erythema in fair skin but not in darker skin. The global solar UVI was developed as a friendly measure of biologically effective UVR for public awareness of the risks of UVR exposure and to promote sun protection [1.2003]. Weather forecasts in many countries include a forecast of the solar UV index to guide the public to sun exposure. Anyway, it is does not represent the effective doses of body parts differently inclined from the horizontal one [29.1999; 2.2003; 2.2006].

Epidemiologists usually measure personal UVR doses by recalled exposure over a number of years. This can include a measure of the number of sunburns experienced at various times in life, hours spent outdoors during recreational activities or for

work. For example, many studies on the effects of UVR exposure on the eye have quantified ocular exposure by adjusting ambient UVR (years in a location for which average ambient UVR is known) in the use of a hat, sunglasses and surface albedo. However, such indices are particularly inaccurate and the estimation of the risk factor exposure level of individuals in epidemiological studies is imprecise, expressed in varying "natural" units which have no fixed relationship to the physical units used to measure ambient UVR.

Even if networks for reliable measurements of ground level UVR exist, this would not accurately represent the population distribution of individual UVR exposure [14.2003]. One problem is the geometrical difference between a horizontally fixed detector and the curved body surface that will produce significant deviations in exposure, even though several attempts to quantify such deviations have recently been proposed [14.2004; 18.2004; 3.2006].

As already mentioned, behavioural and cultural differences mean that for any ground level measure of UVR, there may be a hundred-fold difference in personal UVR exposure. It would be erroneous to interpret highly precise estimates of ground-level UVR as accurate estimates of personal UVR exposure. Furthermore, variations in skin pigmentation and the use of sunscreens determine the exposure to biological structures in the context of variations in ambient UVR.

1.5 Effects of absent or excess solar UVR

Environmental toxicity for most environmental risk factors increases monotonically with increasing exposure, so that the theoretical minimum results in the lowest physically achievable level of exposure, while for solar UVR there is clearly not a monotonic association between health risks and exposure [12.2004; 17.2006]. Some UVR exposure is required for the induction of synthesis of vitamin D, which is essential for musculo-skeletal health [2.1976; 1.2005]. A scenario of no UVR exposure would lead to a vastly increase in disease load due to the

increase in vitamin D deficiency [4.1992]. Conventionally it is believed that this causes effects on calcium and phosphorus levels and eventually rickets, osteomalacia and osteoporosis. Recent research suggests that vitamin D may also have an extremely important role in the immune system, such that even subclinical hypovitaminosis D may have a causal role in the development of several cancers and contribute to the development of autoimmune disorders such as multiple sclerosis and type 1 diabetes. A new hypothesis on the relationship between vitamin D and epidemic influenza was also proposed in a very recent work [10.2006]. On the other hand, excessive exposure to ultraviolet radiation is a relatively new problem, resulting from less clothing, migration of paleskinned peoples to areas of high ambient UVR and behavioural practices such as sunbathing [5.1992; 10.1995; 14.1996; 31.1999; 10.2000; 4.2001; 4.2002; 16.2003; 6.2004; 15.2004; 19.2004; 4.2006].

The theoretical minimum risk is therefore the turning point of the exposure-response curve [11.2000]. For UVR exposure this would equate to the minimum population distribution of UVR exposure that maintains vitamin D sufficiency, given the current diet [25.1998]. This distribution is, as yet, undefined, and varies depending on age, sex and skin type [22.1998]. There are both direct (e.g. skin cancers) and indirect effects (e.g. altering food productivity of plant and aquatic ecosystems) of ultraviolet radiation on human health. Table 1.3 presents a summary of the most recent outcomes.

Exposure of the whole body to 1 MED is equivalent to ingesting 10000 IU (International Units) of vitamin D. Thus, exposure of 6-10% (an arm, a lower leg, or face and hands) of the body surface to 1 MED is then equivalent to ingesting 600-1000 IU. The current recommended daily intake of vitamin D for children is 400 IU and for adults 200 IU, although recent research suggests that this should be increased to 600 IU (actually, some studies suggest a daily intake of up to 4000 IU) in the absence of sunlight exposure [14.2006]. Daily exposure of 6-10% of the body surface to 1 MED should be sufficient to maintain vitamin D

amount (>50 nmol/l). Recent research, anyway, suggests that the lower level of vitamin D sufficiency should be raised to at least 80 nmol/l.

Using available global data on annual ambient UVR, it should be possible to calculate the mean daily UVR exposure required to maintain vitamin D sufficiency at any location for a particular skin type [16.2004; 17.2004; 13.2005]. This has not been done yet. The amount of UVB at higher latitudes is insufficient to produce vitamin D over the winter months so inhabitants of such areas should achieve higher levels of vitamin D synthesis in other seasons and rely on stored vitamin D over the winter. This level of exposure would result in a zero incidence of cutaneous melanoma and an odds ratio of 1.0 for developing basal cell carcinoma.

Propaganda regarding sun avoidance and protection have been used widely for more than twenty years. A reduction in sunbathing and increased sun protection after intensive health promotion campaigns have been observed [2.2000]. Such a decrease in exposure is relatively low but could cause a significant decrease in incidence of skin cancers and UVR-related eye diseases. A better choice might be to lead people towards a theoretical minimum risk of disease [2.2005; 5.2005].

For UVR personal exposure there are some difficulties when using the comparative risk assessment methodology of burden of disease assessment: even if there is a theoretical exposure required to maintain vitamin D levels and to achieve a minimum disease burden, there is a lack of data that transfer this theoretical value into a measurable population exposure distribution [1.2006].

The exposure distribution of populations is still unclear, because data on ambient UVR do not easily interpret actual population exposure distribution. Epidemiological studies have not accurately managed to measure past UVR exposure but rather use measures such as the number of sunburns or estimated hours in the sun. Furthermore, these imprecise measures are based on recall of events in the past [8.2004].

Table 1.3 Candidate, and selected, health outcomes to be assessed for the burden of disease related to ultraviolet radiation [19.2006]

Outcomes associated with UVR	Strong evidence of causality	Included in the Burden of Disease study
Immune effects		
Acute		
Suppression of cell-mediated immunity		
Increased susceptibility to infection		
Impairment of prophylactic immunization		
Activation of latent virus infection - herpes labialis	Activation of latent virus infection - herpes labialis	Activation of latent virus infection - herpes labialis
Chronic		
Activation of latent virus infection - papilloma virus		
Rheumatoid arthritis*		
Type 1 diabetes mellitus*		
Multiple sclerosis*		
Effects on the eyes		
Acute		
Acute photokeratitis and conjunctivitis	Acute photokeratitis and conjunctivitis	
Acute solar retinopathy	Acute solar retinopathy	
Chronic		
Climatic droplet keratopathy		
Pterygium	Pterygium	Pterygium
Pinguecula		
Squamous cell carcinoma of the cornea	Squamous cell carcinoma of the cornea	Squamous cell carcinoma of the cornea
Squamous cell carcinoma of the conjunctiva	Squamous cell carcinoma of the conjunctiva	Squamous cell carcinoma of the conjunctiva
Cataract	Cortical cataract	Cortical cataract
Ocular melanoma		
Macular degeneration		
Effects on the skin		
Acute		
Sunburn	Sunburn	Sunburn
Photodermatoses	Photodermatoses	
Chronic		
Cutaneous malignant melanoma	Cutaneous malignant melanoma	Cutaneous malignant melanoma
Cancer of the lip		
Basal cell carcinoma of the skin	Basal cell carcinoma of the skin	Basal cell carcinoma of the skin
Squamous cell carcinoma of the skin	Squamous cell carcinoma of the skin	Squamous cell carcinoma of the skin
Chronic sun damage/solar keratoses	Chronic sun damage/solar keratoses	Solar keratoses
Other direct effects		
Acute		
Medication reactions		
Chronic		
Vitamin D production* - rickets, osteoporosis -tuberculosis	Vitamin D production - rickets, osteomalacia, osteoporosis	Vitamin D production - rickets, osteomalacia, osteoporosis
Non-Hodgkins lymphoma*		
Other cancers *- -Prostate -Breast -Colon		
Hypertension*		
Psychiatric disorders* -Seasonal affective disorder -Schizophrenia -General well-being		
Indirect effects		
Effect on climate, food supply, disease vectors, atmospheric chemistry		

* Possible beneficial effects of adequate UVR exposure

1.6 Climate change, ozone depletion and the impact on ultraviolet exposure of human skin

More recently, there has been an increased awareness of the interactions between ozone depletion and climate change (global warming), which could influence human exposure to terrestrial UV [3.2004; 11.2005].

Since the late 1970s significant decrease in total ozone on a global scale has taken place while in the 1990s the loss of ozone in the northern hemisphere was proceeding with a loss rate of about 6% per decade over mid-latitudes (30–50°N) in winter and early spring [13.2004]. The loss in summer months, when UV levels are much higher and people are exposed more frequently to the sun, is about 3% per decade. At mid-latitudes ozone depletion now appears to be slowing down to 4% in winter/spring and 2% in summer/autumn in the northern regions [7.2006].

All other factors being constant, calculations for the northern hemisphere based on the measured ozone trends for the period 1979–1992 indicate that the terrestrial erythemally effective UV radiation should have increased by less than 1% per decade at 15°N to about 3% per decade at 30–40°N and 5% per decade at 50–60°N [13.2003; 18.2003]. These predictions have not generated from ground based UV monitoring programmes. Reasons offered to account for this apparent discrepancy include the limited period of most UV monitoring networks, accuracy of instrument calibration and long-term stability of monitoring equipment, year-to-year fluctuations in cloud cover and an increase in ozone and aerosols present in the lower atmosphere due to pollution. However, international inter-comparisons between instrumentation are improving data quality and reliability.

Anyway, the climatology of terrestrial UV is predicted to change in the future as a consequence of changes not only in total ozone but also in other atmospheric variables that are influenced by changes in climate. Results of model calculations indicate that generally there will only be slight changes in ambient UV over the next decade. By the mid-part of this century, UV levels will return

to those found in 1980, provided that all other factors remain constant [7.2006].

This assumption is unlikely and factors that could influence recovery include non-compliance with the Montreal protocol and subsequent amendments, interactions between ozone depletion and global warming and future volcanic eruptions [2.1992; 20.1997].

Slaper provided the most sophisticated attempt to estimate the impact of ozone depletion on skin cancer incidence [13.1996]. These estimates suggest that the increased risk of skin cancer due to ozone depletion would not have been adequately controlled by implementation of the Montreal Protocol alone, but can be achieved through implementation of its later amendments. Under the Montreal Amendments, incidences of all types of skin cancer in north-west Europe will rise around the mid-part of this century to an additional incidence of about 90 per million. Thereafter the increase in disease rates attributable to ozone depletion is expected to return almost to zero by the end of the next century and, as skin cancer typically results from several decades of UV exposure, the response of the disease will follow later than changes in exposure [6.2002].

It should be noted that the calculated risks do imply full compliance with restrictions on the production and consumption of ozone-depleting chemicals throughout the world. If, in the future, compliance does not continue, damage to the ozone layer could be greater than hitherto expected and biological impacts could be more severe [7.2002].

These quantitative risk estimates concerning skin cancer are valid if all other factors that determine risk (such as human behaviour) are not modified. This is, of course, extremely unlikely. Given the uncertainties that exist regarding not only atmospheric change but also human behaviour, it is likely to prove impossible to look back at the end of this century and be certain what effect ozone depletion had on skin cancer incidence worldwide.

Much attention has been given to stratospheric ozone depletion but what has frequently been overlooked is that climate change induced by greenhouse-gases can also influence ambient UV through the indirect influence of global warming on total ozone and other variables, such as clouds and aerosols [6.2003].

It is noteworthy to consider that the impact of changes in ambient temperature could influence people's behaviour and the time they spend outdoors. A change to warmer conditions is predicted to occur. These average temperature changes will be accompanied by an increased frequency of extreme temperature events and high summer temperatures, such as in the summer 2003, will become more frequent. Furthermore, it is not just temperatures that will change, but also the amount and frequency of rainfall. Winters will become wetter and summers may become drier. Clearly such changes in climate could encourage behaviour that would increase population exposure to sunlight and the health risks associated with it [5.2003].

Experimental studies on animals have shown that elevated temperatures enhance UV-induced skin cancer in comparison with that at room temperature. Assuming that ambient temperature would have a similar effect in humans, de Gruijl et al. [6.2003] speculated that long-term rise of temperature by 2°C as a consequence of climate change would increase the carcinogenic effectiveness of solar UV by 10%.

The combined effect of ozone depletion and global warming would enhance the excess incidence by about 20%, which would result in excess skin cancers. With the protection of the ozone layer now well-established, the effect of rising temperatures on skin cancer incidence, especially on people living at high latitudes, may soon be greater than that of ozone depletion. Moreover, this effect will increase with further rises in temperature so efforts analogous to the Montreal protocol are needed to mitigate the adverse consequences of climate change on human skin.

2. PRESENT INVESTIGATION

2.1 Aim of the study

The assessment of human UV exposure is generally a complex issue. This survey arose from the need to characterize the exposure to solar UVR of the Italian population. Such need, matured from some epidemiologic evidences all over the world (section 1.5), has been better justified by the possibility to collect data of personal UV exposure, for the first time, on a representative Mediterranean population. Italians, in fact, are becoming more and more heterogeneous due to the important migratory fluxes from the south of the world. In addition the greater facility of movement within the European Union has contributed to distribute people genetically adapted to living at different latitudes. Recent studies (section 1.6) have also suggested that, among the possible consequences of the climatic changes, there could be an excess of exposure of human beings to solar UVR. This can derive from the combined effect of the stratospheric ozone losses and the global warming which leads to a greater tendency of the population to stay outdoors.

In this study, after an introduction on the background (chapter 1), the description of the materials and the methodologies adopted are presented in chapter 3. This is followed by chapters on the plans and how the *in vivo* experiments with volunteers were carried out (chapter 4) and on the analysis and discussion of the results (chapter 5).

The primary aim of this study is firstly to provide and validate a methodology for recording the level of exposure for different body postures and then to combine the information derived from possible biological indicators with such exposure data. Several erythemal dosimeters have been developed (section 3.2). We used photosensitive film, made by polysulphone (PS) polymer whose absorbance properties change on exposure to UV radiation (section 3.3). PS dosimetry enabled measurements of the exposure of differently oriented surfaces and in remote and not easily accessible places. In all *in vivo* campaigns, the volunteers under

different environmental conditions wore PS dosimeters (section 4.2). In particular, the groups involved in the field experiments were selected according to how much they were representative of a leisure time activity (sections 4.2.1, 4.2.2, 4.2.5) or of a working activity (sections 4.2.3) or both (section 4.2.4).The results were quantified in terms of Exposure Ratio ER (section 3.4.1). In such a way, being ER an adimensional parameter, the results are not time dependent if the habits of the people of the selected group remain the same throughout time.

The first results consisted on the data collection of the personal UV exposure in terms of Exposure Ratio of the selected groups, which are added to the global dataset. Such dataset, derived from studies obtained with questionnaires, diaries, observations, models and measures, is becoming an important vehicle to formulate guidelines for the exposure to non ionizing radiations and to adopt protective measures.

Polysulphone dosimetry was thoroughly studied during this research and an important contribution to the understanding of the calibration curves was given (section 4.1).

In addition some biological indicators, used to identify possible effects, were considered with measures of personal exposure. Colorimetric measures (section 3.4.2) and skin temperature data were systematically taken during the experiments. In some cases, it was possible to add further information like free radical (FR) amounts in the plasma, the phototype according to Fitzpatrick's classification and information on the use of sunscreens or medicals.

A schematic diagram of the suggested methodology is offered in the next section.

2.2 The proposed methodology

The methodology proposed in the present investigation (chapter 3) is schematically reported in Figure 2.1. Starting from the availability of PS dosimeters and calibrated ambient UV instrumentation (PS+UV resources), it is possible to retrieve the dosimeter calibration curve for the site and time of the year in

which the experiment is carried out. Thus, the value of Exposure Ratio is reached after campaigns with the volunteers and information can then be transferred through the literature in the existing dataset of personal exposures (Exposure dataset).

During the experiments, it is possible to perform pre- and post-exposure measurements both of colorimetric parameters (Colorimetry) and skin temperature (Skin temperature). The obtained series of data (L, a, b, T) for each volunteer therefore constitute, after having operated proper quality check and quality assurance tests, the input to the multivariate approach through the Principal Components Analysis (PCA). It is then possible to search for correlations (Correlation matrix) among the principal components and Exposure Ratio. In most cases it is not possible to reach meaningful linear relationships and a classification in groups (Cluster Analysis) becomes necessary.

Finally, the interpretation can be supported by the information derived from not systematic measures of categorical type, like free radicals, the questionnaires or the visual analysis (Ancillary data) and eventually parameterized in a model (Interpretation-Model).

Figure 2.1 Simplified flux diagram of the proposed methodology

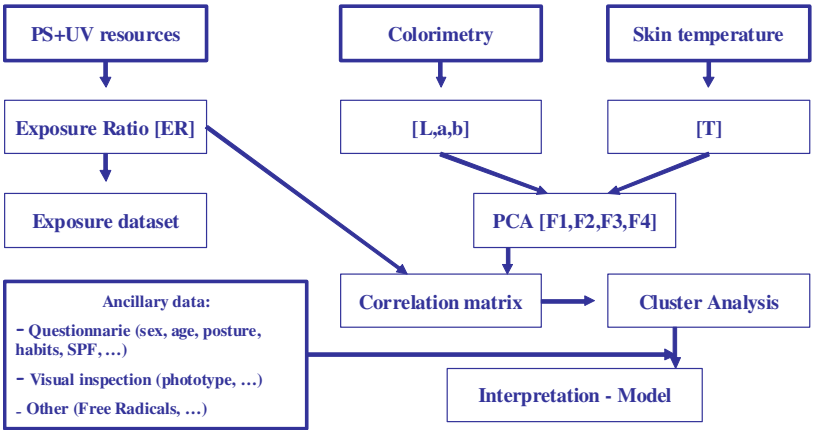

3. MATERIALS AND METHODS

3.1 Introduction

Surveys, questionnaires and time diary reports can help to quantify the average time spent outdoors which can then be converted into a personal UV dose, if the ambient UV doses, i.e. the incident weighed irradiance on a given surface over a specified period of time, are known. Self-reports were used successfully to assess sun protection in sun exposure studies together with the knowledge of the negative health effects of over UV exposure, attitudes toward sun exposure and sun protection and to record sunburn episodes. People were commissioned to report their ‘‘usual’’ behaviour and/or the duration of their sun exposure (e.g. time spent outdoors). The use of self reports is a good tool in understanding population exposure once levels of ambient UV are known. They were used successfully among children and adolescents. However, recall and response bias errors must be considered as well as any a priori assumptions. In fact the error increments with increasing distance between the meter site and the exposed individual. Moreover, there are limited opportunities for extracting the specific information that would help the development of guidelines for sun-related behaviour, reducing excess exposure or increasing inadequate exposure for vitamin D synthesis.

Some studies have used models for determining personal UV doses. By using a well defined set of rules and procedures, an equation for calculating personal UV exposure can be determined and the collected information are used as input to the model. A well-known model used to estimate erythemal UV exposure requires factors related to ambient UV levels, sun protection, body postures in different settings, outdoor activity, timing and duration of exposure. Assumptions and generalizations are made for each factor and the model assumes that any factors do not change during the measurement period. When a scenario is assumed, the model is run for that scenario to estimate cumulative UV exposure. Overall, modelling is a relatively simple method for

estimating exposure but it has not been adequately validated for the use. If direct measurements are used within a model, a sample of a few days is often used to represent a longer time pattern and this, too, cannot give an accurate assessment of exposures.

On the other hand, personal exposures can be measured with dosimeters, using polysulphone or spore-containing biofilms or portable data-loggers. In Table 3.1 a summary of studies measuring or assessing youth (childhood and adolescent) exposure during their activities is reported.

In the present study, we have chosen polysulphone dosimetry as the most accurate methodology. All the experiments were conducted keeping in mind that as much data as possible should have been collected for a correct interpretation of results. Beside necessary personal information (sex and age) and personal exposures (expressed as fraction of the total ambient radiation), colorimetric and skin temperature data were systematically taken during the experiments. In some cases, it was possible to add further information like free radicals amount, the phototype according to Fitzpatrick's classification (Table1.2) and information on the use of sunscreens or medicals.

Data were then analysed by means of well known statistical multivariate approaches, namely PCA (Principal Component Analysis) and Cluster Analysis, useful when variables are not only correlated but are also large in number, making the data interpretation difficult.

In addition a model was developed to interpret the results and estimate short and long term doses.

Table 3.1 Studies measuring or assessing childhood and adolescent UV exposure and related activities [3.2005]

Reference; country where study conducted	Group characteristics; age; (*n*, sample size)	Study duration, season	UV measurement/ assessment method (body site where reported)	Activity assessment method; recall period
Melville *et al.* (44); USA	Sports players and scouts; 8–18 years (126)	1–3 days, summer	PSF (cheek, forehead, arm)	Observation (logbook); not reported
Fritschi *et al.* (26); Australia	Adolescents; 13–15 years (972)	4 days, summer	Questionnaire	Self-report (diary); daily
Grob *et al.* (22); France	Toddlers, 3 years (150); adolescents, 13–14 years (200)	1 season, summer	Questionnaire	Self-report (questionnaire); 9 months later
Diffey *et al.* (40); UK	Schoolchildren; 9–10 years and 14–15 years (180)	13 weeks, summer	PSF (chest)	Self-report (diary); daily
Dwyer *et al.* (45); Tasmania	Schoolchildren; 14–15 years (125)	4 days, late spring	PSF (hand) Questionnaire	Self-report (questionnaire); 10 months later
Mayer *et al.* (46); USA	Children; 6–9 years (58)	8 weeks, summer	Colorimeter Questionnaire	Self-report (questionnaire); daily
Robinson *et al.* (47); USA	Adolescents; 11–19 years (658)	45 days, summer	Questionnaire	Self-report (questionnaire); week
Gies *et al.* (41); Australia	Schoolchildren; 12 years (112)	8 days, summer	PSF (shoulder)	Self-report (diary); daily
Kimlin *et al.* (48); Australia	Adolescents; 15–16 years (*n* not given)	2 days, summer	PSF (shoulder)	Self-report (diary); daily
Moise *et al.* (50,51); Australia	Infants, age not given; and children, 2.5 years (115)	12 days; spring, autumn	PSF (shoulder, chest)	Self-report (diary); daily
Moise *et al.* (52); Australia	Schoolchildren; 12–13 years (70)	5 school days, winter	Model Questionnaire	Self-report (questionnaire); usual, no recall
Milne *et al.* (42,53); Australia	Schoolchildren (age and *n* not given)	1 day, spring	PSF (shoulder)	Observation (logbook)
O'Riordan *et al.* (54); Australia	Infants; age not given (21)	4 days; winter, spring	PSF (wrist)	Parental report (questionnaire); 4 days
Parisi and Kimlin (55); Australia	Schoolchildren (age and *n* not given)	1 month, summer	Model	Self-report (questionnaire, school); usual exposure
Parisi *et al.* (56); Australia	Schoolchildren; 0–19 years (142)	4 months, 1 year	Model	Self-report (diary); daily
Autier *et al.* (57); Europe	Young adults; 18–24 (58)	3 months, summer	Electronic dosimeter (ground)	Self-report (diary); daily
Godar *et al.* (10); USA	Schoolchildren; 0–19 years (2000)	2 years	Survey: National Human Activity Pattern Survey (1992–1994)	Self-report (survey); not given
Cokkinides *et al.* (58); USA	Schoolchildren; age not given (1192)	1 year	Survey	Self-report (questionnaire); maximum 1 year later
Termorshuizen *et al.* (59); The Netherlands	Children; 1 year (910)	6 weeks, spring	Questionnaire Model	Parental report (questionnaire); 6 weeks later
Severi *et al.* (60); Europe	Schoolchildren; 6–7 years (631)	6 years, holidays only	Questionnaire	Parental report (questionnaire), 6 years later
Guy *et al.* (61); South Africa	Schoolchildren; 4–9, 13–14 years (30)	7 days, summer	PSF (lapel)	Self-report (diary); daily
Livingston *et al.* (62); Australia	Schoolchildren; 7–12 years (78 032)	3 years, summer	Questionnaire	Self-report (questionnaire); maximum 1 year later
Stanton *et al.* (63); Australia	Child-care children; 3–5 years (49)	4 days, autumn	PSF (both wrists, back)	Video recordings
Sullivan *et al.* (64); Australia	Schoolchildren; 9–15 years (35)	1 day, autumn	PSF (lapel)	Self-report (diary); daily
Godar *et al.* (65); USA	School subjects; 1–18 years (*n* not given)	3 years	Survey: National Human Activity Pattern Survey (1992–1994)	Self-report (survey); not given
Boldeman *et al.* (66); Sweden	Schoolchildren; 1–6 years (62)	11 school days, summer	Spore dosimeter (shoulder)	Observation (logbook)
Thieden *et al.* (67,100); Denmark	Schoolchildren; 4–18 years (127)	3 years	Electronic dosimeter (wrist)	Self-report (diary); daily
Castanedo-Cazares *et al.* (68); Mexico	Schoolchildren; 9–19 years (80)	1 year (school days only), autumn	Observation	Observation (logbook, watch); daily
Ono *et al.* (49); Japan	Schoolchildren; 10–11 years (~175)	7 days, 1 year	Spore dosimeter (upper arm) UV-colouring labels	Logbook (unidentified recorder)

3.2 Personal UV dosimetry

Personal exposure to UVR can be measured using physical, chemical or biological dosimeters. A dosimeter indicates the effect of UV irradiance on a specific biological system when a

measurable property changes in a reproducible manner after exposure to UV [4.1987]. A dosimeter is calibrated in physical units against another instrument that measures UV (e.g. a spectroradiometer or a broad-band radiometer) [15.1996]. A personal dosimeter is capable of evaluating UV exposure in realistic conditions that include the changing of position and surface orientation with respect to the source of radiation [5.1988; 11.1995; 3.2000]. The suitability of a dosimeter depends on its specific response spectrum. A dosimeter should be precise, accurate, reliable, inexpensive, independent from temperature and humidity and have a reproducible biological response. Most dosimeters, used to measure personal UV exposure, have a response that resembles the erythemal action spectrum defined by the Commission Internationale d'Eclairage (CIE) and weigh UV at different wavelengths according to the extent to which it induces erythema.

Physical dosimeters

Miniature electro-optical UV sensors have made it possible to construct small UV detectors capable of being electrically paired to a portable data logger carried in a trouser pocket, worn on a belt or clipped to glasses [8.2005]. So, it is possible to record UV exposure on a second-by-second basis, which permits a clearer understanding of human behaviour in sunlight. Anyway, these dosimeters have limitations [9.2005]: the quantity of data stored can be conditioned by the processing time; the UV semiconductors of electronic instruments may not behave in the same way as their biological counterparts; the complexity of the operating system may result in considerable power consumption, which reduces the weight/lifetime ratio; the price may be high; a satisfactory cosine response may be difficult to achieve; and environmental durability and temperature independence may be less than optimal. However, it is possible to overcome each of these limitations. Since electronic and digital dosimeters are reusable, the cost can be spread over a longer period,

waterproofing can be achieved with sealants, and lithium batteries extend the durability, but not the weight, of the power source.

In this study, ambient and personal UV doses were determined also using X2000-4 GigaHertz electronic dosimeters (Figure 3.1).

Figure 3.1 The X2000-4 GigaHertz electronic dosimeter worn by a volunteer during a field experiment

The X2000-4 electronic dosimeters are small and easy to use. They are powered by batteries during exposure and can be set up in not easily accessible areas. The electronic dosimeter is equipped with two photovoltaic cells, one reproducing the erythemal action spectrum, the other having a response which is approximately constant in the UVA range (the UVB contribution is negligible). The instrument response is cosine corrected. The acquisition sampling rate can be set using the dedicated software and, in this study, a frequency of 1 Hz was adopted. The absolute calibration of the electronic dosimeters was certified by Gigahertz-Optik in 2005.

Another example of a portable datalogger is the ‘‘Sunsaver^{TM},, wristband, which gives time-stamped readings every 10 minutes (with 75 compounded readings). The Sunsaver^{TM} wristband houses a digital watch, a data-logger and a silicon carbide photodiode (model JECF1-IDE; Laser Components, Olching, Germany) as the sensor, which has a spectral response similar to the CIE erythemal action spectrum [9.2000].

Chemical dosimeters

The use of chemical methods, which measure the chemical change produced by the radiation, is called actinometry. These techniques usually form the basis of personal ultraviolet dosimeters. The most commonly used material for studies of personal UV dosimetry is the thermoplastic polysulphone (PS, Figure 3.2) [1.1976; 3.1978]. When the film is exposed to UV radiation at wavelengths mainly in the UVB waveband, its UV absorption increases. The increase in absorbance measured at a wavelength of 330 nm increases with UV dose. The film (usually 40–50 mm thick) is mounted in cardboard or plastic photographic holders. Applications of UV dosimetry with polysulphone film have included:

- sun exposure of children;
- sun exposure from different leisure pursuits;
- sun exposure from different occupations;
- anatomical distribution of sunlight in humans and animals;
- clinical photosensitivity studies;
- UV exposure of patients from therapeutic light sources;
- UV exposure of workers in industry.

More details on polysulphone dosimetry will be given in the next paragraph.

Figure 3.2 The polysulphone (PS) dosimeter (on the left) compared with the size of a broad-band radiometer

Biological dosimeters

Biological dosimeters may comprise either biomolecules (for example provitamin D-3, uracil and DNA); bacteriophages (for example T7); or spores (for example Bacillus subtillis, applied in ‘‘DLR-Biofilm’’ and Biosense Viospor). Such dosimeters are small, require no external power source and calculate the biological effect for a specific waveband and reaction. Biological dosimeters all record cumulative UV exposure and eventually reach saturation.

The bacteriophage T7 has been used to monitor ambient UV radiation and, when combined with an appropriate optical filter, a spectral response similar to the action spectrum for erythema in human skin can be achieved.

One type of biofilm used to measure personal UV exposures is made using spores from Bacillus subtilis [6.1994]. The spores are isolated and immobilized in agarose on a biofilm (Figure 3.3). These spores have an action spectrum for inactivation of germination similar to the absorption spectrum of DNA but can be modified to reflect the erythemal response of human skin by using appropriate filters. Each badge has its own ‘‘dark control’’ and both the dark control and the exposed parts of the badge are incubated in a nutrient broth for about 4 hours to allow spore germination and synthesis of proteins. After staining with Coomassie blue for the presence of proteins, the absorbance at 590 nm is measured using a spectrophotometer. Some studies used biofilms to measure UV exposures in extreme conditions: sports, high elevations, extremely cold regions like the Antarctica and in a spacecraft orbiting around the earth. Spore dosimeters proved useful for the long-term measurement of the UV exposure of mountain guides who wore one dosimeter per month, attached to a vertical surface on a cap or glasses. The UV-B passing through car windows was also tested but, as expected, only UV-A passed through the glass (this is also true for windows in buildings). To quantify youth UV exposure, it was reported the use of VioSpor, a biological UV-sensitive photofilm with a filter-optic system and protective case, described as UV-sensitive

artificial skin. The highly sensitive DNA molecules of immobilized spores produce a responsivity profile that corresponds to that of human skin for triggering sunburn. They allow measurement of cumulative UV dose and are not reusable. UV exposure for preschool children was also estimated in both a shady and a sunny playground using a pair of spore dosimeters per subject, which were worn for 11 days, thereby providing a measure of cumulative UV exposure.

An innovative method of biological UV dosimetry based on an in vitro model of previtamin D photosynthesis has been suggested [7.1994; 35.1999]. This dosimeter is still being tested, but has the potential to measure vitamin D levels in individuals as well as UV exposure.

A new biological UV dosimeter, using skin autofluorescence to calculate personal exposure, has been proposed. An in vivo studywas conducted with 131 healthy volunteers, including 23 children and adolescents, fluorescence was measured from sun-exposed and sun-protected skin, and corrected for the impact of pigmentation and redness. Personal exposure data were collected using questionnaires and electronic dosimeters for a summer period. The results obtained suggest that collagen-linked skin fluorescence might be a reliable measure of personal photodamage and UV exposure.

Figure 3.3 The DLR-Biofilm used on a volunteer in a space research experiment (courtesy Dr. Gerda Horneck)

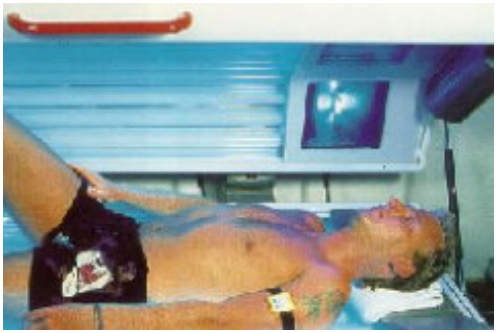

3.3 Polysulphone dosimetry

Polysulphone dosimetry is a widely tested methodology for assessing ultraviolet radiation exposure [7.1989; 9.2004]. The use of PS dosimeters for a reliable quantification of personal doses requires the calibration curves to be determined, due to the discrepancy between PS and CIE spectra (Figure 3.4) [26.1999; 1.2000]. These curves are obtained by measuring the ambient erythemal effective UV dose (ambient UV dose) and the corresponding change in PS film absorbance (ΔA at 330 nm), prior and post exposure [15.2003; 17.2003]. The absorbance of unexposed PS films with a thickness of 40 μm at 330 nm ranges from 0.1 to 0.2 depending on the batch, with increased values after the exposure to UV radiation [30.1999]. Under prolonged exposures the film reaches saturation at values of ΔA greater than about 0.4 [8.2001]. Diffey showed that the best data fit, mainly for $\Delta A > 0.3$, is given by the following equation:

$$D = c(\Delta A + \Delta A^2 + 9 \cdot \Delta A^3) \qquad (1.3)$$

where D (erythemal dose) is expressed in kJ m^{-2}. He found the value of the coefficient c equal to 2 kJ m^{-2} from a field campaign carried out on a summer day (1 July 1986) and on an autumn day (2 October 1986) at a site located at 55 °N.

During this study, several field campaigns using polysulphone dosimeters were carried out (see section 4.1).

Usually, the PS film (PSF) is mounted in a cardboard or photographic holder to form a badge that is secured to the desired surface using a pin, Velcro or tape. The first known study to measure adolescents' UV exposure using PSF was in 1988. PS badges have since been applied in studies to measure personal occupational UV exposure, exposure during other activities, anatomical differences in UV exposure and the influence of sun protection on UV exposure.

The popularity of this badge in scientific research is due to: spectral sensitivity similar to the photobiological response of

erythema; it is an economical means of quantifying personal cumulative erythemal UV exposure; it is temperature independent; it readily undergoes changes in surface properties (among which absorbance) when exposed to UV; it can be miniaturized to form a simple, small badge that requires no power source; it is sufficiently versatile to be attached to a variety of surfaces and anatomic sites; it may comprise multiple apertures to increase the reliability of measurements; it is waterproof and can be used in water sports (if the mounting is waterproof). Validity testing with diary records has found a reasonable correlation of UV exposure [19.1997]. PSF badges have been used in many studies to measure child and adolescent UV exposure [12.1996; 19.2003; 5.2004; 3.2005]. In the earliest study, PSF badges were attached with Band-Aids to the adolescents' hands and upper arms for 3 days in spring. More recently, a study used PSF badges attached to the lapel to measure cumulative UV exposure of 35 schoolchildren during a single day in autumn. In other studies, PSF badges have been attached to different parts of the body including the wrist, cheek, forehead, chest and shoulder [17.1997; 24.1998]. The choice of specific parts of the body is determined by badge attachment capabilities [13.2006], worst exposure conditions and for the comfort of the user [23.1998; 28.1999; 34.1999; 6.2000; 7.2000; 8.2000]. The lapel site provides a good approximation of the UV exposure received by the hands and the face, whereas the top of the shoulder is used to obtain measures of the worst-case scenario [8.2002; 2.2004; 5.2006; 9.2006; 18.2006]. In our experiments, PSF badges were attached to the upper part of the arms, the back (under the nape), the chest and the forehead.

PSF use as UV dosimeter has limitations: it does not permit an assessment of the magnitude and change in exposure rate during the measurement period and provides only a cumulative erythemal UV dose; the sensitivity of PS extends up to wavelengths of 330 nm, whereas the biological effectiveness of UV-B is in the wavelength range 280–320 nm; the dose–response of PS is dependent on film thickness and film of the same thickness should be used in any one particular study; pre- and post-exposure

absorbance measurements may be labour intensive, depending on the dexterity of the operator; PSF does not take into account any combined effect of UV-A with UV-B because it measures only the UV-B biologically effective UV exposure; it shows batch variation and a slight dark reaction (absorbance increases slightly when kept in the dark post-exposure); surface contamination must also be considered; badges may be difficult to keep intact, unwrinkled and clean, in particular when placed on young children, and cleaning and improved measurement techniques to overcome wrinkling are necessary.

Recently, PSF with a filter that allows extension of the measurement range and exposure period has been developed and tested [18.1997; 1.2004]. This means that personal UV exposure studies may use PS to quantify cumulative UV exposure continuously for between 3 and 6 days. Anyway, in this study we used dosimeters whose saturation is reached after some hours, depending on the amount of ambient radiation.

Figure 3.4 CIE and PS action spectra normalized at 295 nm

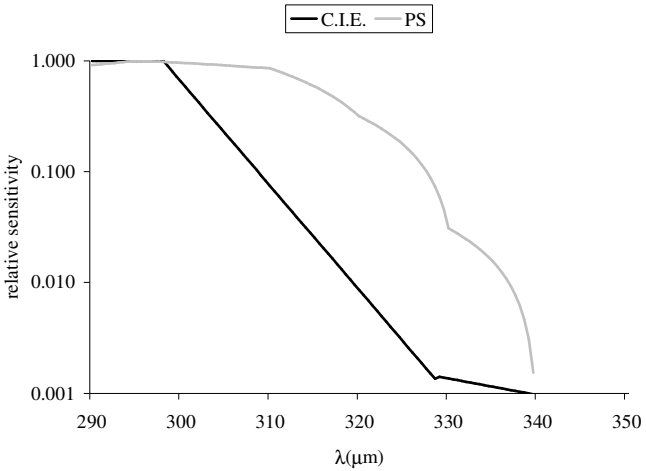

3.4 Data collected

3.4.1 Exposure Ratio

There is no universally accepted measure for quantifying personal UV exposure [4.2005]. Nevertheless, such measures are required to document baseline levels, make comparisons, develop preventive programs and compare and assess the impact of interventions. Moreover, every measure should be the result of:

- personal factors (activity type and movement, skin sensitivity, orientation of the exposed body part to the sun and the time spent outdoors);
- equipment (sun protection worn, i.e. sunscreen, hat etc.);
- physical factors (environmental factors, distal or proximal);
- social environmental factors (i.e. availability of shade).

In the present study, we decided to express personal exposures by means of the Exposure Ratio (ER) between the erythemally weighed absorbed dose as measured by the PS dosimeter and the corresponding ambient dose on a horizontal plane. The measure of ER has the advantage of being independent from the environmental parameters if referred to the same area under the same conditions and if the exposed population behaves in the same way during outdoor activities. Under such limitations, Ratio can characterize the exposure of a group of people during, for example, their working activities or leisure time. For this reason, ER will be used in the next sections to express the results of the field experiments.

3.4.2 Colorimetry

It is quite difficult to study and record skin colour changes quantitatively, as individual perception of colour is complex and subjective [5.2002]. Several studies have showed that both reflectance spectrophotometers and tri-stimulus colorimeters are very useful in the study of the quantitative evaluation of UV-induced erythema and pigmentation, the severity of diseases and the efficacy of treatment modalities [3.2002]. A colorimeter was

used to assess UV exposure of children both before and after a telephone interview conducted with parents. Before their use, information is needed on skin colour variation between different parts of the body to account for variation in skin thickness, blood supply, ambient meteorological conditions (temperature and humidity) and level of activity before measurement [7.2004; 20.2004; 7.2005]. Instruments must also be placed on identical sites before and after exposure to UVR and freckles and moles must be identified to prevent them from obscuring readings. One way of validating colorimeter data may be that of using visual inspection by a dermatologist to identify erythema and rate the level of damage.

The tristimulus colorimeter expresses colour in three dimensions in a similar way in which the human eye perceives colour. The measuring head is gently compressed against the body, a xenon lamp fires, causing a flash, and optical fibers lead the reflected light plus emitted light to silicon photocells for analysis of primary stimulus values for red, green and blue light. Although colorimeters are portable, simple and quick for quantifying erythema with reasonable accuracy, they are costly and error may result if measures are taken with an incorrect pressure.

The Minolta Spectrophotometer CM26000d (Minolta, Osaka, Japan), shown in Figure 3.5, was used in our study [10.2002; 11.2002]. It is based on the physical measurement of reflected light, through an integrating sphere, at specific wavelengths (400–700 nm at 10 nm steps), corresponding to the spectrum of visible light. A number of light filters are built in. Results are displayed as a graph showing reflectance vs. wavelength. With this instrument it is possible to convert and display results as colorimetric values in the (L, a, b) system calculated from spectral data, as recommended by the Commission Internationale de l'Eclairage: the L value (luminance) gives the relative brightness ranging from total black (L=0) to total white (L=100); the a value represents the balance between red (positive value) and green

(negative value); and the *b* value represents the balance between yellow (positive value) and blue (negative value).

Figure 3.5 The Minolta Spectrophotometer CM26000d used to measure skin colour on a volunteer during an experiment

The colorimeter was recommended for the objective evaluation of erythema in the (*L*, *a*, *b*) colour space [12.2005]. The overall data, for an easier colorimetric analysis, can be represented, respectively, in the planes of *L* vs. *a*, *L* vs. *b* and *a* vs. *b*. The *L* and *a* plane indicates luminance vs. red chrominance. In this plane the intensity of the red component of skin colour is visible and the change of red chrominance in erythema response can be observed by serial plotting. The *L* and *b* plane represents luminance vs. yellow chrominance. It shows pigmentary change in skin related to the melanin content. The *a* and *b* plane of red and yellow chrominances give information to understand the concepts of shade of skin colouration, saturation or chroma, relatively, apart from luminance. In each plane, the acquired tanning, quantified at defined periods, is plotted via vectors. The origin of vector represents the original skin colour, the length gives the intensity of acquired tanning, and the direction gives the shade of tanning.

The visual evaluation of the intensity of constitutional skin colour is correlated with the *L* and *b* component. The sectors of skin colour defined are limited by radii, originating from the central point (*L*=50, *a*=*b*=0) of the *Lab* volume and have angles with the *b>0* axis, called category angles.

In the experiments discussed in the present study, Minolta Spectrophotometer measures were taken before and after exposure of PS dosimeters worn by volunteers with Observer 10° and Primary Illuminant D65. For each measure, a not exposed and an exposed site were taken into account and the changes between the two sites, before and after exposure, were used as biological indicators. In the following, the changes will be indicated by the same letters of the parameters, that is:

$$L = \left(L_{after}^{\exp} - L_{after}^{n-\exp}\right) - \left(L_{before}^{\exp} - L_{before}^{n-\exp}\right) \tag{2.3}$$

$$a = \left(a_{after}^{\exp} - a_{after}^{n-\exp}\right) - \left(a_{before}^{\exp} - a_{before}^{n-\exp}\right) \tag{3.3}$$

$$b = \left(b_{after}^{\exp} - b_{after}^{n-\exp}\right) - \left(b_{before}^{\exp} - b_{before}^{n-\exp}\right) \tag{4.3}$$

where the *exp* and *n-exp* exponents stay for “exposed” and “not exposed” site. Usually, the measures on the not exposed site do not change in the pre- and post-exposure conditions and can be eliminated. If the expressions (2.3), (3.3) and (4.3) are positive, then the corresponding parameter has increased its value. Evaluation of the constituent melanin was thus possible, besides information on skin colour changes due to short term or long term exposure. The standardized relative changes were used in the statistical analysis.

3.4.3 Skin temperature

Human skin is constantly exposed to solar radiation of all wavelengths ranging from 290 to 4000 nm, which include, besides the ultraviolet (UV) portion, visible light (400–700 nm) and infrared (IR) radiation (700–4000 nm). Of total incident solar

energy, more than half is comprised in the IR range. The solar IR radiation reaching the earth's surface is mostly near-IR, that induces molecular vibrations and rotations increasing temperature of the receiving systems, such as skin. Moreover, some effects occurring at the interface between skin and air (e.g. sweating) can change the value of skin temperature. Thus, in order to separate the effects due to the solar UVR on human skin and that due to the heat generated by IR radiation or other causes, measures of skin temperature were taken during the experiments with volunteers.

A PT-3LF Portable Non-contact Thermometer (Optex, Japan) was used to measure skin temperature before and after exposure, following the same procedure of colorimetric data (Figure 3.6). A temperature change was thus defined as:

$$T = \left(T_{after}^{\exp} - T_{after}^{n-\exp}\right) - \left(T_{before}^{\exp} - T_{before}^{n-\exp}\right) \qquad (5.3)$$

The instrument (planned mainly for applications in electric wiring, motors and machines, freezers and refrigerators) resulted in being quick (response after 1.5 s), safe and reliable (repeatability ±1°C of reading value) also for its new use on human body. With a field of view of 30/1000 mm, it uses a sighting method based on a coaxial laser marker. Optics are made of a silicon lens and its sensing element by a thermopile working in the range 8-14 μm. Its accuracy is ±1% of reading value. It can work adjusting the emissivity ratio ε from 0.95 (dark bodies) to 0.70 (bright bodies). Due to its battery power supply and the reduced weight (200 g) and dimensions, it proved to be useful in all field campaigns carried out.

Figure 3.6 The Optex Portable Non-contact Thermometer PT-3LF used to measure skin temperature on a volunteer during an experiment

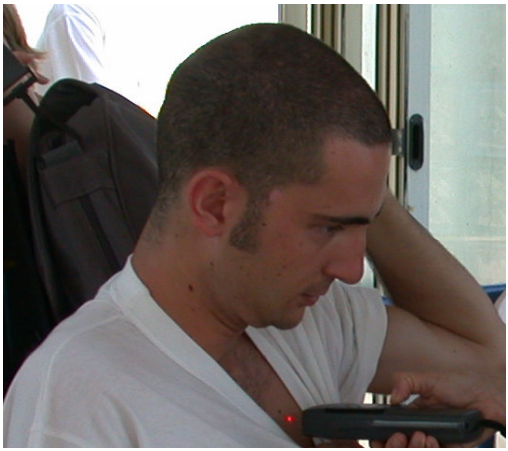

3.4.4 Ancillary data

Free radicals

Free radicals (FR) are toxic substances that can cause oxidative damage to major constituents of biological systems. On the other hand, antioxidants are defined as any substance that significantly prevents the pro-oxidant–initiated oxidation of a substrate. Consequently, it was suggested that it might be possible to reduce FR damage and thus cancer risk through [11.2004]:

(1) caloric reduction, that is, lowering the level of FR reactions arising in the course of normal metabolism;

(2) minimize dietary components that increase the level of FR reactions (e.g. polyunsaturated fats);

(3) supplement the diet with one or more FR reaction inhibitors (antioxidants).

Both the phenolic antioxidant butylated hydroxytoluene (BHT) and the carotenoid β-carotene have been shown to influence ultraviolet carcinogenesis. However, there is a lack of correlation between physicochemical and pathophysiological responses in both cases: whereas the influence on UV carcinogenesis of both

antioxidants has been reported to diminish as the level of dietary fat decreases [15.2006], the mode of BHT's action in inhibiting UV carcinogenesis appears to be related to UV dose diminution through increased spectral absorbance of the stratum corneum while β-carotene has no such effect and may actually exacerbate UV carcinogenesis under certain dietary conditions. This paradox points to the complex relationship between chemical mechanisms and biological mode of action of antioxidants. Recent clinical and experimental data suggest that antioxidant supplementation of the complex and intricately balanced natural antioxidant defense system as a cancer prevention strategy will demand extreme caution.

Until recently, determination of FR plasma levels and the effect of antioxidant therapy on these levels has been difficult. Anyway, a portable, free radicals determination system called D-Roms test (by Diacron, Grosseto, Italy) was recently developed [33.1999]. The D-Roms test is based on the ability of transition metals to catalyse in the presence of peroxides with formation of FRs which are trapped by an alchilamine. The alchilamine reacts forming a coloured radical detectable at 505 nm. The reagents utilised are the cromogen (*R1*, an alchilamine) and a pH 4.8 buffer (*R2*). Ten microlitres of hemolysis-free serum are to 1 ml of *R2* and to 10 microl of *R1*. The sample is mixed, incubated for 1 minute at 37°C and read for optical density. After another minute, the sample is read again. The average *delta A/min* is multiplied by a *K* factor and calculated using serum with defined value. Reference values of FR are reported in Table 3.2.

The D-Roms test provides a simple, inexpensive and practical method to identify subjects with a high level of oxidative stress and to demonstrate the effect of any treatment or additive stress. In this study, it was used on a sample of the volunteers (those who accepted blood analysis) for the short-term experiment of sun bathers and the long-term study of the vineyard growers.

Table 3.2 Reference values of the D-Roms test [33.1999]

Values	FR (Caratelli Units: CU)
Below normal *	<250
Normal	250-300
Border	300-320
Light oxidative stress	320-340
Oxidative stress	340-400
Strong oxidative stress	400-500
Very strong oxidative stress	>500

* It should be noted that values <250 Carratelli Units may be found in patients under cortisonic or antioxidative treatment

Other data

A complete view of the sample of volunteers can be accomplished only when some other data are added to those described above. They are in many cases categorical (or reducible to categorical) and they are useful to interpret the output of statistical analysis.

Here is the list of such ancillary data and the way they were recorded:

Sex: categorical variable, recorded through questionnaires;

Age: categorical variable, recorded through questionnaires;

Phototype: categorical variable, recorded through visual inspection of a dermatologist;

Use of sunscreens or other protection tools: categorical variable, recorded through questionnaires (in some cases it was possible to know the type of sunscreen or hat);

Particular habits or needs: categorical variable, recorded through questionnaires (the frequency of search for shade and typical posture held during the experiments were taken into consideration; highly sensitive to the recall of volunteers and, thus, affected by a greater uncertainty)

3.5 Multivariate exploratory techniques

3.5.1 Nonparametric statistics: Sign Test

The Sign Test is a nonparametric test alternative to the t-test for dependent samples. The test is applicable to situations when we have two measures (e.g., under two conditions) for each subject and want to establish if the two measurements (or conditions) are different. The only assumption required by this test is that the number of subjects (cases) is sufficient and the underlying distribution of the variable of interest is continuous; no assumptions regarding the nature or shape of the underlying distribution are required. The test simply computes the number of times (across subjects) in which the value of the first variable (*A*) is larger than that of the second variable (*B*). Under the null hypothesis (stating that the two variables are not different from each other) we expect this to be the case about 50% of the time. Based on the binomial distribution we can compute a *z* value for the observed number of cases where *A*>*B*, and compute the associated tail probability for that *z* value.

We used the Sign Test to analyse colorimetric (*L*, *a*, *b*) and skin temperature (*T*) data. First we asked if there was a difference between the exposed and the not exposed body-parts before exposure. This was necessary to justify the correctness of the choice of the non exposed part. Then, we were interested to know if there was a change in the exposed site after exposure to sun and the test was applied to colorimetric data of the same variable before and after (assuming that the colorimetric measures pre- and post-exposure were correctly executed). The results for each experiment are described in chapter 4. It is necessary to mention here that, for every set of data analysed, a table like Table 3.3 was obtained but not reported.

Table 3.3 Example table for Sign Test results

Pair of variables	**N. of cases**	**Percent A<B**	**z**	**p-level**
(the two variables involved)	(the number of cases to be analyzed)	(the percent of cases *A*<*B*)	(the value of *z* for *A*>*B*)	(the associated tail probability)

3.5.2 Principal Component Analysis

Data are often collected on variables that are not only correlated but are also large in number. This makes the interpretation of the data and the detection of its structure difficult. By transforming the original variables to a smaller number of uncorrelated variables, Principal Components Analysis (PCA) makes these two tasks easier [8.1995].

For the data collected on p variables for N cases, PCA performs analyses in the N-dimensional space defined by P variables and P-dimensional space defined by N cases. The computation of factors in PCA basically consists of diagonalizing a symmetric matrix: correlation matrix or covariance matrix (depending on whether it is necessary that the data be standardized or centred on the mean values). In both cases, the result is a new set of variables (*principal components*) that are linear combinations of the original variables and are uncorrelated. The new variables thus generated are smaller in number, and yet account for the inherent variation of the data to the maximum possible extent. In fact, in this way, a new space (*factor space*) is generated onto which the cases and the variables can be projected and classified into categories.

In PCA analysis of points in the vector space of cases, straight lines are sought that best fit the clouds of points in the P-dimensional vector space, R_p, of the cases, in the least squares sense. The objective is to obtain a set of orthogonal vectors. Each vector of this set is proportional to the factor axis of the space, R_n, of variables, and can generate a straight line in R_p with the least squares property. These vectors are called the *factor axes* and are further used for computing the *factor coordinates* of the points (cases) in the space R_p. Projection of the cases onto the factor space G_q, generated by the set of factors, can reveal the hidden data structure.

Consequently, a lower dimensional vector subspace is recovered, that represents the original vector space. Although the first factor is extracted so as to capture the variance to the maximum extent, it can seldom entirely capture the variance. What remains should, therefore, be recovered by another (second)

factor and so on. However, the number of factors thus extracted will never exceed the number of original variables.

3.5.3 Cluster Analysis

Cluster analysis actually encompasses a number of different classification algorithms. A general question facing researchers in many areas of inquiry is how to organize observed data into meaningful structures, that is to develop taxonomies. Cluster analysis is not as much a typical statistical test as it is a collection of different algorithms that "put objects into clusters". Unlike many other statistical procedures, cluster analysis methods are mostly used when we do not have any a priori hypotheses but are still in the exploratory phase of our research. In a sense, cluster analysis finds the "most significant solution possible." Therefore, statistical significance testing in the traditional sense of this term is really not appropriate, even in cases when *p*-levels are reported. The general categories of cluster analysis methods are Joining (Tree Clustering), Two-way Joining (Block Clustering) and K-means Clustering. In this work we used the last one [8.1995].

It is useful when we have hypotheses concerning the number *k* of clusters in our cases or variables. If so, we may want to ask to form exactly *k* clusters that are to be as distinct as possible. In general, the *k*-means method will produce exactly *k* different clusters of greatest possible distinction. The program will start with *k* random clusters, and then move objects between those clusters with the goal to minimize variability within clusters and maximize variability between clusters. This is analogous to ANOVA in reverse, in the sense that the significance test in ANOVA evaluates the variability between groups against the within-group variability when computing the significance test for the hypothesis that the means in the groups are different from each other. In *k*-means clustering, the program tries to move objects (e.g., cases) in and out of groups (clusters) to get the most significant ANOVA results.

Usually, in the result of a *k*-means clustering analysis, we would examine the means for each cluster on each dimension to

assess how distinct our *k* clusters are. Ideally, we would obtain very different means for most, if not all dimensions, used in the analysis. The magnitude of the *F* values from the analysis of variance performed on each dimension is another indication of how well the respective dimension discriminates between clusters. The output of *k*-means clustering is usually expressed as a spreadsheet with the Euclidean distances (below the diagonal) and squared Euclidean distances (above the diagonal) between cluster centres. Specifically, this matrix shows the Euclidean distances between clusters, computed from the respective cluster means on the dimensions used for the classification.

4. RESULTS

4.1 Variability among polysulphone calibration curves

The variability among the calibration curves obtained during 14 field experiments (E01…E14) carried out in different environmental conditions (urban, rural and semi-rural sites) was first analysed. Field campaigns were performed during 2004 and 2005 at three Italian sites between 41.9°N and 43.3°N, for solar zenith angle ranging from about 20° to 70°. The observed variability among the calibration curves was interpreted taking into account the site of the field experiment and important factors modulating the UV spectrum at the earth's surface.

The purpose was to combine the information deriving from the empirical relation between the erythemal effective UV dose and the PS absorbance change with its mathematical explanation.

A parameterization of the calibration curves, represented by a coefficient multiplying a cubic polynomial function, was also proposed. It was shown that the multiplying coefficient depends on the spectral shape of the UV radiation, which is mainly affected by the total ozone amount and the solar zenith angle, while the cubic polynomial function is assumed to be dependent on the PS photodegradation mechanisms only. This polynomial function, first proposed by Diffey on an empirical basis, is here explained in Appendix II, based on the theoretical expression of the PS response found by Krins et al [21.1998].

4.1.1. Calibration curves of polysulphone films

A large variability was observed between the PS calibration curves (Figure 4.1). The same variability can be observed also by comparing the Diffey curve to those of other studies (Figure 4.2), such as a curve obtained in Antarctica in 2002 during the summer season (ISS) and those obtained by Kimlin in the USA (K1, K2, K3 curves) and in Australia (K4, K5 curves). The variability observed amounts to much more than 10%, which is the relative error associated with doses estimated by equation (1.3), and it is clearly related to different ambient conditions [1.2001]. It is

noteworthy that such a large variability cannot be attributed only to different thickness (all dosimeters are 40 μm thick) and batch.

Figure 4.1 Calibration curves presented for experiments E01…E14 and the Diffey cubic polynomial (the highest curve). Data points from calibrations are also reported (black dots) [9.2006].

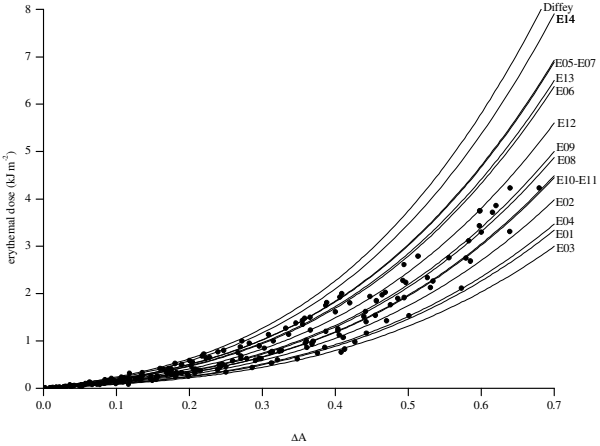

Figure 4.2 Comparison among different calibration curves: Diffey [7.1989], ISS [7. 2003], K1, K2, K3, K4, K5 (Kimlin, personal communication (2005)).

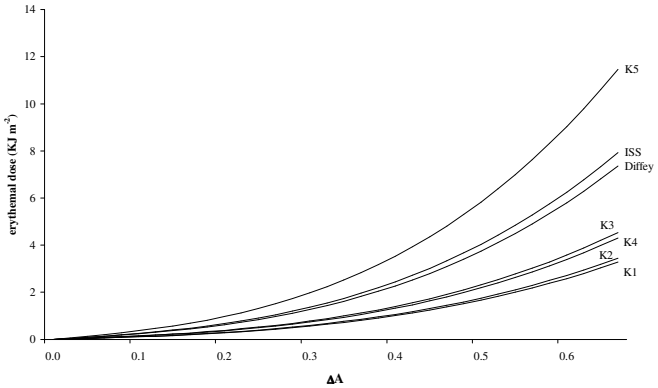

In order to study this large variability among PS calibration curves in the local environmental conditions of middle-latitude sites, 14 field campaigns were carried out: six at an urban site (Rome, city centre); five at a semi-rural site (Monteporzio Catone); three at a rural site (S Felice, Tuscany). All sites are located between 41.9 and 43.3°N. Six campaigns were held during summer 2004 and 2005, two in winter 2004 and 2005, four in spring 2005 and two in autumn 2005. All field campaigns were conducted under almost completely clear sky conditions and for a SZA in the range from 20° to 70°. The polysulphone film was mounted on a plastic holder with a central hole of about 1 cm^2 and three batches were used. Calibration curves were obtained using a number of dosimeters ranging from 10 to 20, located on a horizontal flat plane and exposed for different appropriate time intervals. Absorbance, before and after exposure to solar UV radiation, was measured in the laboratory either by a standard UV spectrophotometer (Perkin Elmer Lambda 5 UV-Vis double beam Spectrometer) or by a miniaturized and portable spectroradiometric system (Ocean Optics-Avantes AVS-SD 2000). In the latter case, a sample holder micrometry movement system moves the PS badge with high precision during irradiation by a xenon pulsed lamp and the absorbance was measured at the 330 nm emission peak of the source. More details on the spectroradiometer system can be found in Sisto et al [8.2001]. The two reading methods were carefully compared using different film batches and no discrepancy was found in the change of optical absorbance at 330 nm.

4.1.2. Measurements of ambient UV doses

The use of dosimeters requires a calibration using well-calibrated solar UV instruments such as spectroradiometers or broad-band radiometers. In this study ambient UV doses were measured by broad-band radiometers (model UVB-1, Yankee Environmental System, MA, USA) and by X2000-4 electronic dosimeters (Gigahertz-Optik, Pucheim, Germany). The YES radiometer has a spectral response similar to that of skin erythema

and it measures the erythemal dose rate between 280 and 400 nm. The waveband is selected by means of the detector and of coloured glass filters. A phosphor filter converts incoming UVB radiation to green light, which is then measured by a solid-state photo-detector. The YES radiometer is equipped with an internal temperature control system for the phosphor and related optical components. The system heats these components at a fixed temperature of 45°C in the ambient temperature range between −40°C and +40°C. YES measurement is sampled at 1 min averages.

Two YES radiometers were used in this study. One belongs to the Solar Radiometry Observatory, University of Rome 'Sapienza' (41.9°N, 12.5°E, 75 m asl). This radiometer (named here as the URO radiometer) is installed on the roof of a building on the University Campus (in the centre of Rome) and it has been working reliably since 2000. The Solar Radiometry Observatory is one of the stations that regularly measures UV irradiance in Italy, and it also has a Brewer spectrophotometer (operational since 1992) for measurements of UV spectral irradiance. Ambient UV doses agree with those measured by the Brewer spectrophotometer at Rome 'Sapienza', under clear sky conditions, with ±10% uncertainty. The URO radiometer was calibrated at the European Reference Centre for Ultraviolet Radiation Measurements (Joint Research Centre, Ispra, Italy) in 2004.

The other YES radiometer (named here as the ISPESL radiometer) belongs to the ISPESL (Istituto Superiore per la Prevenzione E la Sicurezza sul Lavoro), Monteporzio Catone (41.8°N, 12.7°E, 300 m asl). This semi-rural site is about 30 km southeast of Rome. The performance of the ISPESL radiometer was tested during several field experiments using the URO radiometer as the reference instrument. The mean percentage difference between the two instruments during all field experiments was less than 5% showing their good agreement.

A complementary method for measuring ambient UV doses using X2000-4 electronic dosimeters was also used in this study.

The X2000-4 electronic dosimeters are small and easy to use. They are powered by batteries during exposure and can be set up in not easily accessible areas. The electronic dosimeter is equipped with two photovoltaic cells, one reproducing the erythemal action spectrum, the other having a response which is approximately constant in the UVA range (the UVB contribution is negligible). The instrument response is cosine corrected.

The acquisition sampling rate can be set using the dedicated software and, in this study, a frequency of 1 Hz was adopted. The absolute calibration of the electronic dosimeters was certified by Gigahertz-Optik in 2005.

4.1.3 Calibration curves from different instruments

A comparison between the calibration curves obtained with broad-band radiometers and electronic dosimeters was carried out on 28 July 2005 in Rome under clear sky conditions. Ambient doses were calculated beginning with dose rates as 1 min averages of the irradiance values. Electronic dosimeters were exposed on a flat horizontal plane near the radiometer so that all instruments had the same field of view of 2π. Twenty PS dosimeters were used for differing time intervals starting at 7.00 UT.

Calibration curves obtained from the two different instruments are plotted in Figure 4.3, showing a good agreement: the percentage difference (X2000 – YES)/YES is –9%. This result supports the use of electronic dosimeters to obtain calibration curves during field campaigns of personal solar exposure in sites where it is not possible to install radiometers. In this case it is however recommended to assess the agreement between the calibration curves of a well-calibrated standard UV instrument and electronic dosimeters.

The PS calibration curve for each of the 14 field campaigns was obtained by measuring ambient UV doses by means of YES radiometers or electronic dosimeters. Collected data for each campaign were best fitted using a cubic polynomial function with the same form of equation (1.3) but different values of the c coefficient. The dates and sites of the field experiments are listed

in chronological order in Table 4.1, while the calibration curves are plotted in Figure 4.1 together with the Diffey curve. Values of c from the best fit procedure and its goodness (R) are also reported in Table 4.1 From Figure 4.1 it can be seen that the calibration curves show a large variability, which is reflected in the values of the coefficient c, varying within a factor of more than 2. This effect cannot be due to differences among the PS dosimeters. Urban calibration curves have the smallest c values (average 0.94 ± 0.02 kJ m^{-2}), which increase in the semi-rural and rural sites (average 1.41 ± 0.04 kJ m^{-2} and 1.44 ± 0.03 kJ m^{-2}, respectively). Moreover, Table 4.1 shows that there is variability among the calibration curves even within the same month.

Table 4.1 List of 14 calibration curves and the corresponding value of c (with the associated standard error). R is a measure of the goodness of the polynomial fit. Rome, Monteporzio and S. Felice are respectively urban, semi-rural and rural sites [9.2006].

	Date(dd/mm/yyyy)	Site	(c±Δc) kJm^{-2}	R
E01	22/07/2004	Rome	0.78±0.03	0.98
E02	13/12/2004	Rome	0.93±0.01	0.99
E03	04/02/2005	Rome	0.70±0.02	0.99
E04	09/03/2005	Monteporzio	0.81±0.03	0.99
E05	21/03/2005	Monteporzio	1.61±0.05	0.99
E06	06/04/2005	Monteporzio	1.49±0.04	0.99
E07	22/04/2005	S.Felice	1.62±0.03	0.99
E08	21/06/2005	Rome	1.14±0.02	0.99
E09	12/07/2005	S.Felice	1.17±0.03	0.99
E10	20/07/2005	Rome	1.04±0.02	0.99
E11	28/07/2005	Rome	1.05±0.01	0.99
E12	15/09/2005	Monteporzio	1.31±0.03	0.99
E13	12/10/2005	S.Felice	1.52±0.04	0.99
E14	04/11/2005	Monteporzio	1.85±0.04	0.99

Figure 4.3 PS calibration curves on 28 July 2005 obtained using URO YES radiometer data and the average of the two GigaHertz Optic X2000–4 electronic dosimeters. The calibration equations are, respectively, $D = 1.1(\Delta A + \Delta A^2 + 9\Delta A^3)$ for the YES and $D = 1.0(\Delta A + \Delta A^2 + 9\Delta A^3)$ for the electronic devices. Data points from calibration are also reported (black dots) [9.2006].

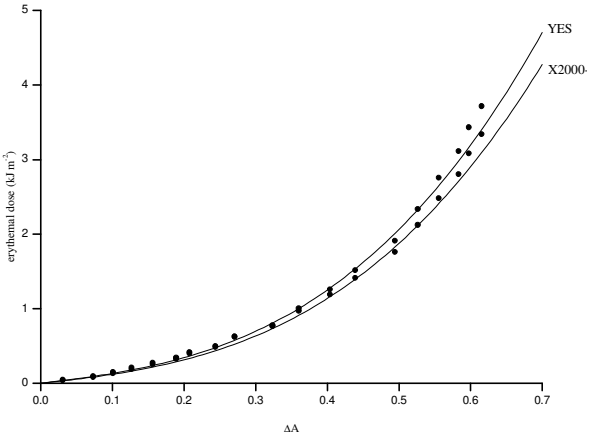

4.1.4 Explanation of the observed variability

A mathematical interpretation of equation (1.3) is given in the Appendix II using a perturbative method, but it should be reminded that a complete justification of the coefficients in brackets is empirical.

Data collected from the field experiments indicate that the variability of the *c* coefficient could be attributed to the different environmental conditions during each field campaign. Keeping in mind that the polysulphone and the erythema have different responses beyond 300 nm (Figure 3.4), special attention was focused on the total ozone amounts and solar zenith angle ranges. In order to investigate their effect on the calibration patterns, the STAR radiative transfer model (Ruggaber 1994) was used under clear sky conditions in an urban, a semi-rural and a rural scenario. The agreement between the UV measurements and the modelled values was already assessed in a field campaign in Rome. Here

the model was used to calculate spectral irradiances from 280 to 400 nm with 0.5 nm wavelength steps, total ozone values O_3 ranging from 200 to 500 DU in steps of 50 DU and SZA ranging from 20 to 70° in steps of 10°. The sites were differentiated taking into account surface albedo, boundary layer height and tropospheric aerosol type, while the same standard values of stratospheric aerosol and vertical profiles of ozone, temperature and humidity, named US profiles were used. Modelled spectral irradiances were then convolved with the CIE erythema action spectrum and the PS action spectrum, and integrated over the entire wavelength range.

According to Krins et al [1.2001], the *g* factor was determined as follows:

$$g = \frac{\int I(\lambda) S_{ery}(\lambda) d\lambda}{\int I(\lambda) S_{PS}(\lambda) d\lambda} \tag{1.4}$$

where $I(\lambda)$ is the solar spectral irradiance at the earth's surface, $S_{ery}(\lambda)$ the CIE erythema action spectrum and $S_{PS}(\lambda)$ the polysulphone action spectrum. In the Appendix II we show that *c* can be expressed by dividing *g* by the constant $\alpha = 7.4 \times 10^{-5}$ m^2 J^{-1}. The behaviour of *g* follows the variability of $I(\lambda)$, which is affected by atmospheric and geometric parameters. The model was used to find out which factors play a major role in the fluctuation of *g*. No significant discrepancies were found in *g* values owing to the characterization of the three sites in terms of typical aerosol loading and surface albedo.

The analysis showed that total ozone and SZA are the main parameters affecting the variability of *g*. Values of *g* as a function of O_3 amounts and SZA, summarized in Table 4.2, show that significant variations of *g* are related to lower O_3 and SZA values, while at higher O_3 and SZA levels no changes occur. This indicates that *g* variability is mainly modulated by changes of solar UVB irradiance where the erythemal action spectrum is

more effective. This is in agreement with the results shown by Krins et al. [1.2001].

Table 4.2 Values of *g* as a function of total ozone (first column on the left, values in DU) and SZA (upper row, in degrees) [9.2006].

O3/SZA	**20**	**30**	**40**	**50**	**60**	**70**
500	0.07	0.06	0.06	0.06	0.06	0.06
450	0.07	0.07	0.06	0.06	0.06	0.06
400	0.07	0.07	0.07	0.06	0.06	0.06
350	0.08	0.08	0.07	0.07	0.06	0.06
300	0.09	0.08	0.08	0.07	0.06	0.06
250	0.10	0.09	0.09	0.08	0.07	0.06
200	0.12	0.11	0.10	0.09	0.08	0.07

The values in Table 4.2 allow us to estimate c (see Table 4.3).

Table 4.3 Modelled values of *c* as a function of total O_3 (first column on the left, values in DU) and SZA (upper row, in degrees) [9.2006].

O3/SZA	**20**	**30**	**40**	**50**	**60**	**70**
500	0.90	0.87	0.83	0.79	0.76	0.76
450	0.95	0.91	0.87	0.82	0.77	0.75
400	1.01	0.97	0.91	0.85	0.79	0.75
350	1.09	1.04	0.97	0.90	0.82	0.78
300	1.20	1.14	1.06	0.97	0.87	0.77
250	1.35	1.28	1.18	1.07	0.95	0.83
200	1.56	1.48	1.36	1.22	1.06	0.91

In order to interpret the results, it is useful to distinguish two regions in Table 4.3:

• the first region (dark grey) highlights that for $O_3 \leq 300$ DU and SZA$\leq 40°$ the *c* values show a great variability (from 1.06 to 1.56 kJ m^{-2});

• the second (light grey) refers to $O_3 \geq 400$ DU and SZA$\geq 50°$, where the *c* values are on average stable around 0.8 kJ m^{-2}.

A comparison between modelled (Table 4.3) and measured (Table 4.1) c values was performed taking into account four groups of total O_3 amounts (from 250 to 400 DU at 50 DU steps). Calibration curves, representative of each group, were then determined using the mean modelled and measured value of c in equation (1.3). The results for two different total ozone amounts (250 and 400 DU), representative of middle-latitude sites, are plotted in Figure 4.4. The error bar assigned to each data point in Figure 4.4 is 10% for the measured c and 20% for the modelled c. A comparison indicates that the calibration curves are consistent for O_3=400 DU (measured c=1.22, modelled c=0.96) where the percentage difference, (measured − modelled)/measured, is 21%. In the case of O_3=250 DU (measured c=1.45, modelled c=0.95) the percentage difference is 34%.

Figure 4.4 Measured (black) and modelled (grey) calibration curves for two different groups (left: O_3 = 250 DU, SZA > 50°; right: O_3 = 400 DU, SZA < 50°). The error bars are drawn as described in the text [9.2006].

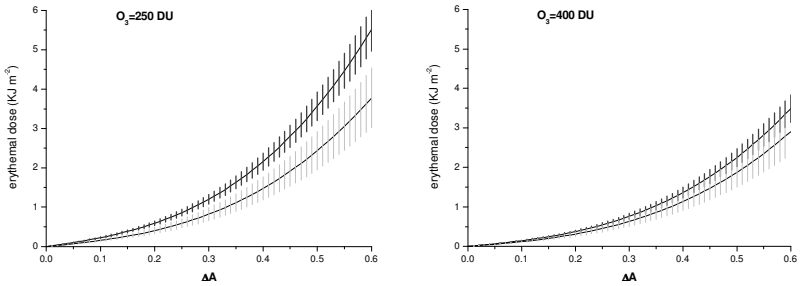

The calibration curve is best fitted by a cubic expression with a multiplying coefficient c which is a function of g (see equation (1.3)). A mathematical interpretation is presented in the Appendix II, showing that the curve was obtained expanding the polysulphone response function to the limit of small doses and inverting the relation between the absorbance variation and the absorbed dose. It can be assessed that the multiplying coefficient

is affected by the solar UV spectrum at the earth's surface whilst the expression in brackets depends on the photoinduced reaction of polysulphone film dosimeters.

The mismatch between the polysulphone spectral curve and the CIE erythemal action spectrum is responsible for the variability among polysulphone calibration curves. Since the erythemally weighed irradiance is much more sensitive to the UVB radiation than the irradiance weighted by the polysulphone response function, *c* follows total ozone fluctuations and solar zenith angle changes. Similar results were shown by Krins et al. [1.2001]

The solar zenith angle is involved in the radiation absorption law:

$$I(SZA) = I(0)e^{-\frac{\alpha}{\cos(SZA)}} \tag{2.4}$$

where *I(SZA)* is the direct beam radiation at a fixed wavelength reaching the earth's surface at SZA, *I(0)* is the irradiance at the top of the atmosphere and α is the atmospheric extinction coefficient.

For small angles, the following equation is obtained:

$$I(SZA) = I(0)\left[1-\alpha(1-\frac{1}{2}SZA^2+..)\right] \tag{3.4}$$

Equation (3.4) yields that, for sufficiently small values of SZA, the dependence on the solar zenith angle is a second-order polynomial law. For increasing values of total ozone amount, the SZA dependence becomes negligible.

A best fitting procedure to describe the measured g values as functions of O_3 and SZA was performed by using the following relationship:

$$g(O3, SZA) = g(200,20) - a \cdot O3 + b \cdot SZA - \overset{\prime}{b} \cdot (SZA)^2 \tag{4.4}$$

where *g(200,20)* is the *g* value at O_3=200 DU and SZA=20°.

If *g(200,20)*=0.12, the best fit (R^2=0.93) to the measured values of g, according to equation (4.4), gives

$$a = 1.30 \cdot 10^{-4} DU^{-1}$$
$$b = 7.76 \cdot 10^{-4} (\text{degree})^{-1}$$
$$\hat{b} = 1.78 \cdot 10^{-5} (\text{degree})^{-2}$$

4.2 In vivo experiments

The experiments carried out during the study are now described. For each of them, a table giving information on place, date, duration, number of volunteers and body-site of the PS dosimeter is presented. Results of Exposure Ratio, colorimetry parameters and skin-temperatures are then given, through the correlation matrices, the PCA and the Cluster Analysis.

Participation was on a voluntary basis with the approval of the host institutions. In case of school children, parents issued a written consent.

4.2.1 Schoolchildren

The schoolchildren study arose from the possibility to carry out an experiment of solar UV dosimetry on an easily controllable population and from the need to acquire data for embryo database on the of solar UVR dose in particular among children and adolescents [6.2006; 11.2006]. The objective of this study was to test if during the average time spent outdoors, children were exposed to a minimal UV dose for the production of vitamin D or on the contrary such UV exposure was excessive. In both cases an assessment of physical outdoor environment can be useful for local authorities for seeking of adequate outdoor environments mainly for children and to recommend behavior modifications. The school, located in a high density built area of Rome with a tree surrounded public park, was selected on the basis that the children could also stay outdoors during the lessons. Moreover, since the experiment was carried out in a period of high solar irradiance, it turns out that results can be considered as upper limit

values for the UV exposure of elementary school students in an urban site at mid latitudes. Many other studies dealt with the same problem in the case of primary and elementary school children [4.2000; 5.2000; 5.2001; 6.2001; 7.2001; 3.2003; 11.2003; 4.2004; 10.2005].

Table 4.4 gives a descriptive summary of the experiment. The children were aged 6-7 years. Schoolchildren were followed by the staff responsible for the experiment during their exposure in the sun. Measurements were performed for 3 work days: 9 and 25 May 2005 and 7 June 2006. Exposures occurred during recreation time, from 10.00 to 12.00 local time or from 13.30 to 14.30 local time. Calibration curves were obtained for 9 and 25 May under similar meteorological conditions, giving an average value of c=(1.17±0.03), for the 7 June c=(0.80±0.03).

Table 4.4 Schoolchildren: descriptive table

Site	Date	Time	Volunteers	PS position
Rome	09/05/2005	Recreation time	17	1 on the chest
Scuola Elementare	25/05/2005	13.30-14.30 LT	17	
"Ada Negri"	07/06/2006	10.00-12.00 LT	13	

Colorimetric and skin temperature measures to all participating children were taken before and after exposure. Each child was equipped with a PS dosimeter placed on its chest. The comparison among doses absorbed in each of the three days showed that these values were consistent (as average and standard deviations), independently from the day of the experiment. For this reason it was possible to group the days of exposure as if it were a unique experiment with 47 volunteers. The average Exposure Ratio was found to be 0.07, with a standard deviation of 0.03. The median was 0.07 with the upper quartile 0.08 and the lower quartile 0.06. Minimum and maximum values were 0.01 and 0.15 respectively.

Some of the values of Exposure Ratios were particularly low. They were related to absorbance changes ΔA_{330}<0.030. The results showed that children were not extremely exposed to the sun

during recreation time outdoors. Regarding the sufficient vitamin D dose, the calibration curve, analogous to the erythema calibration curve, was determined. Such a curve can be derived from the erythema calibration curve taking into account the definition of *g* in equation (2) (section 4.1.4), modified by the vitamin D action spectrum, which lies in between the eryhtema and the PS action spectra (Figure 3.4):

$$g_{vitD} = \frac{\int I(\lambda)S_{vitD}(\lambda)d\lambda}{\int I(\lambda)S_{PS}(\lambda)d\lambda} = \frac{\int I(\lambda)S_{vitD}(\lambda)d\lambda}{\int I(\lambda)S_{ery}(\lambda)d\lambda} \cdot \frac{\int I(\lambda)S_{ery}(\lambda)d\lambda}{\int I(\lambda)S_{PS}(\lambda)d\lambda} = g\frac{\int I(\lambda)S_{vitD}(\lambda)d\lambda}{\int I(\lambda)S_{ery}(\lambda)d\lambda} \quad (6)$$

Keeping in mind that α (section 4.1.4) is a constant, it is possible to find a relationship between the erythemal *c* and the vitamin D coefficient (c_{vitD}):

$$c_{vitD} = c\frac{\int I(\lambda)S_{vitD}(\lambda)d\lambda}{\int I(\lambda)S_{ery}(\lambda)d\lambda} \quad (7)$$

Spectral irradiances were measured by Brewer spectrophotometer located in the campus of the University of Rome "Sapienza". An example of such a procedure is shown in Figure 4.5, where the calibration curves for the erythema and the vitamin D are plotted for 7 June 2006. The conversion factor (the ratio between integrals in equation (7)) is, in this case, equal to 3.4. In the same figure, the line corresponding to 1 MED and 1 SED (section 1.4) and the value of 0.25 MED, a possible estimate for a sufficient production of vitamin D with a 6-10% of the body exposed, are also plotted (section 1.5).

Colorimetric and skin temperature data were analyzed using a correlation matrix (Table 4.5), the PCA and, then processed by means of a cluster analysis (Figure 4.6).

A discussion is provided in paragraph 5.1.

Figure 4.5 Schoolchildren: vitamin D (red) and erythemal (blue) calibration curves (Rome, 07 June 2006)

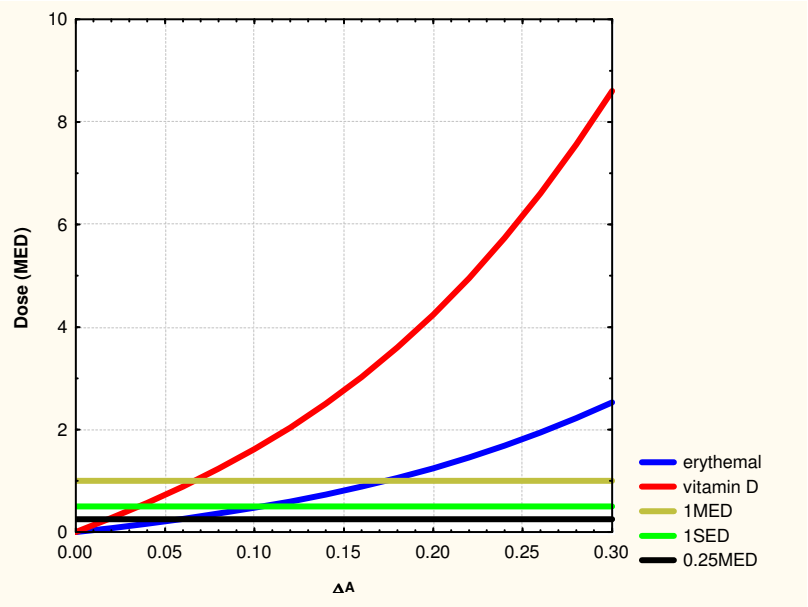

Table 4.5 Schoolchildren: correlation matrix

	L	a	b	T	ER_{chest}	F1 (55%)	F2 (23%)	F3 (12%)	F4 (9%)
L	1.00	**-0.55**	0.24	-0.21	0.09	**-0.65**	**0.66**	-0.21	0.30
a	**-0.55**	1.00	-0.39	0.46	-0.30	**0.82**	-0.29	-0.27	0.41
b	0.24	-0.39	1.00	**-0.53**	0.11	**-0.73**	-0.45	**-0.50**	-0.12
T	-0.21	0.46	**-0.53**	1.00	-0.30	**0.75**	0.45	-0.37	-0.31
ER_{chest}	0.09	-0.30	0.11	-0.30	1.00	-0.28	-0.04	0.24	-0.05
F1 (55%)	**-0.65**	**0.82**	**-0.73**	**0.75**	-0.28	1.00	-0.00	-0.00	0.00
F2 (23%)	**0.66**	-0.29	-0.45	0.45	-0.04	-0.00	1.00	-0.00	-0.00
F3 (12%)	-0.21	-0.27	**-0.50**	-0.37	0.24	-0.00	-0.00	1.00	0.00
F4 (9%)	0.30	0.41	-0.12	-0.31	-0.05	0.00	-0.00	0.00	1.00

Figure 4.6 Schoolchildren: cluster analysis
(R_chest indicates the ER of the chest)

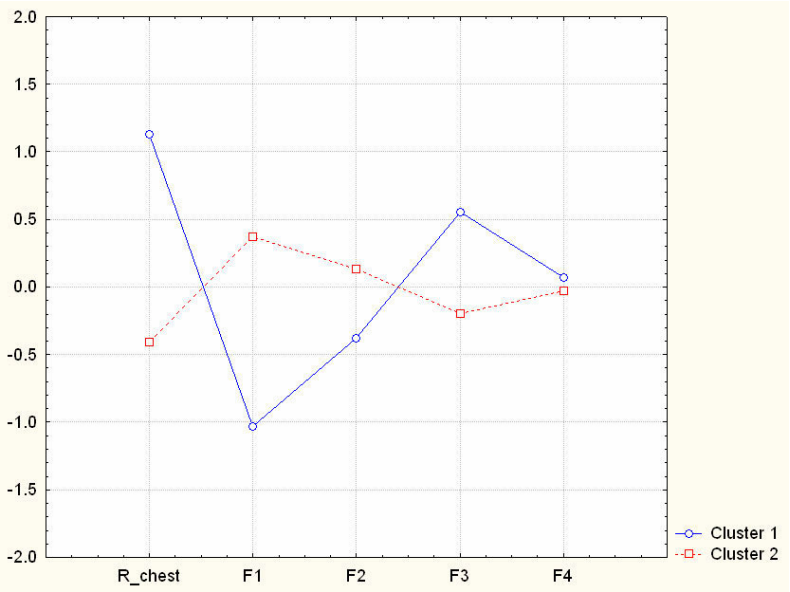

4.2.2 Sun bathers

The purpose of this study was to investigate the UV exposure of three groups of Italian beachgoers (group 1: 17 individuals already sun-tanned; group 2: 11 individuals with no previous exposure, i.e. non sun-tanned; group 3: 9 individuals with an abnormally high sensitivity to the first exposure, i.e. photosensitive).

Individuals belonging to the latter group experienced signs of violent cutaneous manifestations (photodermatoses) after the first solar exposure. Such signs are visible either as localized or extended reddening, or as bubbles and/or vesicles [12.2003]. Photodermatoses represent a rather wide cutaneous pathology whose origin is not very clear, with a high incidence mainly on the breast area in women.

In this field experiment, carried out on 27 May 2005 at a

Mediterranean sea side resort (about 30 km west from Rome), the volunteers wore PS dosimeters on their chest and measurements of skin colorimetry and skin temperature pre-post exposure as useful markers of personal response to UV doses were taken. Some of the volunteers also used the electronic dosimeter (Figure 3.1).

In addition 16 (5 of which photosensitive) out of the 37 volunteers accepted blood tests to measure the quantity of free radicals in their plasma (section 3.4.4), the day before and two days after the exposure.

Table 4.6 summarizes the information on the experiment. Volunteers were followed by the staff responsible for the experiment during their exposure time (11.20 - 13.30 local time). Shadowed places (beach umbrella and indoor rooms) were also available. They were asked to avoid sunscreen protection during the experiment and to fill in a questionnaire (see Appendix III) which reported both the time intervals spent in the shade and their exposure posture. The calibration curve was obtained from ambient UV doses measured by a broad-band radiometer (model UVB-1, Yankee Environmental System, MA, USA). The curve was characterized by a value of c equal to 0.63±0.01.

The mean (and the median) value of the Exposure Ratio was equal to 0.19, with a standard deviation of 0.07 and a range of values between 0.09 and 0.42. The upper quartile was 0.22 and the lower quartile was 0.14.

Table 4.6 Sun bathers: descriptive table

Site	Date	Time	Volunteers	PS position
Fregene (RM) Stabilimento "Lido"	27/05/2005	11.20-13.30 LT	37	1 on the chest

Eight out of the 9 photosensitive individuals showed first symptoms of photodermatoses, diagnosed by a dermatologist of Phototherapy Laboratory of S. Gallicano Institute in Rome,

approximately after 1 hour of exposure and their dosimeters were withdrawn. A ninth volunteer, belonging to group 1, showed signs of photodermatoses.

Colorimetric and skin temperature data were analyzed using a correlation matrix (Table 4.7), the PCA and then processed by means of a cluster analysis (Figure 4.7). A characterization of the three groups was accomplished and presented in Table 4.8.

In order to better understand the role of Exposure Ratio and of the other variables in the appearance of photodermatoses, some results were presented as scatterplot diagram of the principal components F1 vs ER (Figure 4.8) and F3 vs ER (Figure 4.9). A Box-Whiskers diagram was used to understand if the amount of free radicals in the plasma could change before and after exposure (Figure 4.10). A discussion is provided in section 5.1.

Table 4.7 Sun bathers: correlation matrix

	L	a	B	T	ER_{chest}	F1 (60%)	F2 (22%)	F3 (11%)	F4 (7%)
L	1.00	**-0.66**	**0.62**	0.32	-0.22	**0.88**	-0.20	0.04	0.43
a	**-0.66**	1.00	-0.49	-0.16	0.10	**-0.78**	0.46	-0.31	0.29
b	**0.62**	-0.49	1.00	0.43	-0.42	**0.84**	0.12	**-0.50**	-0.16
T	0.32	-0.16	0.43	1.00	-0.11	**0.55**	**0.79**	0.27	-0.03
ER_{chest}	-0.22	0.10	-0.42	-0.11	1.00	-0.29	-0.06	0.34	0.03
F1 (60%)	**0.88**	**-0.78**	**0.84**	**0.55**	-0.29	1.00	-0.00	0.00	0.00
F2 (22%)	-0.20	0.46	0.12	**0.79**	-0.06	-0.00	1.00	-0.00	0.00
F3 (11%)	0.04	-0.31	**-0.50**	0.27	0.34	0.00	-0.00	1.00	0.00
F4 (7%)	0.43	0.29	-0.16	-0.03	0.03	0.00	0.00	0.00	1.00

Figure 4.7 Sun bathers: cluster analysis (R_chest indicates the ER of the chest)

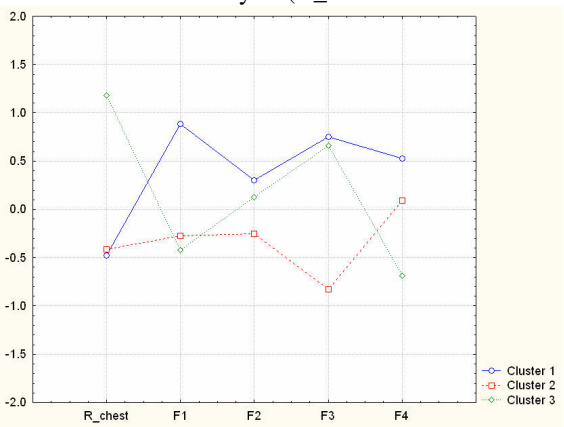

Table 4.8 Sun bathers: characterization of the three groups of volunteers. The number of *Subjects* is followed by the sum of males (*M*) and females (*F*); in the column *Age* the minimum and the maximum values for the group are reported; *Time*, *Dose*, *ER* are mean values of the group; *Phototype* lists the phototypes in the group; the *Shadow* and the *Posture* (*st*=standing; *ly*=lying; *si*=sitting; *be*=bent) mean values are reported as percentage; *FR* is the mean percentage free radical change pre-post exposure; *L*, *a*, *b* and *T* are the mean absolute changes pre-post exposure.

Group	Subjects (M+F)	Age	Time (min)	Dose (J m^{-2})	ER	Phototype	Shadow (%)	Posture (%)				FR (%)	L	a	b	T (°C)
								st	ly	si	be					
1	17 (9+8)	21-47	115	235	0.19	2-3-4	12	50	36	14	0	-1	-3.2	-0.7	-4.6	-1
2	11 (6+5)	20-54	113	236	0.19	2-3	9	44	35	19	3	+6	-4.7	+0.7	-6.8	-3
3	9 (3+6)	20-52	99	217	0.21	2-3	8	36	49	15	0	0	-4.3	+0.5	-6.8	-1

Figure 4.8 Sun bathers: Exposure Ratio on the chest (R_chest), F1, photodermatoses (marked by arrows)

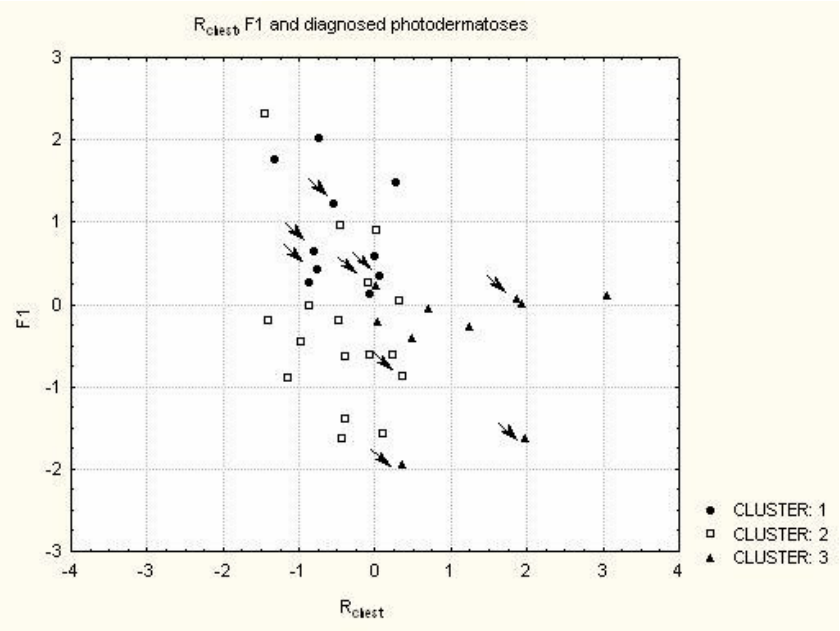

Figure 4.9 Sun bathers: Exposure Ratio on the chest (Rchest), F3, photodermatoses (marked by arrows)

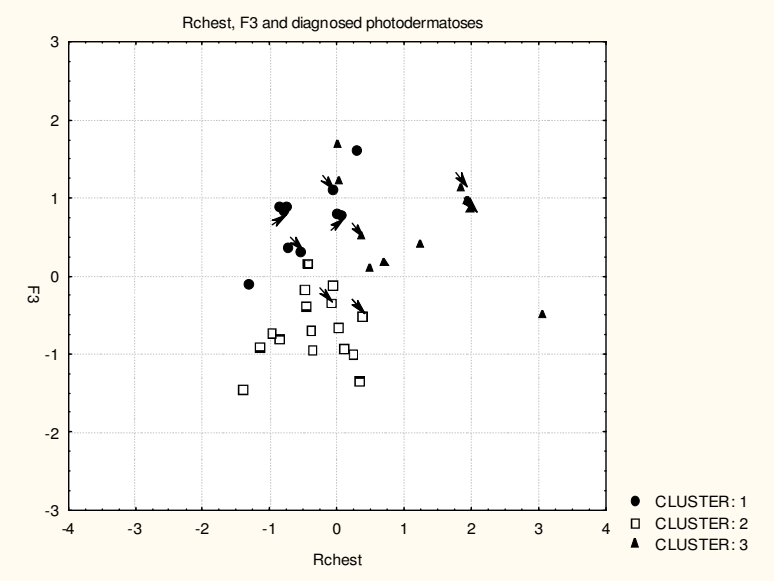

Figure 4.10 Sun bathers: Free radicals in the plasma pre and post exposure (16 out of 37 volunteers)

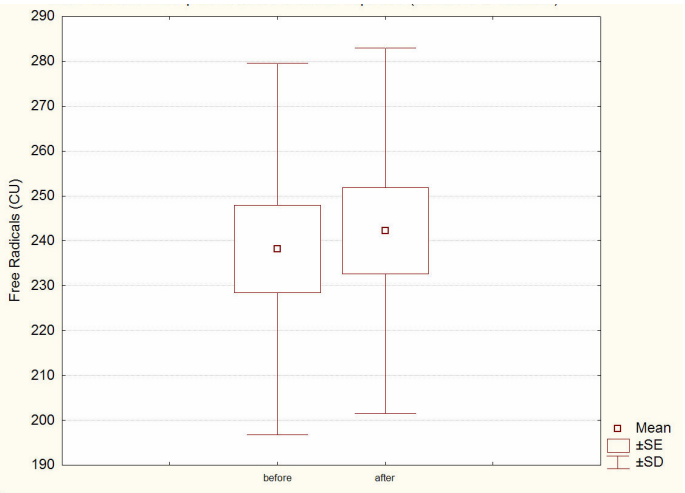

4.2.3 Vineyard growers

In the study on the vineyard growers of an agricultural company in Tuscany the problem of long term exposure to the solar radiation has been studied [8.2003; 6.2005]. The volunteers have been followed during three seasons (spring, summer and autumn) when their activity at the open air is higher. Due to the changing job duties in each season, the typical posture changes, too.

Three experiments have been therefore carried out: from 20 to 22 april 2005 (spring); from 12 to 13 July 2005 (summer); from 11 to 12 October 2005 (autumn). Every experiment has consisted of a continuous exposure for the entire day of job (from 8.00 to 17.00 local time), involving a total of 96 volunteers. They were asked to wear a PS dosimeter on the upper part of the back, under the nape, and on the upper part of the left arm. All of them have undergone to measures of colorimetry and skin temperature before and after the exposure. Moreover, 10 of them have accepted a withdrawal of blood before the exposure in spring and at the end of the exposure in summer for measuring the amount of free radicals in the plasma. Table 4.9 collects the descriptive information of the experiment.

Table 4.9 Vineyard growers: descriptive table

Site	Date	Time	Volunteers	PS position
Castelnuovo B.ga (SI) Agricola S.Felice	20-22/04/2005 12-13/07/2005 11-12/10/2005	8.00-17.00 LT	23 39 34	1 on the back 1 on the left arm

With their help, information on the use of protections (hats and dresses; nobody made use of solar cream), on the time intervals spent in the shade (during the lunch break) and on the assumed posture. For each experiment, a calibration curve has been determined in situ (Table 4.1).

Exposure Ratio shows an average value of 0.71 (median 0.69) for the dosimeter located on the back, with a standard deviation of

0.26 and an excursion between minimum and maximum of 0.18 and 1.30. For the dosimeter on the arm, instead, the average value of ER goes down to 0.46 (median 0.42), with standard deviation 0.20 and excursion minimum-maximum between 0.12 and 0.92. Colorimetric (*L*, *a*, *b*) and skin temperature (*T*) data have been elaborated as shown in the correlation matrix (Table 4.10), in which the Exposure Ratio between dose on the arm and dose on the back ($ER_{arm/back}$) also appears. It, differently from ER_{chest} and ER_{back}, is maintained approximately constant from one season to the other. Figure 4.11 shows the outcome of the cluster analysis.

Table 4.10 Vineyard growers: correlation matrix

	L	**a**	**b**	**T**	**ER_{back}**	**ER_{arm}**	**$ER_{arm/back}$**	**F1 (58%)**	**F2 (21%)**	**F3 (12%)**	**F4 (9%)**
L	1.00	**-0.62**	**0.54**	-0.25	-0.17	-0.03	0.21	**-0.83**	-0.20	0.40	-0.34
a	**-0.62**	1.00	**-0.58**	0.32	0.16	0.04	-0.18	**0.86**	0.09	-0.13	-0.48
b	**0.54**	**-0.58**	1.00	-0.23	-0.12	-0.03	0.10	**-0.80**	-0.23	**-0.53**	-0.13
T	-0.25	0.32	-0.23	1.00	0.00	-0.01	-0.02	**0.50**	**-0.86**	0.04	0.06
ER_{back}	-0.17	0.16	-0.12	0.00	1.00	**0.79**	-0.13	0.16	0.09	-0.06	-0.01
ER_{arm}	-0.03	0.04	-0.03	-0.01	**0.79**	1.00	0.46	0.03	0.03	-0.00	-0.01
$ER_{arm/back}$	0.21	-0.18	0.10	-0.02	-0.13	0.46	1.00	-0.18	-0.08	0.12	0.01
F1 (58%)	**-0.83**	**0.86**	**-0.80**	**0.50**	0.16	0.03	-0.18	1.00	0.00	0.00	-0.00
F2 (21%)	-0.20	0.09	-0.23	**-0.86**	0.09	0.03	-0.08	0.00	1.00	-0.00	-0.00
F3 (12%)	0.40	-0.13	**-0.53**	0.04	-0.06	-0.00	0.12	0.00	-0.00	1.00	-0.00
F4 (9%)	-0.34	-0.48	-0.13	0.06	-0.01	-0.01	0.01	-0.00	-0.00	-0.00	1.00

At last, the temporal behavior between spring and summer of the amount of free radicals in the plasma is plotted in a Box-Whiskers diagram in Fig. 4.12. A discussion of the results is provided in section 5.1.

Figure 4.11 Vineyard growers: cluster analysis
(R_back, R_arm, R_arm/back indicate respectively the ER of the back, of the arm and the ratio between the two)

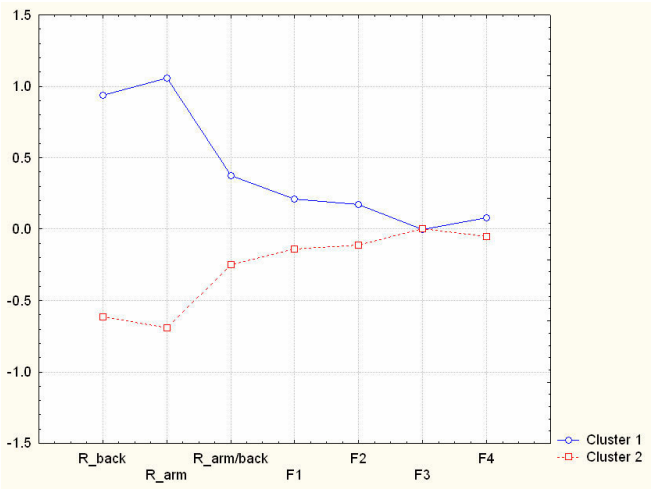

Figure 4.12 Sun bathers: Free radicals in the plasma in spring and summer
(10 volunteers)

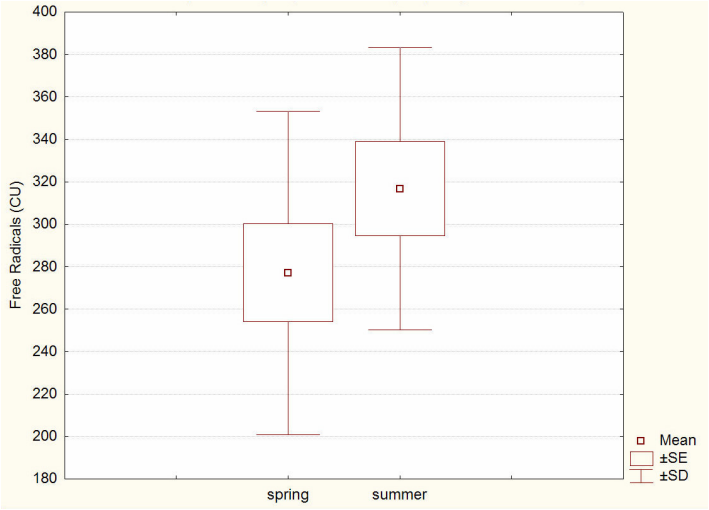

4.2.4 Skiers

The experiment with the skiing teachers and the skiers has been carried out at La Thuile (Aosta), between the locality Les Suches (2176 m), where most of the volunteers had been exposed while skiing, and Les Granges (1644 m), where a small group of people had instead skied. Eighty-three volunteers took part in the experiment and a PS dosimeter was applied to their hats corresponding to their foreheads, so as to nearly simulate exposition of a vertically oriented body portion. Indeed, consequences of the elevated exposure to solar UV radiation in high mountain turn out to be serious on the upper part of the ears, the nose and the lower lip [9.2005].

The experiment was performed from 31 March to the 4 April 2006, during the open timetable of the ski tracks (from 8.00 to 16.00 LT), under conditions of mostly good weather. Each experiment consisted of 3 successive exposures covering the entire day of exposure. Because of the elevated radiation, in fact, PS dosimeters needed to be changed almost every two hours in order to avoid saturation. All the volunteers were subject to colorimetric and skin temperature measurements before and after the exposure. Table 4.11 is a synthesis of the descriptive information of the experiment. With the help of volunteers, information on the use of protections (creams, hats, sunglasses and clothes), on the eventual time intervals spent in the shade (during the lunch break) and on the typical posture (depending also on the type of ski discipline) were collected (Appendix IV).

Table 4.11 Skiers: descriptive table

Site	Date	Time	Volunteers	PS position
La Thuile (AO)	31/03-04/04/2006	8.00-16.00 LT	83	1 on the forehead

Because of the different skiing altitudes and the need to test the reliability of Table 4.3 for an elevated albedo due to the fresh snow (not included in the simulations of the model described in

section 4.1.4), three simultaneous calibration curves were determined on 31 March 2006 (first day of the experiment) at Saint Cristophe (569 m of quota, semi-rural site), Les Granges and Les Suches. Results are shown in Figure 4.13. The *c* values, starting from the highest locality, are respectively: 1.69±0.02, 1.47±0.01 and 1.24±0.01. Measured values of *c* are higher than those obtained from Table 4.3 when 330 DU of total ozone and SZA values between 41° and 58° are considered. In particular, the percentage differences between measured and theoretical values, i.e. (measured-modeled) /measured, are: 25% for Saint Cristophe, 35% for Les Granges and 44% for Les Suches. A confirmation of the validity of the model with albedo values comparable to those of non snowy sites was obtained by the calibration curves, in the same localities, at the end of autumn 2006, in absence of snow.

Table 4.12 Skiers: correlation matrix

	L	**a**	**b**	**T**	**ER1**	**ER2**	**ER3**	**F1 (47%)**	**F2 (26%)**	**F3 (17%)**	**F4 (10%)**
L	1.00	**-0.44**	**0.41**	0.19	0.02	-0.07	0.00	**-0.80**	**0.67**	0.27	**0.54**
a	**-0.44**	1.00	-0.22	0.29	-0.24	0.08	-0.08	**0.75**	0.14	**-0.54**	**0.34**
b	**0.41**	-0.22	1.00	-0.10	-0.19	-0.06	0.17	**-0.69**	**0.38**	**-0.63**	-0.19
T	0.19	0.29	-0.10	1.00	0.06	-0.22	**-0.42**	0.20	**0.78**	0.14	0.14
ER1	0.02	-0.24	-0.19	0.06	1.00	**0.51**	0.17	-0.03	-0.06	**0.34**	-0.10
ER2	-0.07	0.08	-0.06	-0.22	**0.51**	1.00	**0.36**	0.06	-0.17	-0.05	0.10
ER3	0.00	-0.08	0.17	**-0.42**	0.17	**0.36**	1.00	-0.16	-0.24	-0.18	0.00
F1 (47%)	**-0.80**	**0.75**	**-0.69**	0.20	-0.03	0.06	-0.16	1.00	-0.31	-0.09	-0.02
F2 (26%)	**0.67**	0.14	**0.38**	**0.78**	-0.06	-0.17	-0.24	-0.31	1.00	-0.08	**0.42**
F3 (17%)	0.27	**-0.54**	**-0.63**	0.14	**0.34**	-0.05	-0.18	-0.09	-0.08	1.00	0.13
F4 (10%)	**0.54**	**0.34**	-0.19	0.14	-0.10	0.10	0.00	-0.02	**0.42**	0.13	1.00

Exposure Ratios show an average value of 1.01 (median 1.03) as obtained from the entire dataset, with a standard deviation of 0.31 and an excursion between minimum and maximum of 0.32 and 1.75. Colorimetric data (*L*, *a*, *b*) and skin temperature values (*T*) have been processed to find correlations as shown in Table 4.12. The table also presents the values of ER relating to the 3 sequences of exposure (ER1, ER2 and ER3). In such a way, it is possible to investigate also on the possible correlations between

the Exposure Ratios obtained at different times of the day. Figure 4.14 shows the results of cluster analysis. As for the other experiments, a discussion of the results is provided in section 5.1.

Figure 4.13 Skiers: simultaneous calibration curves for three different locations of same latitude and longitude but different altitude (Les Suches 2176 m, Les Granges 1644 m, Saint Cristophe 569 m). Data refer to 31 March 2006. Calibration equations are respectively: $D=1.7(\Delta A + \Delta A^2 + 9\Delta A^3)$; $D=1.5(\Delta A + \Delta A^2 + 9\Delta A^3)$; $D=1.2(\Delta A + \Delta A^2 + 9\Delta A^3)$.

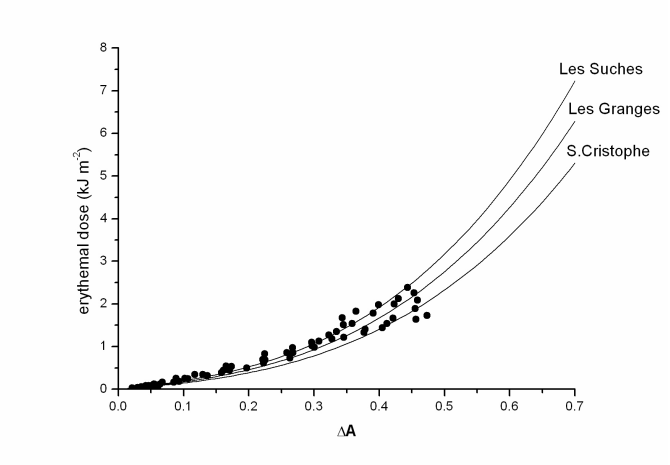

Figure 4.14 Skiers: cluster analsyis (R1, R2 and R3 indicate respectively the ER of the forehead in three successive time intervals during the exposure)

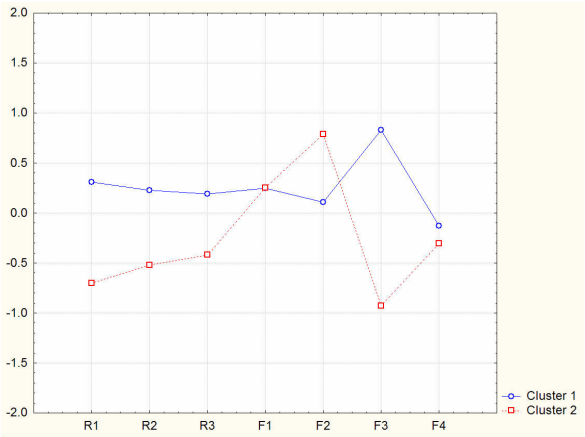

4.2.5 Hikers

In order to confirm the Exposure Ratio of the skiers experiment, the measure of personal doses was repeated on voluntary hikers in a mountain site without snow (Adamello, peak at 3539 m) on 23 July 2006. Using a theoretical curve of calibration, with daily ozone equal to 313 DU and an interval of SZA between 26° and 73°, a value of *c* equal to 0.96±0.02 was determined for such experiment.

The experiment was carried out from 7.30 to 13.30 local time (Table 4.13), under good weather conditions in the first part of the day and gradually worsening in the second part. The experiment included 3 successive exposures in order to cover the entire interval of time. Fifteen volunteers wore a PS dosimeter on their chest and the remaining 12 on their hat, in correspondence of the forehead. In such a way it was possible to carry out comparisons with the skiers experiment. The volunteers themselves compiled a questionnaire (Appendix IV) on the use of protections (creams, hats, sunglasses and clothes), on the eventual periods spent in the shade and on the most frequent posture. In this experiment, however, it was not possible to execute measures of colorimetry and skin temperature.

ER shows an average value of 0.27 (median 0.24) for the PS dosimeter placed on the forehead, with a standard deviation of 0.19, a minimum of 0.05 and a maximum of 0.66. For the dosimeter located on the chest, the average value of the Exposure Ratio diminishes to 0.11 (median 0.07), with a standard deviation of 0.08 and an excursion minimum-maximum between 0.04 and 0.27.

Table 4.13 Hikers: descriptive table

Site	Date	Time	Volunteers	PS position
Adamello (TN)	23/07/2006	7.30-13.30 LT	27	1 on the chest or forehead

4.2.6 Summary of the experiments with volunteers

Table 4.14 is a summary of the Exposure Ratios for the 5 experiments. The number in brackets beside each group of volunteers is the number of cases used for the analysis. The uncertainty on the value of ER is between 15% and 20%, depending upon the UV resource used for the calibration (a spectrophotometer or a broad-band radiometer, respectively). Since the dosimeters have been placed on different parts of the body during the various experiments, it is not possible to operate comparisons among them in all cases. The table, anyway, suggests some of such comparisons for dosimeters placed on the chest (schoolchildren, sun bathers, hikers) and on the forehead (skiers, hikers) while the case of the vineyard growers is apart. In most cases, the distribution of the Exposure Ratio is not normal and for this reason, besides the average and standard deviation, the median, the upper and the lower quartile are reported.

Synthesizing and comparing the (*L*, *a*, *b*, *T*) series of data in a unique table was avoided. Indeed, such parameters turn out to be mainly influenced from the phototype of the chosen group of individuals, the duration of exposure and the protection used by the volunteers.

Table 4.14 Exposure Ratio: results from 5 experiments. The number in brackets beside each group of volunteers is the number of cases included in the analysis. The uncertainty on the value of ER is between 15% and 20%, depending upon the UV resource used for the calibration

ER_{Chest}	**Mean**	**stdv**	**MAX**	**min**	**median**	**up.quart.**	**low.quart.**
Schoolchildren (47)	**0.07**	0.03	0.15	0.01	**0.07**	0.08	0.06
Sun bathers (37)	**0.19**	0.07	0.42	0.09	**0.19**	0.22	0.14
Hikers (15)	**0.11**	0.08	0.27	0.04	**0.07**	0.26	0.05
$ER_{Forehead}$	**Mean**	**Stdv**	**MAX**	**min**	**median**	**up.quart.**	**low.quart.**
Skiers (83)	**1.01**	0.31	1.75	0.32	**1.03**	1.72	0.75
Hikers (12)	**0.27**	0.19	0.66	0.05	**0.24**	0.35	0.13
ER_{Back}	**Mean**	**stdv**	**MAX**	**min**	**median**	**up.quart.**	**low.quart.**
Vineyard growers (96)	**0.71**	0.26	1.30	0.18	**0.69**	0.92	0.52
$ER_{Arm/Amb}$	**Mean**	**stdv**	**MAX**	**min**	**median**	**up.quart.**	**low.quart.**
Vineyard growers (96)	**0.46**	0.20	0.92	0.12	**0.42**	0.61	0.29

4.3 A model to estimate short and long-term doses

The experiments exposed in section 4.2 took place in some days of typical exposure, assuming that results could represent with good approximation a group of people in their working or recreational activity. In the case of schoolchildren (section 4.2.1) the repeatability of the ER measures in two consecutive years was verified while for the vineyard growers (section 4.2.3) an attempt to monitor their exposure habits during three different seasons was performed.

Exposure Ratios of Table 4.14 can be therefore used, with the due limitations, to determine short and long term doses of the categories under study or, by extension, of those groups that is thought to show similar behavior [4.2003]. It is obvious that the more uncertain the exposure behavior is, the less reliable the estimation obtained on the basis of a not representative ER will be. It is therefore preferable to carry out a type study for each particular group taken in consideration [27.1999]. It is also important to notice that the availability of a mean (or median) value, of a maximum and a minimum (or an upper and lower quartile) constitutes a reference for the estimate of the dose in the average and in the worse condition, respectively. A simple empirical model to estimate the personal dose that uses, among other things, the values of ER, is expressed by equation (7.4):

$$Dose = \sum_{time} \sum_{bodysite} \frac{ER \cdot AE \cdot AI}{PF} \qquad (7.4)$$

where:

- *ER* comes from the experiments, as above described;
- *AE* indicates the ambient erythemal dose as measured from a UV radiometer on a horizontal surface;
- *AI* is the activity index, meant as the fraction of time when the subject is exposed;
- *PF* is the protection factor, represented by a sunscreen, a hat or other. Its determination requires particular attention, being equal to 1 when protection is missing, greater than 1 otherwise.

The ratio determined by *ER*, *AE*, *AI* and *PF* must be summed on the number of portions of the body (*bodysite*) and on the time intervals (*time*) in which we want to obtain the estimated dose.

An example, shown in Figure 4.15, can help to understand. Let us consider one of the sun bather volunteers (section 4.2.2), who exposed from 11.20 to 13.34 local time (i.e. from 9.20 to 11.34 UT). From the absorbance change of his PS dosimeter, placed on his chest, an *ER* value of 0.21 can be determined. Moreover, it can be extracted from the questionnaire that the volunteer did not protect himself during exposure (*PF*=1). The blue curve of Figure 4.15 represents the ambient erythemal irradiance (*AE*) while the area under such a curve is the dose absorbed from a 1 square meter horizontal surface exposed from dawn to sunset. The volunteer, instead, has only exposed himself for a fraction of time (*AI*) and the resulting curve is shown as the red one, so that the underlying area reduces a lot. However, such an area still does not correspond to the dose absorbed from the chest of the volunteer, since it must be modulated by the Exposure Ratio. The result is the green curve, reducing again the value of the absorbed dose. The final result is equal to 313 J m^{-2} for the modeled absorbed dose, very close to the measured value of 308 J m^{-2}.

The dose estimation turns out to be particularly good in this case, because the ER obtained from the volunteer himself has been used. If an estimate of representative doses for an entire population is needed, we should make use of the average (or median) value and of the upper and lower references, with a resulting uncertainty range in the final result. Calculations for the experiment of sun bathers when all data are used are reported in Table 4.15. From the error propagation of equation (7.4), we have estimated an uncertainty on the dose between 20% and 30%, depending on the uncertainty of UV radiometers (spectrophotometers or broad-band radiometers, respectively). Equation (7.4) can be of interest in epidemiological studies, when correlations between long time cumulative doses (for the duration of the entire life, for example) and the incidence of some

pathologies are analyzed [9.2001; 12.2006]. This aspect, however, goes beyond the scopes of this study.

Figure 4.15 Example of model application

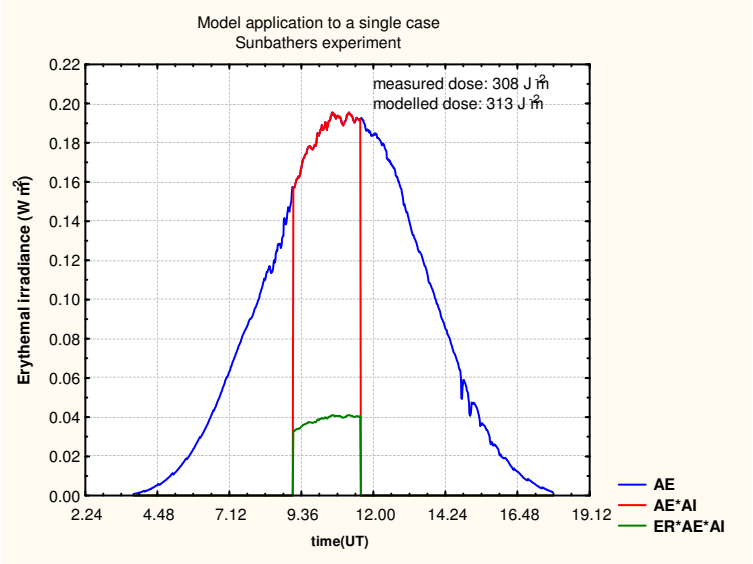

Table 4.15 Results of model calculations for the doses of sun bathers. ER is chosen both as a different value for each volunteer (*Single*) and as the same value for all cases (*Mean*, *Minimum*, *Maximum*). The second column shows the results of the mean percentage difference, while the third one reports the correlation coefficient (*R*) between modelled and measured values.

ER	**% diff modelled-measured**	**R modelled vs measured**
Single	+1.9	0.999
Mean	-11.8	0.460
Minimum	-58.2	0.460
Maximum	+95.0	0.460

DISCUSSION AND CONCLUSIONS

5.1 Discussions of results

The calibration curves of PS dosimeters depend on the total ozone amount and the SZA. Such dependency is, in first approximation, linear in the ozone and quadratic in the SZA (equation (4.4)). It was assessed that it is necessary to determine a calibration curve for each personal exposure experiment. The curve can be considered valid until the environmental conditions remain approximately constant in the measurement site. Doses obtained from the calibration curves have an uncertainty determined by the coefficient *c*, i.e. around ± 10%. If a field calibration is not feasible, a theoretical estimate (Table 4.3) is possible when the daily ozone amount and the SZA interval are known. In this case, the estimated dose uncertainty increases to 20%. Moreover, it is important to notice that Table 4.3 was obtained with the assumption of surface albedo under snow free conditions. The discrepancy with calibration curves derived in sites with higher albedo was verified in the skiers experiment (section 4.2.4).

Table 4.14 allows the comparison of Exposure Ratios obtained from dosimeters placed on the same body-part. Exposure Ratios on the chest are the lowest, mainly because the dosimeter is in a nearly vertical position. The values vary from the mean of 0.07 for the schoolchildren to 0.19 for the sun bathers, with an intermediate of 0.11 for the hikers. The same relationship stands for the maximum values (0.15 for the schoolchildren, 0.27 for the hikers, 0.42 for the sun bathers) while the minimum values of sun bathers and hikers are almost equal (0.08 and 0.07, respectively). A possible interpretation of such differences can be found both in the greater mobility of children during their play activities in the open space and the shady environments of the school garden. The Exposure Ratio for schoolchildren is confirmed by several papers. Regarding hikers, the low value of ER can be due to the relative position of their chest towards the sun. In fact, during the trekking the chest is shaded more than in the case of sun bathers, who

normally modify their own posture following the sun. It should be remembered that the ER does not represent the amount of the effective absorbed dose by an individual. Instead, the personal dose is determined multiplying the Exposure Ratio by the ambient UV dose (i.e UV doses received by a horizontal surface) which depends on the place and the period of the year.

The comparison between the ER values on the forehead of skiers and hikers clearly shows the combined effect of snow albedo and posture on the face exposure: a mean value of 1.01 (practically the entire available dose on a horizontal surface) for the skiers and the value of 0.27 for the hikers. For some skiers, such an elevated average ER was significantly high as indicated by the maximum 1.75 and the upper quartile 1.72. In the skiers experiment, 3 dosimeters for each volunteer were used from 8.00 to 16.00 local time and changed about every two hours. It is worth noting in Table 4.12 that the corresponding ratios ER1, ER2 and ER3 turn out to be weakly correlated (ER1 with ER2 and ER2 with ER3), probably due to the different snow reflections on the skiing tracks in the morning and afternoon.

The vineyard growers experiment is not comparable to the others, due to the different position of the dosimeters. Only the ER on the arm can be considered an indicator of vertical exposure (mean 0.46). The high ER on the back (0.71 for the mean and 1.30 as the maximum value) was mostly due to the fact that many of the job duties carried out by the workers required a folded back posture, forcing the nape to being almost horizontal. From Table 4.10 it can also be observed that the ER on the back and that on the arm have a correlation coefficient of 0.79 (significance level $p<0.05$). The ratio between the two Exposure Ratios, moreover, slightly changed in the course of the experiments: 0.58 in spring, 0.61 in summer, 0.72 in autumn.

The calibration curve for the production of vitamin D, obtained starting from the erythemal calibration (Figure 4.5), could be a further tool to find the optimal sun exposure level. In our case, we meant to put into evidence how the presence of a garden in a school could be helpful to improve the quality of life of the

children and the school staff, for example by optimizing the recreation timetable.

The statistical analysis in the (*L*, *a*, *b*, *T*) space turned out of not easy interpretation in many cases. The Sign Test allowed to verify, for all the involved subjects, a significant difference between the values of *L* and *a* in the exposed body-part with respect to the not-exposed (equations (2.3) and (3.3)) while such difference is not always statistically significant for *b* and *T* (equations (4.3) and (5.3)). This justifies the correctness of the choice of the non exposed part from the point of view of melanin and, presumably, blood circulation. Exposure, on the other hand, did not always cause modification of one or more of the (*L*, *a*, *b*, *T*) parameters. This could take place either when the absorbed dose was small (due to short exposure time or low irradiance) or when the skin was already photoprotected. Moreover, the correlation matrices confirm the well known relationships between *L*, *a* and *b*: negative correlation for *L* vs. *a* and positive for *L* vs. *b*.

In the schoolchildren study, the grouping in two clusters (Figure 4.6) separated the cases of above and below mean ER on the chest. If we take into account the first principal component F1 and its correlations (Table 4.5), we see that to the first cluster belong the cases in which *L* and *b* show a slight decrease while *a* and *T* have a weak increase. Such result is somewhat unexpected and probably due to the reduced change of biological indicators determined by the measurement site characteristics and the short time of exposure.

The study on sun bathers shows characteristics nearly complementary to the previous one. If, in fact, we take cluster 3 into consideration, it comprises the cases with high ER on the chest and low values of the first principal component F1. Looking at Table 4.7, it can be noted that low F1 values were associated to slightly increasing values of *L* and *b* and weakly decreasing values of *a* and *T*. Table 4.8 shows a characterization of the three groups of volunteers: individuals already sun-tanned (group 1); individuals with no previous exposure, i.e. non sun-tanned (group

2); individuals with an abnormally high sensitivity to the first exposure, i.e. photosensitive (group 3). ER values of the three groups are comparable within the error uncertainty, while colorimetric and skin temperature parameters changes of photosensitive individuals are the same of non sun-tanned ones. Further considerations could be made looking at Figures 4.8, 4.9 and 4.10. From the first, it can be observed that the diagnosed photodermatoses (marked with an arrow) mainly corresponded to mean or below mean ER. The second figure, instead, adds to the same information the important consideration that diagnosed photodermatoses had above mean values of the third principal component F3, corresponding to negative values of *b* (and, consequently, of *L*). It seems that the rise of photodermatoses was not principally due to high absorbed doses but to the genetic characteristics of the individuals. From Figure 4.10, finally, it can be observed that no changes of free radicals in the plasma were present, before and after exposure, probably due to the short exposure time.

In the vineyard growers experiment, the grouping in 2 clusters (Figure 4.11) is mainly determined by the ER (on the arm and the back) while the principal components seem to play a minor role. If we consider F1 in cluster 1 and look at Table 4.10, we find a weak decrease of *L* and *b* and an increase of *a* and *T* (i.e. a browning, probably due to the production of melanin, and a consequent reddening, coupled with a temperature increase due to the prolonged exposure under normal conditions). Figure 4.12, at last, shows that the change in the amount of free radicals in the plasma was not statistically significant even on a long time scale, although a tendency to increase could be thought of.

The grouping in 2 clusters in the skiers experiment (Figure 4.14) is clearly determined by the ER (ER1, ER2 and ER3) and the principal components F2 and F3. In cluster 1, with the highest Exposure Ratios, the cases with F2 near to the average and F3 above it fall. Table 4.12 indicates that F3 is negatively correlated to *a* and *b*, therefore it can be thought that high ratios corresponded to a decrease in reddening and yellowness, probably

due to the low external temperatures. As already evidenced, the hikers experiment confirmed the hypothesis by which the increase of personal exposure due to elevation is widely exceeded from the snow albedo reflection.

5.2 Conclusions

The study proposed a methodology for the characterization of personal exposure to solar ultraviolet radiation (UVR). Such methodology (section 2.2), validated through *in vivo* experiments, is mainly based on the determination of the doses absorbed from different body-sites, expressed by their ratio with the ambient available dose on a horizontal surface. The resulting Exposure Ratio ER (section 3.4.1) is one of the commonly used parameters for personal UV dosimetry studies. The doses absorbed from portions of the body of the exposed subjects were determined through the technique of the polysulphone (PS) dosimetry (section 3.3). The proposed methodology made use also of colorimetric parameters (section 3.4.2), skin temperature (section 3.4.3) and of the additional information that could be collected during experiments with human subjects (section 3.4.4). All data were analysed by means of multivariate statistics (PCA and Cluster Analysis).

In the first part of the experimental activity, the study contributed to the interpretation of the PS dosimeters calibration curves finding that they, in the event of applications under not controlled conditions, must be executed contextually to the measures on the exposed subjects. The calibration curves, in fact, show a variability due to the geometry of the radiation (through the solar zenith angle, SZA) and to the atmospheric transparency in the UV range (mainly due to ozone, O_3). The proposed explanation (section 4.1) was presented in a scientific publication printed on *Physics in Medicines in Biology* in the month of August 2006.

As far as Exposure Ratio is concerned, its uncertainty is between 15% and 20% (depending on the instrument used for the calibration of the PS dosimeters), resulting from 5 experiments

(section 4.2) carried out on different Italian sites (urban, coastal, rural and mountain) in different seasons of the year. The main scope of the accomplished studies was to supply information on the exposure habits on groups of the Italian population under working (like the vineyard growers or skiing teachers) or recreational activities (like the schoolchildren during the hour of recreation at school, the sun bathers, the skiers and the hikers).

The results can be summarised as follows:

- Schoolchildren (section 4.2.1): an average (and median) value of 0.07 for the ER on the chest was found, ranging from a minimum of 0.01 to a maximum of 0.15. Since such value turned out to be the lowest among all the experiments and the study was carried out when the irradiance was higher during the school-year (May-June) in one of the few Rome schools having a garden for the recreation, we asked whether the absorbed dose allowed a sufficient production of vitamin D. Although this last question is object of recent research, it was found that some children of the sample showed inadequate modalities of exposure. A survey among the children and their parents indicated that such insufficiency could be recovered during the summer months, when the hours of sunlight exposure increase. However, the problem regarding whether the well-being of the individuals is due to the yearly production of vitamin D or on short intervals of time remains unsolved. It should be noted that some of the subjects of this study were not Caucasian.

- Sun bathers (section 4.2.2): the ER on the chest supplied an average and a median value of 0.19, with a high variability due to the variability of postures (minimum of 0.09 for the subjects mostly in motion and maximum of 0.42 for those lying down). The study, proposed to supply indications on the relationship between the absorbed doses and the development of photodermatoses, evidenced that these last ones were not necessarily linked to the high values of ER but they depended mainly on the genetic characteristics of the individuals, which probably reacted to the exposure with a slow production of melanin. It was also found that the measure of the free radicals in

the plasma did not show meaningful variations on the temporal scale of 3 days.

- Vineyard growers (section 4.2.3): this experiment, carried out in three different seasons (spring, summer and autumn) in order to characterize the personal exposure during the entire solar year, supplied an average value of 0.71 (median 0.69) for the nape and of 0.46 (median 0.42) for the arm, with an elevated variability due to the different atmospheric conditions and the change of jobs between one season and another. The interpretation in terms of skin temperature and colorimetric parameters was not easy while a tendency to the increase of free radicals in the plasma between spring and summer existed (even though not statistically meaningful). Some of the workers in this experiment were not Italian.

- Skiers (section 4.2.4): the study clearly showed how the contour conditions can determine ER values greater than 1, i.e. personal doses higher than the ambient horizontally available. In fact, in this case an average value of 1.01 (median 1.03) was obtained for the ER on the forehead, with a variability between 0.32 and 1.75, determined from the snow albedo that can nearly double the amount of intercepted irradiance. The absolute value of the doses was however high, as shown from the calibration curves, too. No difference, instead, was found between the skiing teachers and the skiers. The multivariate analysis, although also in this case of difficult interpretation, showed that the parameters mainly involved in the characterization of the groups were a, b and T.

- Hikers (section 4.2.5): planned in order to confirm the evidence coming from the study with the skiers, this last experiment supplied for the ER on the forehead an average value of 0.27 and a median one of 0.24 (range of variability between 0.05 and 0.66) and for the ER on the chest an average value of 0.11 and a median one of 0.07 (range of variability between 0.04 and 0.27).Carried out on mountains without snow, the study confirmed the determining role of the snow albedo in the experiment with the skiers.

The proposed empirical model (section 4.3) was tested for the sun bather volunteers, showing that the agreement between modelled and measured values gradually decreases passing from a single ER value for each volunteer to an average one (respectively from +1.9% to -11.8%). Due to the fact that in most cases a mean ER value is available, it can be concluded that a model underestimates short and long term doses by at least 10% the measured ones, with an uncertainty ranging from 15% to 20%.

In conclusion, this investigation has reached the scopes that were prefixed for the acquaintance of the ER for groups of the Italian population. A link with biological indicators, on the other hand, has shown to be more difficult to find, although the proposed original methodology has been well established and future studies could eventually confirm its validity.

Appendix I: Radiometric quantities and units

Quantities of UV radiation are expressed using radiometric terminology (see Table AI.I). Terms relating to a beam of radiation passing through space are the "radiant energy" and "radiant flux". Terms relating to a source of radiation are the "radiation intensity" and the "radiance". The term "irradiance", which is the most commonly used term in photobiology, relates to the object (e.g. human body) struck by the radiation. The radiometric quantities in Table AI.I may also be expressed in terms of wavelength by adding the prefix "spectral". The time integral of the irradiance is strictly termed the "radiant exposure" but is sometimes expressed as "exposure dose" or simply "dose". The term dose in photobiology is analogous to the term "energy fluence" in radiobiology and not to "absorbed dose".

Table AI.I: Radiometric terms and units [1.2002]

Term	Unit	Symbol
Wavelength	nm	λ
Radiant energy	J	Q
Radiant flux	W	ϕ
Radiant intensity	$W \cdot sr^{-1}$	I
Radiance	$W \cdot m^{-2} \cdot sr^{-1}$	L
Irradiance	$W \cdot m^{-2}$	E
Radiant exposure	$J \cdot m^{-2}$	H

Appendix II: Cubic form of the calibration curve

Starting from the best fit of the polysulphone calibration curves to a polynomial function of the type:

$$D = c(\Delta A + a\Delta A^2 + b\Delta A^3) \quad \text{(A.1)}$$

in this work the variability of the polysulphone calibration curves is parameterized by varying the overall coefficient c and leaving the $(\Delta A + a\Delta A^2 + b\Delta A^3)$ term unchanged. This approach was suggested by Diffey [7.1989]. Here we try to give a theoretical interpretation of equation (A.1).

The mismatch between the polysulphone action spectrum $S_{PS}(\lambda)$ and the C.I.E. erythemal action spectrum $S_{ery}(\lambda)$ causes the dependence of the polysulphone absorbance on the UV radiation exposure and is responsible for the variability of the polysulphone calibration curves.

The polysulphone response function at 330 nm for monochromatic radiation of 306 nm and polysulphone film thickness of 26 μm was studied by Krins *et al* [21.1998; 26.1999], and is given by the following expression:

$$\Delta A = -\log[A + B\exp(-\frac{D_{PS}}{D_1}) + C\exp(-\frac{D_{PS}}{D_2})] \quad \text{(A.2)}$$

where: D_{PS} is the dose weighted by the polysulphone action spectrum; D_1 and D_2 are threshold doses; A, B, C are non dimensional coefficients satisfying the condition

$$A + B + C = 1 \quad \text{(A.3)}$$

The polysulphone absorbance variation is strongly dependent on the film thickness, so the coefficients given for 26 μm thickness are not valid in the case of 40 μm thickness dosimeters. Anyway, here we assume that the functional dependence of ΔA on D_{PS} is always given by equation (A.2) and that the polysulphone thickness only affects the values of the coefficients.

In order to determine A, B, C, D_1 and D_2 in the case of 40 μm thickness polysulphone films we use the values of absorbance variations found by Diffey [7.1989] irradiating the dosimeters with two different calibration lamps (helarium and fluorescent lamp), whose absolute power spectra are known. Equation (A.2) can be used if D_{PS} is known. We determine D_{PS} following the definition of *g* given by Krins *et al* [21.1998], where $H(\lambda)$ is the lamp spectral irradiance:

$$g = \frac{\int S_{ery}(\lambda)H(\lambda)d\lambda}{\int S_{PS}(\lambda)H(\lambda)d\lambda} = \frac{D_{ery}}{D_{PS}} \quad \text{(A.4)}$$

By using the calibration lamps power spectra, we calculate the ratio between the C.I.E. dose, D_{ery}, and the PS dose, D_{PS}. The obtained *g* values are *g*=0.20 in the case of helarium lamp and *g*=0.60 for the solar fluorescent lamp. Thus, they can be used to find the D_{PS} values helpful for best fitting to the function given by equation (A.2) leaving the five parameters free.

We find the following best fitted parameter values for the polysulphone response function in the case of 40 μm thickness:

A=-0.017
B=0.142
C=0.875
D_1=2413 Jm^{-2}
D_2=58759 Jm^{-2}

If we study equation (A.2) in the limit:

$$\frac{D_{PS}}{D_1}, \frac{D_{PS}}{D2} << 1 \quad \text{(A.5)}$$

we obtain

$$\Delta A \cong -\log(A + B(1 - \frac{D_{PS}}{D_1} + \frac{1}{2}\frac{D^2_{PS}}{D^2_1} - \frac{1}{3!}\frac{D^3_{PS}}{D^3_1}) + C(1 - \frac{D_{PS}}{D_2} + \frac{1}{2}\frac{D^2_{PS}}{D^2 2} - \frac{1}{3!}\frac{D^3_{PS}}{D^3 2})) = \log\left(1 - (\frac{B}{D_1} + \frac{C}{D_2})D_{PS} + \frac{1}{2}(\frac{B}{D_1^2} + \frac{C}{D_2^2})D^2_{PS} - \frac{1}{3!}(\frac{B}{D_1^3} + \frac{C}{D_2^3})D^3_{PS}\right)$$

(A.6)

Then, defining:

$$\alpha = (\frac{B}{D_1} + \frac{C}{D_2}); \beta = \frac{1}{2}(\frac{B}{D_1^2} + \frac{C}{D_2^2}); \gamma = \frac{1}{3!}(\frac{B}{D_1^3} + \frac{C}{D_2^3}) \qquad \text{(A.7)}$$

and taking into account that $\alpha << 1$, $\beta \sim o(\alpha^2)$, $\gamma \sim o(\alpha^3)$, we find:

$$\Delta A \cong -\log\left(1 - \alpha D_{PS} + \beta D_{PS}^2 - \gamma D_{PS}^3\right) \cong \alpha D_{PS} - \beta D_{PS}^2 + \gamma D_{PS}^3 = \alpha D_{PS}\,(1 - \frac{\beta}{\alpha} D_{PS} + \frac{\gamma}{\alpha} D_{PS}^2) \qquad \text{(A.8)}$$

Inverting this relation the following equation holds:

$$D_{PS} \cong \frac{\Delta A}{\alpha}\left(1 + \frac{\beta}{\alpha} D_{PS} - \frac{\gamma}{\alpha} D_{PS}^2 + \frac{\beta^2}{\alpha^2} D_{PS}^2 + ..\right) \qquad \text{(A.9)}$$

Keeping the terms up to ΔA^3:

$$D_{PS} \cong \frac{\Delta A}{\alpha}\left(1 + \frac{\beta}{\alpha}\frac{\Delta A}{\alpha}(1 + \frac{\beta}{\alpha}\frac{\Delta A}{\alpha}) + (\frac{\beta^2}{\alpha^2} - \frac{\gamma}{\alpha})(\frac{\Delta A}{\alpha})^2 + ..\right) = \frac{\Delta A}{\alpha}\left(1 + \frac{\beta}{\alpha}\frac{\Delta A}{\alpha} + (\frac{2\beta^2}{\alpha^2} - \frac{\gamma}{\alpha})(\frac{\Delta A}{\alpha})^2 + ..\right) \qquad \text{(A.10)}$$

Using the definition given by equation (A.4), the relationship between the radiant exposure weighted by the C.I.E. erythemal spectrum D_{ery} and the polysulphone absorbance variation is obtained, valid in the limit of small doses:

$$D_{ery} = g\,\frac{\Delta A}{\alpha}\left(1 + \frac{\beta}{\alpha}\frac{\Delta A}{\alpha} + \left(\frac{2\beta^2}{\alpha^2} - \frac{\gamma}{\alpha}\right)\left[\frac{\Delta A}{\alpha}\right]^2\right) \qquad \text{(A.11)}$$

The obtained calibration curve is a third order polynomial law, without the constant term, with a multiplying coefficient that is a function of the ratio *g* between the radiant exposure weighted by the C.I.E. erythemal curve and the radiant exposure weighted by the polysulphone spectral efficiency. All the dependence on the spectrum is in the multiplying coefficient whilst the expression in parenthesis in equation (A.11) is independent of the measured spectrum, being an intrinsic characteristic of the photoinduced reaction of polysulphone film dosimeters. The *g* values can be estimated using equation (A.12):

$$g = 1000 \cdot c \cdot \alpha \quad \text{(A.12)}$$

Values found by equation (A.12) seem to agree well with experimental data. The average of the estimated and measured g values obtained in three different field experiments performed in Rome during 2004 and 2005, where spectral UV irradiance data were available, are respectively 0.07 and 0.08.

Appendix III: Questionnaire for sun bathers

QUESTIONNAIRE FOR SUN BATHERS

Fill in please the following questionnaire, that will help us to interpret the results collected with your collaboration. Thank you!

Date: Name:

Sex: M ☐ F ☐

Dosimeter number: ☐

Part A: Fill in the following table, describing your activities every half hour (column "Description of activity"). If your activities in the half hour are more than one, describe each of them. Mark also with a cross the positions of your body that best represent your activity (column "Body posture"). If the same activity lasts more than half hour, write "as above" (column "Description of activity"):

Time	Description of activity	Body posture							
		Supine	Sitting	Bent	On the knees	Standing	Walking	Running	Other
11.00-11.30									
11.30-12.00									
12.00-12.30									
12.30-13.00									
13.00-13.30									
13.30-14.00									

Part B: Fill in with black spots the following table indicating the time intervals you are in the shadow (under a beach umbrella, nearby a building etc…):

11.00	11.15	11.30	11.45	12.00	12.15	12.30	12.45	13.00	13.15	13.30	13.45	14.00

Part C: Answer, please, to the following questions, marking your choice with a cross:

Do you think you have protected yourself during the exposure, today? ☐ Yes ☐ No

Would you say today is a typical day for the season? ☐ Yes ☐ No

Do you usually spend more or less time in the sun compared with what you have reported in Part B? ☐ More ☐ Same ☐ Less

How would you define the weather today? (You can choose more than one answer)

☐ Sunny
☐ Partly cloudy
☐ Very cloudy
☐ Overcast
☐ Rainy
☐ Stormy

Appendix IV: Questionnaire for skiers and hikers

QUESTIONNAIRE FOR SKIERS

Fill in please the following questionnaire, that will help us to interpret the results collected with your collaboration. Thank you!

1) Date: Name:

2) Fill in with the sequence of dosimeters you wear:

3) Fill in with a cross to describe your activity between one dosimeter change and the following:

Time	At sun	Partially at sun	In the shadow	Standing	Skiing	On the skilift

4) Fill in with the time and duration of breaks in closed rooms:

QUESTIONNAIRE FOR HIKERS

Fill in please the following questionnaire, that will help us to interpret the results collected with your collaboration. Thank you!

1) Date: Name:

2) Fill in with the sequence of dosimeters you wear:

3) Fill in with a cross to describe your activity between two dosimeters change:

Time	At sun	Partially at sun	In the shadow	Standing	Walking	Sitting

4) Fill in with the time and duration of breaks in closed rooms:

REFERENCES

(ordered firstly by year and then by the first name of the first author)

1976-1990 (The origins)

1. A. Davis, G.H.W. Deane, B.L. Diffey *Nature, Vol. 261, 169-170,* ***1976*** "Possible dosimeter for ultraviolet radiation"
2. J.F. Leach, A.R. Pingstone, K.A. Hall, F.J. Ensell, J.L. Burton *Aviat Space Environ Med, 47(6), 630-633,* ***1976*** "Interrelation of atmospheric ozone and cholecalciferol (vitamin D_3) production in man"
3. B.L. Diffey and A.Davis *Phys Med Biol, Vol. 23, No.2, 318-323,* ***1978*** "A new dosemeter for the measurement of natural ultraviolet radiation in the study of photodermatoses and drug photosensitivity"
4. B.L. Diffey *Photochem Photobiol, Vol. 46, No.1, 55-70,* ***1987*** "A comparison of dosimeters used for solar ultraviolet radiometry"
5. M.Blumthaler, W. Ambach *Atmos Environ, Vol. 22, N.4, 749-753,* ***1988*** "Human solar ultraviolet radiant exposure in high mountains"
6. T.B. Fitzpatrick *Arch Dermatol, 124, 869-871,* ***1988*** "The validity and practicality of sun-reactive skin types I through VI"
7. B.L.Diffey (editor) *Radiation measurement in photobiology,* ***1989*** Academic Press, London

1991-1999 (First studies)

1. B.L. Diffey *Phys Med Biol, Vol. 36, No.3, 299-328,* ***1991*** "Solar ultraviolet radiation effects on biological systems"
2. B.L. Diffey *Phys Med Biol, Vol. 37, No.12, 2267-2279,* ***1992*** "Stratospheric ozone depletion and the risk of non-melanoma skin cancer in British population"

3. C.Bacci e C.Furetta *La fisica dei medici,* ***1992*** La Nuova Italia Scientifica, Roma
4. C.L. Hanchette and G.G. Schwartz *Cancer, Vol. 70, No.12, 2861-2869,* ***1992*** "Geographic patterns of prostate cancer mortality. Evidence for a protective effect of ultraviolet radiation"
5. International Agency for Research on Cancer *Vol. 55, Lyon France,* ***1992*** "Solar and Ultraviolet Radiation. Monographs on the evaluation of carcinogenic risks to humans"
6. L.E. Quintern, M. Puskeppeleit, P. Rainer, S. Weber, S. el Naggar, U. Eschweiler, G. Horneck *J Photochem Photobiol B: Biol, 22, 59-66,* ***1994*** "Continuous dosimetry of the biologically harmful UV-radiation in Antarctica with the biofilm technique"
7. I.P. Terenetskaya *Biomedical Optics'94, Los Angeles (CA),* ***1994*** "Provitamin D photoisomerization as possible UVB monitor: kinetic study using tunable dye laser"
8. A. Rizzi *Analisi dei dati. Applicazioni dell'informatica alla statistica,* ***1995*** La Nuova Italia Scientifica, Roma
9. A.Webb *J Photochem Photobiol B: Biol, 31, 9-13,* ***1995*** "Measuring UV radiation: a discussion of dosimeter properties, uses and limitations"
10. B.L. Diffey, E.Healy, A.J. Thody, J.L. Rees *The Lancet, Vol. 346, December 23/30, 1713,* ***1995*** "Melanin, melanocytes and melanoma"
11. G. Horneck *J Photochem Photobiol B: Biol, 31, 43-49,* ***1995*** "Quantification of the biological effectiveness of environmental UV radiation"
12. B.L. Diffey, C.J. Gibson, R. Haylock and F.McKinlay *Brit J Dermatol, 134, 1030-1034,* ***1996*** "Outdoor ultraviolet exposure of children and adolescents"
13. H. Slaper, G.J.M. Velders, J.S. Daniel, F.R. de Gruijl, J.C. van der Leun *Nature, Vol. 384, 256-258,* ***1996*** "Estimates of ozone depletion and skin cancer incidence to examine the Vienna Convention achievements"
14. H.M. Gloster and D.G. Brodland *Dermatol Surg, 22, 217-226,* ***1996*** "The epidemiology of skin cancer"

15. P. Knusche and J.Barth *J Photochem Photobiol B: Biol, 36, 77-83, **1996*** "Biologically weighted personal UV dosimetry"
16. A.R. Young *Phys Med Biol, 42, 789-802, **1997*** "Chromophores in human skin"
17. A.V. Parisi and J.C.F.Wong *Phys Med Biol, 42, 2331-2339, **1997*** "The erythemal ultraviolet exposure for humans in greenhouses"
18. A.V. Parisi and J.C.F.Wong *Phys Med Biol, 42, 1263-1275, **1997*** "Erythemal irradiances of filtered ultraviolet radiation"
19. A.V. Parisi, J.C.F. Wong and G.I. Moore *Phys Med Biol, 42, 77-78, **1997*** "Assessment of the exposure to biologically effective UV radiation using a dosimetric technique to evaluate the solar spectrum"
20. M.M. Caldwell and S.D. Flint *Plant Ecol, 128, 67-76, **1997*** "Uses of biological spectra weighting functions and the need of scaling for the ozone reduction problem"
21. A. Krins, B. Dörschel, J. Henniger and P. Knusche *Radiat Prot Dosim, Vol. 78, No.3, 195-204, **1998*** "Mathematical description of the reading of personal UV dosemeters taking polysulphone film as an example"
22. B.L. Diffey *Clin Dermatol, 16, 83-89, **1998*** "Ultraviolet radiation and human health"
23. M.G. Kimlin, J.C.F.Wong, A.V. Parisi *Health Phys, Vol. 74, N.4, 429-434, **1998*** "Simultaneous comparison of the personal UV exposure of two human groups at different altitudes"
24. M.G. Kimlin, A.V. Parisi, J.C.F.Wong *Phys Med Biol. 43, 231-240, **1998*** "The facial distribution of erythemal ultraviolet exposure in south-east Queensland"
25. R.M. Sayre, J.C. Dowdy, J. Shepherd et al. "Vitamin D vs. Erythema: effects of solar angle and artificial sources". In: M.F. Holick, E.G. Jung (editors) *Biological effects of light* Kluwer Academic Publishers, Hingham Mass, 149–152, **1998**
26. A. Krins, B. Dörschel, J. Henniger, P. Knusche and A.Bais *Radiat Prot Dosim, Vol. 83, No.4, 303-307, **1999*** "Readings of polysulphone film after fractionated exposures to UV radiation

and consequences for the calculation of the reading resulting from polychromatic UV radiation"
27. A.V. Parisi, L.R. Meldrum, J.C. Wong, J. Aitken, R.A. Fleming *Phys Med Biol, 44, 2947-2953,* ***1999*** "Lifetime ultraviolet exposure estimates for selected population groups in south-east Queensland"
28. A.V. Parisi, M.G. Kimlin *Phys Med Biol, 44, 2071-2080,* ***1999*** "Comparison of the spectral biologically effective solar ultraviolet radiation in adjacent tree shade and sun"
29. A.V. Parisi, M.G. Kimlin *J Photochem Photobiol B: Biol, 53, 70-74,* ***1999*** "Horizontal and sun-normal spectral biologically effective ultraviolet irradiances"
30. A.V. Parisi, L.R. Meldrum, M.G. Kimlin *Protection Against the Hazards of UVR – Virtual Conference Jan. 18-Feb. 5, Internet Photochemistry&Photobiology www.photobiology.com,* ***1999*** "Polysulphone film thickness and its effects in ultraviolet radiation dosimetry"
31. F.R. de Gruijl *Eur J Cancer, Vol. 35, No. 14, 2003-2009,* ***1999*** "Skin cancer and solar UV radiation"
32. J.C.F. Wong, A.V. Parisi *Protection Against the Hazards of UVR – Virtual Conference Jan. 18-Feb. 5, Internet Photochemistry&Photobiology www.photobiology.com,* ***1999*** "Assessment of ultraviolet radiation exposures in photobiological experiments"
33. M.R. Cesarone, G. Belcaro, M. Carratelli, U. Cornelli, M.T. De Sanctis, L. Incandela, A. Barsotti, R. Terranova, A. Nicolaides *Int Angiol, 18(2), 127-30,* ***1999*** "A simple test to monitor oxidative stress"
34. M.G. Kimlin, A.V. Parisi *Phys Med Biol, 44, 917-926,* ***1999*** "Ultraviolet radiation penetrating vehicle glass: a field based comparative study"
35. O.N. Galkin, I.T. Terenetskaya *J Photochem Photobiol B: Biol, 53, 12-19,* ***1999*** "'Vitamin D' biodosimeter: basic characteristics and potential applications"

2000

1. A. Krins, D. Bolsée, B. Dörschel, D. Gillotay and P. Knusche *Radiat. Prot. Dosim., Vol. 87, No.4, 261-266,* ***2000*** "Angular dependence of the efficiency of the UV sensor polysulphone film"
2. AA.VV. *Atti del Convegno "Rischio Ultravioletto. Esposizione al sole, usi terapeutici e cosmetici, attività industriali" Cavalese (TR) 25-26 marzo 1999,* ***2000*** Giunta della Provincia Autonoma di Trento – Azienda Provinciale per i Servizi Sanitari
3. A.F. Moise *Radiat Prot Dosim, Vol. 91, Nos.1-3, 111-114,* ***2000*** "Ultraviolet exposure, measurement and protection in Townsville, Australia"
4. A.V. Parisi, L.R. Meldrum, J.C.F.Wong, J.Aitken, R.A. Fleming *Photodermatol Photo, 16:19-24,* ***2000*** "Effect of childhood and adolescent ultraviolet exposures on cumulative exposure in South East Queensland schools"
5. A.V. Parisi, M.G. Kimlin *Environmetrics, 11, 563-570,* ***2000*** "Effect of meal break times on solar UV exposure of schoolchildren in a southeast Queensland summer month"
6. A.V. Parisi, M.G. Kimlin, J.C.F. Wong, M. Wilson *J Photochem Photobiol B: Biol. 54, 116-120,* ***2000*** "Diffuse component of solar ultraviolet radiation in tree shade"
7. A.V. Parisi, M.G. Kimlin, J.C.F. Wong, M. Wilson *Phys Med Biol, 45, 349-356,* ***2000*** "Personal exposure distribution of solar erythemal ultraviolet radiation in tree shade over summer"
8. A.V. Parisi, L.R. Meldrum, M.G. Kimlin, J.C. Wong, J. Aitken, J.S. Mainstone *Phys Med Biol, 45, 2253-2262,* ***2000*** "Evaluation of differences in ultraviolet exposure during weekend and weekday activities"
9. E. Thieden, M.S. Ågren, H.C. Wulf *Photodermatol Photo, 16:57-61,* ***2000*** "The wrist is a reliable body site for personal dosimetry of ultraviolet radiation"
10. L. Naldi, A, Di Landro, B. D'Avanzo, F. Parazzini and the GISED *J Am Acad Dermatol Vol. 42, N.3, 446-452,* ***2000*** "Host-

related and environmental risk factors for cutaneous basal cell carcinoma: evidence from an Italian case-control study"
11. M.F. Holick *Radiat Prot Dosim, Vol. 91, Nos.1-3, 65-71, **2000*** "Sunlight and vitamin D: the bone and cancer connections"

2001

1. A. Krins, B. Dörschel, P. Knusche, H.K. Seidlitz and S. Thiel *Radiat Prot Dosim, Vol. 95, No.4, 345-352, **2001*** "Determination of the calibration factor of polysulphone film UV dosemeters for terrestrial solar radiation"
2. A.V. Parisi, M.G. Kimlin, D. Turnbull *J Photochem Photobiol B: Biol, 65, 151-156, **2001*** "Spectral shade ratios on horizontal and sun normal surfaces for single trees and relatively cloud free sky"
3. A.V. Parisi, J.C. Wong, M.G. Kimlin; D. Turnbull; R. Lester *Photodermatol Photo, 17, 55-59, **2001*** "Comparison between seasons of the ultraviolet environment in the shade of trees in Australia"
4. B.K. Armstrong, A. Krickerb . *Photochem Photobiol B: Biol, 63, 8–18, **2001*** "The epidemiology of UV induced skin cancer"
5. D.C. Whiteman, C.A. Whiteman, A.C. Green *Cancer Cause Control, 12, 69-82, **2001*** "Childhood sun exposure as a risk factor for melanoma: a systematic review of epidemiologic studies"
6. D.E. Godar *Photochem Photobiol, 74(6), 787-793, **2001*** "UV doses of American children and adolescents"
7. M. Kimlin and A.V. Parisi *Photodermatol Photo, 17, 130-135, **2001*** "Usage of real-time ultraviolet radiation data to modify the the daily erythemal exposure of primary schoolchildren"
8. R. Sisto, D. Lega, A. Militello *Radiat Prot Dosim, Vol. 97, No.4, 419-422, **2001*** "The calibration of personal dosemeters used for evaluating exposure to solar UV in the workplace"

9. S.R. Feldman, J.R. Dempsey, S. Grummer, J.G. Chen, A.B. Fleischer *J Am Acad Dermatol, Vol. 45, N.5, 718-722, **2001*** "Implications of a utility model for ultraviolet exposure behavior"

2002

1. B.L. Diffey *Photodermatol Photo, 18, 68-74, **2002*** "What is light?"
2. B.L. Diffey *Methods, 28, 4-13, **2002*** "Sources and measurement of ultraviolet radiation"
3. C. De Felice, S. Parrini, A. Barducci, G. Chitano, G. Tonni, G. Latini *Pediat Res, Vol.51, N.1, 100-105, **2002*** "Predictive value of skin color for illness severity in the high-risk newborn"
4. G.I. Harrison and A.R. Young *Methods, 28, 14-19, **2002*** "Ultraviolet radiation-induced erythema in human skin"
5. H. Hönigsmann *Photodermatol Photo, 18,75-81, **2002*** "Erythema and pigmentation"
6. J.C. van der Leun and F.R. de Gruijl *Photochem Photobiol Sci, 1, 324-326, **2002*** "Climate change and skin cancer"
7. J.F. Abarca and C.C. Casiccia *Photodermatol Photo, 18, 294-302, **2002*** "Skin cancer and ultraviolet-B radiation under the Antarctic ozone hole: southern Chile, 1987-2000"
8. M.G. Kimlin, A.V.Parisi, B.D. Carter, D. Turnbull *Int J Biometeorol, 46, 150-156, **2002*** "Comparison of the solar spectral ultraviolet irradiance in motor vehicles with windows in an open and closed position"
9. P. Weihs *Int J Biometeorol, 46, 95-104, **2002*** "Influence of ground reflectivity and topography on erythemal UV radiation on inclined planes"
10. S. Alaluf, D. Atkins, K. Barrett, M. Blount, N. Carter et al. *Pigment Cell Res, 15, 119-126, **2002*** "The impact of epidermal melanin on objective measurements of human skin colour"
11. S.B. Park et al *Photodermatol Photo, 18, 23-28, **2002*** "Time course of ultraviolet-induced skin reactions evaluated by

two different reflectance spectrophotometers: DermaSpectrophotometer and Minolta spectrophotometer CM-2002"
12. WHO (World Health Organization), WMO (World Meteorological Organization), UNEP (United Nations Environment Program), ICNIRP (International Commission on Non-Ionizing Radiation Protection) *Global Solar UV Index. A practical guide*, ***2002***

2003

1. A. Meves, M.H. Repacholi, E.A. Rehfuess *Int J Dermatol, 42, 846-849,* ***2003*** "Global Solar UV Index: a physician's tool for fighting the skin cancer epidemic"
2. A.V. Parisi, J. Sabburg, M.G. Kimlin *Phys Med Biol, 48, 121-129,* ***2003*** "Comparison of biologically damaging spectral solar ultraviolet radiation at a southern hemisphere sub-tropical site"
3. C. Guy, R. Diab, B. Martincigh *Photochem Photobiol, 77(3), 265-270,* ***2003*** "Ultraviolet radiation exposure of children and adolescent in Durban, South Africa"
4. D.E. Godar, F. Urbach, F.P. Gasparro, J.c. van der Leun *Photochem Photobiol, 77(4), 453-457,* ***2003*** "UV doses of young adults"
5. D. Vishvakarman and J.C.F. Wong *Photodermatol Photo, 19, 81-88,* ***2003*** "Description of the use of a risk estimation model to assess the increased risk of non-melanoma skin cancer among outdoor workers in Central Queensland, Australia"
6. F.R. de Gruijl, J. Longstreth, M. Norval, A.P. Cullen, H. Slaper, M.L. Kripke, Y. Takizawa, J.C. van der Leun *Photochem Photobiol Sci, 2(1), 16–28,* ***2003*** "Health effects from stratospheric ozone depletion and interactions with climate change"
7. G.F. Mariutti, E. Bortolin, A. Polichetti, A. Anav, G.R. Casale, M. Di Menno, C. Rafanelli "UV dosimetry in Antarctica

(Baia Terranova) “Analysis of data from polysulphone films and GUV 511 radiometer” *Proceedings of The International Symposium on Optical Science and Technology, Ultraviolet Ground and Space based measurements, models and effects III, Vol. 5156, 254-261,* ***2003***

8. Gruppo di Studio Fotoprotezione e Cancerogenesi Cutanea *La radiazione solare ultravioletta: un rischio per i lavoratori all’apertoo* 45 pagg. ISPESL, ***2003***

9. J.B. Kerr “Understanding the factors that affect surface UV radiation” *Proceedings of The International Symposium on Optical Science and Technology, Ultraviolet Ground and Space based measurements, models and effects III, Vol. 5156, 1-14,* ***2003***

10. J.M. Sabburg, A.V. Parisi, M.G. Kimlin *Atmos Res, 66, 261-272,* ***2003*** “Enhanced spectral UV irradiance: a 1 year preliminary study”

11. J.P. Castanedo-Cázares, V. Lepe, A. Gordillo-Moscoso, B. Moncada *Salud Pública de México Vol.45, NO.6, 439-444,* ***2003*** “Dosis de radiación ultravioleta en escolares mexicanos”

12. M.A. Ramirez, M.M. Warthan, T. Uchida, R.F. Wagner *South Med J, Vol.96, N.7, 652–655,* ***2003*** “Double exposure. Natural and artificial ultraviolet radiation exposure in beachgoers”

13. M.M. Caldwell, C.L. Ballare, J.F. Bornman, S.D. Flint, L.O. Bjoern, A.H. Teramura, G. Kulandaivelu, M. Tevini *Photochem Photobiol Sci, 2(1), 29–38,* ***2003*** “Terrestrial ecosystems, increased solar ultraviolet radiation and interactions with other climatic change factors”

14. M.G. Kimlin, A.V. Parisi, N.D. Downs *Photochem Photobiol Sci, 2, 365-369,* ***2003*** “Human UVA exposures estimated from ambient UVA measurements”

15. M.G. Kimlin “Techniques for assessing human UV exposures” *Proceedings of The International Symposium on Optical Science and Technology, Ultraviolet Ground and Space based measurements, models and effects III, Vol. 5156, 197-206,* ***2003***

16. M. Ichihashi et al *Toxicology, 189, 21-39,* ***2003*** “UV-induced skin damage”

17. N. Kollias, A. Baqer, I. Sadiq, R. Gillies, H. Ou-Yag *Photochem. Photobiol. 78(3), 220-224, **2003*** "Measurement of solar UVB variations by polysulphone film"
18. R.L. McKenzie, L. O. Bjoern, A. Bais, M. Ilyasd *Photochem Photobiol Sci, 2(1), 5–15, **2003*** "Changes in biologically active ultraviolet radiation reaching the Earth's surface"
19. S.S. Sullivan, J.L. Cobb, C.J. Rosen, M.F. Holick, T.C. Chen, M.G. Kimlin, A.V. Parisi *Nutrition Res, 23, 631-644, **2003*** "Assessment of sun exposure in adolescent girls using activity diaries"
20. V.E. Fioletov, J.B. Kerr, L.J.B. McArthur, D.I. Wardle, T.W. Mathews *J Appl Meteor, 42, 417-433, **2003*** "Estimating UV Index Climatology over Canada"
21. V.E. Fioletov, J.B. Kerr, L.J.B. McArthur, D.I. Wardle, T.W. Mathews, M.G. Kimlin, R. Meltzer, N. Krotkov, J.R. Herman *48th SPIE MEETING, S.Diego (CA)* "Estimating UV Index Climatology over North America" ***2003***

2004

1. A.Parisi and M.G. Kimlin "Dosimeter for measurement of UVA exposures" *Proceedings of The International Symposium on Optical Science and Technology, Ultraviolet Ground and Space based measurements, models and effects III, Vol. 5545, 63-70, **2004***
2. A.V. Parisi and N. Downs *Photochem Photobiol Sci, 3(7), 643–647, **2004*** "Variation of the enhanced biologically damaging solar UV due to clouds"
3. B. Diffey *Phys Med Biol, 49, R1-R11, **2004*** "Climate change, ozone depletion and the impact on ultraviolet exposure of human skin"
4. C. Boldemann, H. Dal, U. Wester *Photodermatol Photo, 20, 2-8, **2004*** "Swedish pre-school children's UVR exposure – a comparison between two outdoor environments"

5. C. Oh et al. *J Invest Dermatol, Vol. 123, No.6, 1147-1150,* ***2004*** "Proportion of lifetime UV dose received by children, teenagers and adults based on time-stamped personal dosimetry"
6. E. De Vries and J.W. Coebergh *Eur J Cancer, 40, 2355-2366,* ***2004*** "Cutaneous malignant melanoma in Europe"
7. G. Chaplin *Am J Phys Anthropol, 125, 292-302,* ***2004*** "Geographic distribution of environmental factors influencing human skin coloration"
8. G. Nole, A.W. Johnson *Dermatol Ther, Vol.17, 57-62,* ***2004*** "An analysis of cumulative lifetime solar ultraviolet radiation exposure and the benefits of daily sun protection"
9. G.R. Casale, A.M. Siani, A. Colosimo *Proceedings 'Complexity in the Living 2004' Rome 28-30 September 2004, 108-113,* ***2004*** "Solar ultraviolet radiation at the earth's surface: factors affecting its impact on human beings"
10. G.V.G. Baranoski, A. Krishnaswamy, B. Kimmel *Phys Med Biol, 49, 4799-4809,* ***2004*** "An investigation on the use of data-driven scattering profiles in Monte Carlo simulations of ultraviolet light propagation in skin tissues"
11. H.S. Black *Integrat Cancer Ther, 3(4), 279-293,* ***2004*** "Reassessment of a free radical theory of cancer with emphasis on ultraviolet carcinogenesis"
12. ICNIRP (The International Commission on Non-Ionizing Radiation Protection) *Health Phys, Vol. 87, N.2, 171-186,* ***2004*** "Guidelines on limits of exposure to ultraviolet radiation of wavelengths between 180 nm and 400 nm (incoherent optical radiation)"
13. J.C. van der Leun *Photodermatol Photo, 20, 159-162,* ***2004*** "The ozone layer"
14. J.J, Streicher, W.C. Cuverhous Jr., M.S. Dulberg, R.J. Fornaro *Photochem. Photobiol. 79(1), 40-47,* ***2004*** "Modeling the anatomical distribution of sunlight"
15. M.B. Lens and M. Dawes *Brit J Dermatol, 150, 179-185,* ***2004*** "Global perspectives of contemporary epidemiological trends of cutaneous malignant melanoma"

16. M.G. Kimlin *J Steroid Biochem, 89-90, 479-483,* ***2004*** "The climatology of Vitamin D producing ultraviolet radiation in the United States"
17. M.G. Kimlin and K.A. Schallhorn *Photochem Photobiol Sci, 3, 1060-1070,* ***2004*** "Estimations of the human 'vitamin D' UV exposure in the USA"
18. M. Mech and P. Koepke *Theor Appl Climatol, 77, 151-158,* ***2004*** "Model for UV irradiance on arbitrarily oriented surfaces"
19. M.Z. Prelich and A.S. Jedrzejowska *Dermatol Surg, 30, 248-252,* ***2004*** "Environmental risk factors predisposing to the development of basal cell carcinoma"
20. N.G. Jablonski *Annu Rev Anthropol, 33, 585-623,* ***2004*** "The evolution of human skin and skin color"

2005

1. A.R. Young and S.L. Walker *Photochem Photobiol, 81, 1243-1245,* ***2005*** "UV radiation, vitamin D and human health: an unfolding controversy introduction"
2. A.V. Parisi and C.A. Wilson *Photodermatol Photo, 21, 303-310,* ***2005*** "Pre-vitamin D_3 effective ultraviolet transmission through clothing during simulated wear"
3. C.Y. Wright and A.I. Reeder *Photochem Photobiol, 81, 1331-1342,* ***2005*** "Youth solar ultraviolet radiation exposure, concurrent activities and sun-protective practices: a review"
4. D.E. Godar *Photochem Photobiol, 81, 736-749,* ***2005*** "UV doses worldwide"
5. D.J. Turnbull, A.V. Parisi, M.G. Kimlin *J Steroid Biochem, 96, 431-436,* ***2005*** "Vitamin D effective ultraviolet wavelengths due to scattering in shade"
6. E. Thieden et al *Brit J Dermatol, 153, 795-801,* ***2005*** "Ultraviolet exposure patterns of Irish and Danish gardeners during work and leisure"

7. J. Diamond *Nature, Vol. 435, 283-284,* ***2005*** "Geography and skin colour"
8. J. Heydenreich and H.C. Wulf *Photochem Photobiol, 81, 1138-1144,* ***2005*** "Miniature personal electronic UVR dosimeter with erythema response and time-stamped readings in wristwatch"
9. M. Allen and R. McKenzie *Photochem Photobiol Sci, 4, 429-437,* ***2005*** "Enhanced UV exposure on a ski-field compared with exposures at sea level"
10. M. Ono, N. Munakata, S. Watanabe *Photochem Photobiol, 81, 437-445,* ***2005*** "UV exposure of elementary school children in five Japanese cities"
11. P.R. Epstein *New Engl J Med, 353(14), 1433-1436,* ***2005*** "Climate change and human health"
12. R. Afiero *"Colorimetria della pelle umana"* Tesi finale per la Scuola di Specializzazione in Fisica Sanitaria Università degli Studi di Roma "La Sapienza" A.A.2004-2005 127 pagg. ***2005***
13. O. Engelsen, M. Brustad, L. Aksnes and E. Lund *Photochem Photobiol, 81, 1287-1290,* ***2005*** "Daily duration of vitamin D synthesis in human skin with relation to latitude, total ozone, altitude, ground cover, aerosols and cloud thickness"

2006

1. A.J. Samanek et al *Med J Aus, 184(7), 338-341,* ***2006*** "Estimates of beneficial and harmful sun exposure times during the year for major Australian population centres"
2. A.R. Estevey, M. J. Marı´ny, J. A. Martınez-Lozano, F. Tena, M. P. Utrillas and J. Canada *Photochem Photobiol, 82, 1047-1052,* ***2006*** "UV Index on Tilted Surfaces"
3. A.R. Young *Prog Biophys Mol Bio, 92, 80–85,* ***2006*** "Acute effects of UVR on human eyes and skin"
4. A.V. Parisi, D.J. Turnbull1 and M. G. Kimlin *Phys Med Biol, 51, 3241-3249,* ***2006*** "Influence of solar UVA on erythemal irradiances"

5. C. Tuchinda, S. Srivannaboon, H.W. Lim *J Am Acad Dermatol, Vol. 54, N.5, 845-854,* ***2006*** "Photoprotection by window glass, automobile glass, and sunglasses"
6. D. Wolpowitz and B.A. Gilchest *J Am Acad Dermatol, Vol. 54, N.2, 301-317,* ***2006*** "The vitamin D questions: how much do you need and how should you get it?"
7. E.C. Weatherhead and S.B. Andersen *Nature, Vol. 441, 39-45,* ***2006*** "The search for signs of recovery of the ozone layer"
8. E. Thieden, P.A. Philipsen, H.C. Wulf *Brit J Dermatol, 154, 133-138,* ***2006*** "Ultraviolet radiation exposure pattern in winter compared with summer based on time-stamped personal dosimeter"
9. G.R. Casale, M. Borra, A. Colosimo, M. Colucci, A. Militello, A.M. Siani and R. Sisto: "Variability among polysulphone calibration curves" *Phys Med Biol, 51, 4413-4427,* ***2006***
10. J.J. Cannell, R. Vieth, J.C.Umhau, M.F.Holick, W.B.Grant, S.Madronich, C.F.Garland and E. Giovannucci *Epidemiol Infect, 134, 1129–1140,* ***2006*** "Epidemic influenza and vitamin D"
11. J. Reichrath *Prog Biophys Mol Bio, 92, 9–16,* ***2006*** "The challenge resulting from positive and negative effects of sunlight: How much solar UV exposure is appropriate to balance between risks of vitamin D deficiency and skin cancer?"
12. K. Kojoa, C.T. Jansenc, P. Nybomd, L. Huurtoa, J. Laihiac, T. Ilusa, A. Auvinena, *Environ Res, 101, 123–131,* ***2006*** "Population exposure to ultraviolet radiation in Finland 1920–1995: Exposure trends and a time-series analysis of exposure and cutaneous melanoma incidence"
13. M.G. Kimlin, N. Martinez, A.C. Green, D.C. Whiteman *J Photochem Photobiol B: Biol, 85, 23-27,* ***2006*** "Anatomical distribution of solar ultraviolet exposures among cyclists"
14. O. Gillie *Brit J Dermatol, 154, 1052-1061,* ***2006*** "A new government policy is needed for sunlight and vitamin D"
15. R. Haywood *Photochem Photobiol, 82, 1123-1131,* ***2006*** "Relevance of Sunscreen Application Method, Visible Light and

Sunlight Intensity to Free-radical Protection: A Study of ex vivo Human Skin"
16. R. McKenzie, G. Bodeker, G. Scott, J. Slusser, K. Lantz *Photochem Photobiol Sci, 5, 343-352,* ***2006*** "Geographical differences in erythemally-weighted UV measured at mid-latitude USDA sites"
17. R.P. Gallaghera, T.K. Leea *Prog Biophys Mol Bio, 92, 119–131,* ***2006*** "Adverse effects of ultraviolet radiation: A brief review"
18. T. Gambichler, G. Moussa, N. S. Tomi, V. Paech, P. Altmeyer and A. Kreuter *Photochem Photobiol, 82, 1097-1102,* ***2006*** "Reference Limits for Erythema-effective UV Doses"
19. WHO (World Health Organization) Public Health and the Environment *"Solar Ultraviolet Radiation. Global burden of disease from solar ultraviolet radiation"* Environmental Burden of Disease Series, No. 13-R. Lucas, T. McMichael, W. Smith, B. Armstrong. Editors A. Prüss-Üstün, H. Zeeb, C. Mathers, M. Repacholi ***2006***

Addendum

Scientific contributions from this research (in reverse chronological order)

- Invited speaker at *Corso AIFM (Associazione Italiana di Fisica Medica)* "La gestione delle radiazioni coerenti e non coerenti in ambito sanitario: applicazioni delle Linee Guida della Regione Lombardia. Le sorgenti UV" Milano, IRCCS San Raffaele 15.11.06 (**2006**)

- Sisto R., Borra M., Casale G.R., Militello A., Siani A.M.: "Esposizione a radiazione solare ultravioletta in un comparto agricolo della Toscana" *dBA2006 Rumore, vibrazioni, microclima, campi elettromagnetici, radiazioni ottiche e ionizzanti. Valutazione, prevenzione e bonifica negli ambienti di lavoro*, Modena 12-13 ottobre 2006, pagg. 173-184 (**2006**)

- Casale G.R., Siani A.M., Palmieri S., Campanella L.. "Spectral changes of paper exposed to ambient solar radiation" *1st International Meeting on Chemometrics and Multivariate Analysis Applied to Cultural Heritage and Environment CMA4CH*, Nemi, Rome (Italy), 2-4 October 2006, 61-62, ISBN 88-548-0765-6 (**2006**)

- Casale G.R., Borra M., Colosimo A., Colucci M., Militello A., Siani A.M. and Sisto R.: "Variability among polysulphone calibration curves" *Physics in Medicine and Biology 51, 4413-4427* (**2006**) *

- Sisto R., Borra M., Casale G.R., Colucci M., Militello A., Siani A.M.: "Solar UV radiation exposure in a population of Tuscany vineyard workers" *28th International Congress on Occupational Health*, Milano, 11–16 June 2006, pag.107 (**2006**)

- Sisto R., Borra M., Casale G.R., Colucci M., Militello A., Siani A.M.: "Studio della parametrizzazione delle curve di calibrazione di dosimetri a polisolfone per il monitoraggio dell'esposizione a radiazione solare UV" *Terzo Convegno Nazionale Controllo Ambientale degli agenti fisici: dal monitoraggio alle azioni di risanamento e bonifica*, Biella, 7–8–9 Giugno 2006 (**2006**)

- Casale G.R., Bono N., Siani A.M., Kimlin M.G.: "Response of polysulphone dosimeters exposed under different environmental conditions", *17th International Congress of Biometeorology ICB 2005* - Annalen der Meteorologie, 41(2), 680-683, ISBN 3-88148-405-1 (**2005**) *

- Casale G.R., Siani A.M., Colosimo A.: "Solar ultraviolet radiation at the earth's surface: factors affecting its impact on human beings" *Complexity in the Living 2004* Rome 28-30 September 2004, Rapporti ISTISAN, ISSN 1123-3117, 108-113 (**2004**) *

** the full text is reported in the following pages*

INSTITUTE OF PHYSICS PUBLISHING PHYSICS IN MEDICINE AND BIOLOGY

Phys. Med. Biol. **51** (2006) 4413–4427 doi:10.1088/0031-9155/51/17/019

Variability among polysulphone calibration curves

G R Casale[1], M Borra[2], A Colosimo[3], M Colucci[2], A Militello[2], A M Siani[1] and R Sisto[2]

[1] University of Rome 'La Sapienza', Physics Department, P.le A. Moro 2, I-00185, Rome, Italy
[2] ISPESL, (Istituto Superiore per la Prevenzione E la Sicurezza del Lavoro), Occupational Hygiene Department, Via Fontana Candida 1, I-0040 Monteporzio Catone (RM), Italy
[3] University of Rome 'La Sapienza', Department of Human Physiology and Pharmacology, P.le A. Moro 2, I-00185, Rome, Italy

E-mail: renata.sisto@ispesl.it

Received 7 June 2006, in final form 14 July 2006
Published 15 August 2006
Online at stacks.iop.org/PMB/51/4413

Abstract

Within an epidemiological study regarding the correlation between skin pathologies and personal ultraviolet (UV) exposure due to solar radiation, 14 field campaigns using polysulphone (PS) dosemeters were carried out at three different Italian sites (urban, semi-rural and rural) in every season of the year. A polysulphone calibration curve for each field experiment was obtained by measuring the ambient UV dose under almost clear sky conditions and the corresponding change in the PS film absorbance, prior and post exposure. Ambient UV doses were measured by well-calibrated broad-band radiometers and by electronic dosemeters. The dose-response relation was represented by the typical best fit to a third-degree polynomial and it was parameterized by a coefficient multiplying a cubic polynomial function. It was observed that the fit curves differed from each other in the coefficient only. It was assessed that the multiplying coefficient was affected by the solar UV spectrum at the Earth's surface whilst the polynomial factor depended on the photoinduced reaction of the polysulphone film. The mismatch between the polysulphone spectral curve and the CIE erythemal action spectrum was responsible for the variability among polysulphone calibration curves. The variability of the coefficient was related to the total ozone amount and the solar zenith angle. A mathematical explanation of such a parameterization was also discussed.

1. Introduction

Following the discovery of the Antarctic ozone hole in 1985 and the significant decrease in total ozone at middle latitudes observed since the 1970s, solar ultraviolet (UV) radiation became an important environmental, ecological and atmospheric parameter to be measured and studied (Webb 1998, WMO 2002, van der Leun 2004). Increasing interest has been shown

by the scientific community in human health risks deriving from over-exposure to solar UV radiation. In fact, harmful effects include some kinds of skin cancer and some eye pathologies (de Gruijl 1999, Diffey 2004), whereas the only well-established beneficial effect of solar UV radiation is the production of vitamin D_3 required for skeleton health (Holick 2000).

According to the Commission Internationale de l'Eclairage, CIE, the UV region is subdivided into UVC (100–280 nm), UVB (280–315 nm) and UVA (315–400 nm). The amount of solar ultraviolet radiation reaching the Earth's surface depends on the amount of incoming solar energy, the transmission properties of the atmosphere and the properties of the surface (Webb 1998, Kerr 2003). No UVC radiation reaches the Earth's surface, since it is completely absorbed by ozone and molecular oxygen in the upper atmosphere.

Extensive UV monitoring by means of spectroradiometers and broad-band radiometers started during the 1990s (WMO 2002), although a homogeneous network for UV measurements does not yet exist (Kerr 2003, Seckmeyer 2000). Recently, UV measurements by multi-channel (moderate- and narrow-band) radiometers have also become available (Di Menno *et al* 2002, Bernhard *et al* 2003).

The degree of effectiveness of UV radiation in producing biological damage depends on the 'biologically effective solar exposure', or 'biologically effective dose', i.e. the incident weighted irradiance on a given surface over a specified period of time, expressed in joules per square metre, J m^{-2} (Parisi 2005). The determination of the biologically effective dose requires knowledge of the action spectra of a biological system, i.e., of functions expressing the effectiveness of electromagnetic radiation in causing a specific response in that biological system. The erythemal action spectrum is a weighting function that simulates the damage process occurring in the skin (Diffey and McKinlay 1987). However, although the biological action spectra can help in understanding some biological effects, they do not contain information on the simultaneous effect of multiple wavelengths and feedback mechanisms.

Values of the erythemal ultraviolet irradiance between 280 and 400 nm, i.e. the dose rate, can be measured by broad-band instruments that have a spectral response matching the skin erythemal response or, alternatively, calculated by using spectroradiometers and then weighting the irradiance with the CIE erythemal action spectrum (CIE 1987). Both these instruments yield data of UV radiation incident upon a flat horizontal surface.

Dosimetry is widely used in epidemiological studies to quantify personal solar exposure of humans in different settings, during their ordinary daily activities. In fact, dosimetry enables measurements of the exposure of differently oriented surfaces and it can be used in remote and not easily accessible places (Webb 1995). Several erythemal dosemeters have been developed: electronic solid state dosemeters (El Naggar *et al* 1995, Cockell *et al* 2001, Cockell *et al* 2002), dosemeters based on the metabolism of bacteria (Boldemann *et al* 2004, Quintern *et al* 1994) and dosemeters based on changes in the optical properties of specific materials following exposure to UV radiation (Davis *et al* 1976, Diffey and Davis 1978). This latter methodology involves the use of photosensitive films whose absorbance properties change upon exposure to UV radiation.

The most widely used photosensitive film is made by polysulphone (PS) polymer (Diffey 1989, Parisi *et al* 1997). This polymer undergoes photodegradation when exposed to UV radiation, leading to modification of its absorbance properties in the UV range. The spectral response of polysulphone (Diffey 1989) is similar to that of CIE erythemal (figure 1). Absorbance at a given wavelength is measured before and after exposure and the observed difference depends on the erythemal effective UV dose absorbed by the dosemeter (Diffey 1989). When this technique is used, it is recommended to determine the calibration curve in order to obtain reliable dose estimates (Diffey 1987, Kimlin 2003, Kollias *et al* 2003).

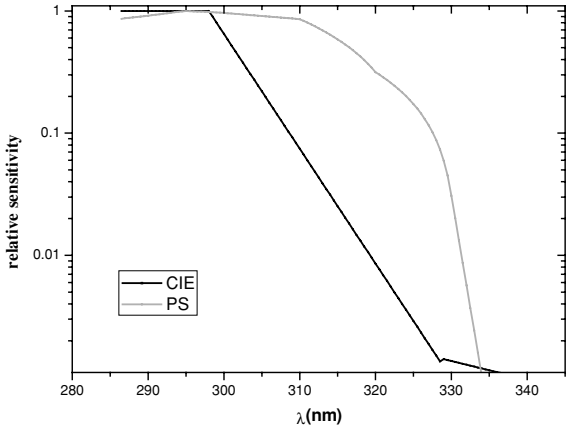

Figure 1. CIE and PS action spectra normalized at 295 nm.

In the present study the variability among the calibration curves obtained during 14 field experiments carried out in different environmental conditions (urban, rural and semi-rural sites) is analysed. Field campaigns were performed during 2004 and 2005 at three Italian sites between 41.9 °N and 43.3 °N, for solar zenith angle (SZA) ranging from about 20° to 70°. The observed variability among the calibration curves is here interpreted taking into account the site of the field experiment and important factors modulating the UV spectrum at the Earth's surface.

The purpose of this study is to combine the information deriving from the empirical relation between the erythemal effective UV dose and the PS absorbance change with its mathematical explanation.

A parameterization of the calibration curves, represented by a coefficient multiplying a cubic polynomial function, is proposed. It is shown that the multiplying coefficient depends on the spectral shape of the UV radiation, which is mainly affected by the total ozone amount and the solar zenith angle, while the cubic polynomial function is assumed to be dependent on the PS photodegradation mechanisms only. This polynomial function, first proposed by Diffey (1987) on an empirical basis, is here explained in the appendix, based on the theoretical expressions for the PS response found by Krins *et al* (1999).

2. Materials and methods

2.1. Calibration curves of polysulphone films

Dosemeters are useful for determining UV doses absorbed by humans on different body parts, mainly when exposure conditions are characterized by high variability during outdoor activities (Parisi *et al* 1997, Kimlin *et al* 1998a). An exhaustive discussion about the properties and limitations of dosemeters was given by Webb (1995).

Polysulphone dosimetry is a widely tested methodology for assessing ultraviolet radiation exposure (Davis *et al* 1976, Diffey 1984, Kimlin *et al* 1998b). The use of PS dosemeters for a reliable quantification of personal doses requires the calibration curves to be determined. These curves are obtained by measuring the ambient erythemal effective UV dose (hereafter called ambient UV dose) and the corresponding change in PS film absorbance (ΔA at 330 nm),

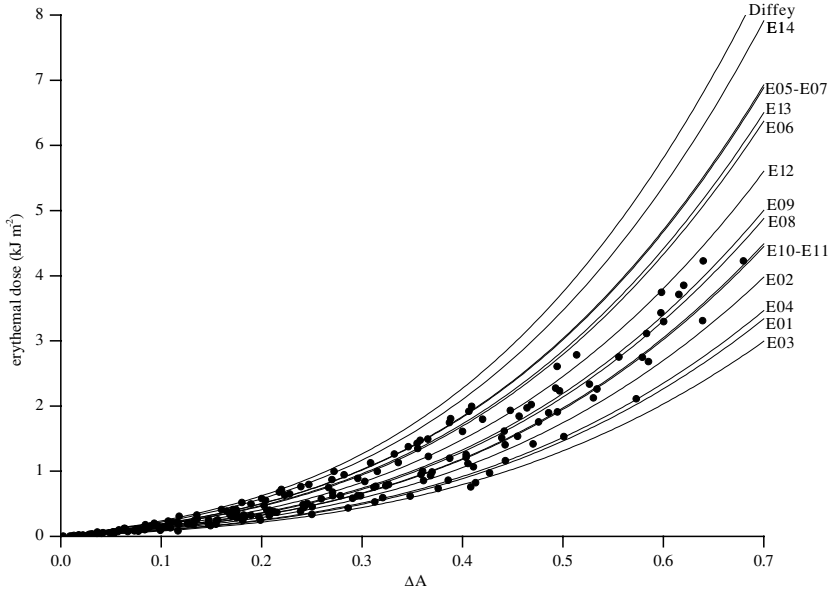

Figure 2. Calibration curves obtained in this study, and the Diffey cubic polynomial (the highest curve). Data points from calibrations are also reported (black dots).

prior and post exposure (Kimlin 2003). The absorbance of unexposed PS films with a thickness of 40 μm at 330 nm ranges from 0.1 to 0.2 depending on the batch, with increased values after the exposure to UV radiation. Under prolonged exposures the film reaches saturation at values of ΔA greater than about 0.4.

Diffey (1987) showed that the best data fit, mainly for $\Delta A > 0.3$, is given by the following equation:

$$D = c(\Delta A + \Delta A^2 + 9\Delta A^3), \tag{1}$$

where D (erythemal dose) is expressed in kJ m^{-2}. He found the value of the coefficient c equal to 2 kJ m^{-2} from a field campaign carried out on a summer day (1 July 1986) and on an autumn day (2 October 1986) at a site located at 55 °N.

In this study, within an epidemiological study regarding the correlation between skin pathologies and personal ultraviolet exposure due to solar radiation, several field campaigns using polysulphone dosemeters were carried out at three Italian sites. A large variability was observed between the PS calibration curves (figure 2). The same variability can be observed also by comparing the Diffey curve to those of other studies (figure 3), such as the curve obtained in Antarctica in 2002 (ISS curve) during the summer season (Mariutti *et al* 2003) and those derived by Kimlin in the USA (K1, K2, K3 curves) and Australia (K4, K5 curves) (Kimlin, personal communication (2005)). The variability observed amounts to much more than 10%, which is the relative error associated with doses estimated by equation (1) (Diffey 1989), and it is clearly related to different ambient conditions. It is noteworthy that such a large variability cannot be attributed only to different thickness (all dosemeters are 40 μm thick) and batch.

In order to study this large variability among PS calibration curves in the local environmental conditions of middle-latitude sites, the following 14 field campaigns were carried out: six at an urban site (Rome, city centre); five at a semi-rural site (Monteporzio

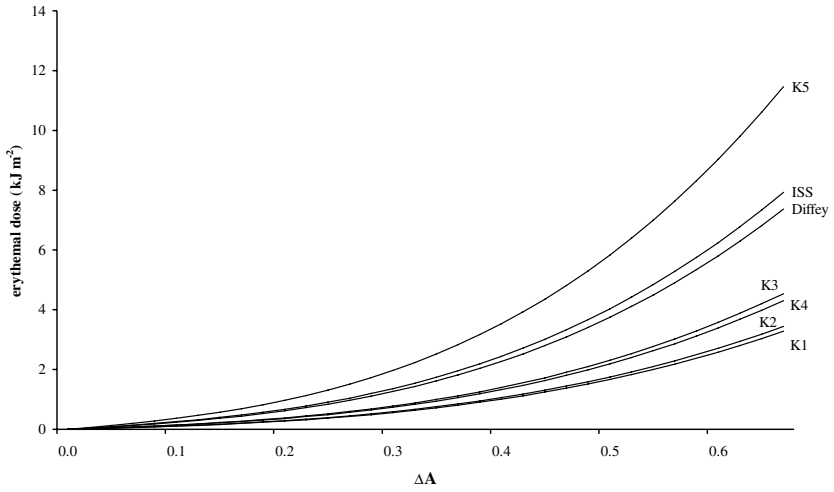

Figure 3. Comparison among different calibration curves: Diffey (1989), ISS (Mariutti *et al* 2003), K1, K2, K3, K4, K5 (Kimlin, personal communication (2005)).

Catone); three at a rural site (S Felice, Tuscany). All sites are located between 41.9 and 43.3 °N. Six campaigns were held during summer 2004 and 2005, two in winter 2004 and 2005, four in spring 2005 and two in autumn 2005. All field campaigns were conducted under almost completely clear sky conditions and for a solar zenith angle (SZA) in the range from 20° to 70°. The polysulphone film was mounted on a plastic holder with a central hole of about 1 cm^2 and three batches were used. Calibration curves were obtained using a number of dosemeters ranging from 10 to 20, located on a horizontal flat plane and exposed for different appropriate time intervals. Absorbance, before and after exposure to solar UV radiation, was measured in the laboratory either by a standard UV spectrophotometer (Perkin Elmer Lambda 5 UV-Vis double beam Spectrometer) or by a miniaturized and portable spectroradiometric system (Ocean Optics-Avantes AVS-SD 2000). In the latter case, a sample holder micrometry movement system moves the PS badge with high precision during irradiation by a xenon pulsed lamp and the absorbance was measured at the 330 nm emission peak of the source. More details on the spectroradiometer system can be found in Sisto *et al* (2001). The two reading methods were carefully compared using different film batches and no discrepancy was found in the change of optical absorbance at 330 nm.

2.2. Measurements of ambient UV doses

The use of dosemeters requires a calibration using well-calibrated solar UV instruments such as spectroradiometers or broad-band radiometers.

In this study ambient UV doses were measured by broad-band radiometers (model UVB-1, Yankee Environmental System, MA, USA) and by X2000-4 electronic dosemeters (Gigahertz-Optik, Pucheim, Germany). The YES radiometer has a spectral response similar to that of skin erythema and it measures the erythemal dose rate between 280 and 400 nm. The waveband is selected by means of the detector and of coloured glass filters. A phosphor filter converts incoming UVB radiation to green light, which is then measured by a solid-state photo-detector. The YES radiometer is equipped with an internal temperature control system for the phosphor

and related optical components. The system heats these components at a fixed temperature of 45 °C in the ambient temperature range between −40 °C and +40 °C. YES measurement is sampled at 1 min averages.

Two YES radiometers were used in this study. One belongs to the Solar Radiometry Observatory, University of Rome 'La Sapienza' (41.9 °N, 12.5 °E, 75 m asl). This radiometer (named here as the URO radiometer) is installed on the roof of a building on the University Campus (in the centre of Rome) and it has been working reliably since 2000. The Solar Radiometry Observatory is one of the stations that regularly measures UV irradiance in Italy, and it also has a Brewer spectrophotometer (operational since 1992) for measurements of UV spectral irradiance. Details can be found in Casale *et al* (2000). Ambient UV doses agree with those measured by the Brewer spectrophotometer at Rome 'La Sapienza', under clear sky conditions, with ±10% uncertainty (Siani *et al* 2003). The URO radiometer was calibrated at the European Reference Centre for Ultraviolet Radiation Measurements (Joint Research Centre, Ispra, Italy) in 2004.

The other YES radiometer (named here as the ISPESL radiometer) belongs to the ISPESL (Istituto Superiore per la Prevenzione E la Sicurezza sul Lavoro), Monteporzio Catone (41.8 °N, 12.7 °E, 300 m asl). This semi-rural site is about 30 km southeast of Rome. The performance of the ISPESL radiometer was tested during several field experiments using the URO radiometer as the reference instrument. The mean percentage difference between the two instruments during all field experiments was less than 5% showing their good agreement.

A complementary method for measuring ambient UV doses using X2000-4 electronic dosemeters was also used in this study. The X2000-4 electronic dosemeters are small and easy to use. They are powered by batteries during exposure and can be set up in not easily accessible areas. The electronic dosemeter is equipped with two photovoltaic cells, one reproducing the erythemal action spectrum, the other having a response which is approximately constant in the UVA range (the UVB contribution is negligible). The instrument response is cosine corrected.

The acquisition sampling rate can be set using the dedicated software and, in this study, a frequency of 1 Hz was adopted. The absolute calibration of the electronic dosemeters was certified by Gigahertz-Optik in 2005.

3. Results

3.1. Calibration curves from different instruments

A comparison between the calibration curves obtained with broad-band radiometers and electronic dosemeters was carried out on 28 July 2005 in Rome under clear sky conditions. Ambient doses were calculated beginning with dose rates as 1 min averages of the irradiance values. Electronic dosemeters were exposed on a flat horizontal plane near the radiometer so that all instruments had the same field of view of 2π. Twenty PS dosemeters were used for differing time intervals starting at 7.00 UT.

Calibration curves obtained from the two different instruments are plotted in figure 4, showing a good agreement: the percentage difference (X2000 − YES)/YES is −9%.

This result supports the use of electronic dosemeters to obtain calibration curves during field campaigns of personal solar exposure in sites where it is not possible to install radiometers. In this case it is however recommended to assess the agreement between the calibration curves of a well-calibrated standard UV instrument and electronic dosemeters.

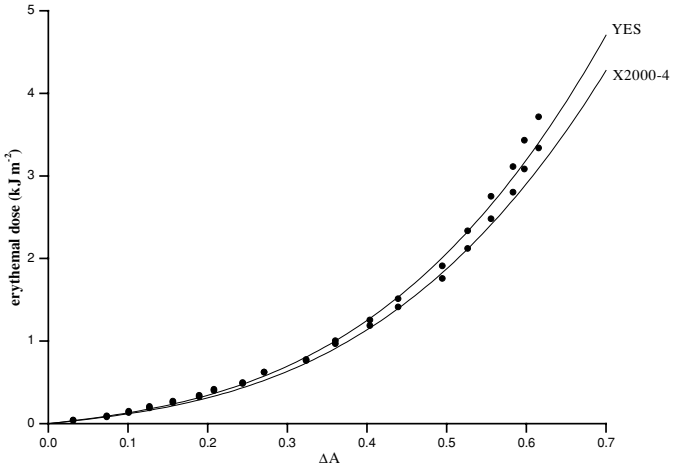

Figure 4. PS calibration curves on 28 July 2005 obtained using URO YES radiometer data and the average of the two GigaHertz Optic X2000–4 electronic dosemeters. The calibration equations are, respectively, $D = 1.1(\Delta A + \Delta A^2 + 9\Delta A^3)$ for the YES and $D = 1.0(\Delta A + \Delta A^2 + 9\Delta A^3)$ for the electronic devices. Data points from calibration are also reported (black dots).

Table 1. List of 14 calibration curves and the corresponding value of c (with the associated standard error). R is a measure of the goodness of the polynomial fit. Rome, Monteporzio and S Felice are respectively urban, semi-rural and rural sites.

	Date (dd/mm/yyyy)	Site	c (kJ m^{-2})	R
E01	22/07/2004	Rome	0.78 ± 0.03	0.98
E02	13/12/2004	Rome	0.93 ± 0.01	0.99
E03	04/02/2005	Rome	0.70 ± 0.02	0.99
E04	09/03/2005	Monteporzio	0.81 ± 0.03	0.99
E05	21/03/2005	Monteporzio	1.61 ± 0.05	0.99
E06	06/04/2005	Monteporzio	1.49 ± 0.04	0.99
E07	22/04/2005	S Felice	1.62 ± 0.03	0.99
E08	21/06/2005	Rome	1.14 ± 0.02	0.99
E09	12/07/2005	S Felice	1.17 ± 0.03	0.99
E10	20/07/2005	Rome	1.04 ± 0.02	0.99
E11	28/07/2005	Rome	1.05 ± 0.01	0.99
E12	15/09/2005	Monteporzio	1.31 ± 0.03	0.99
E13	12/10/2005	S Felice	1.52 ± 0.04	0.99
E14	04/11/2005	Monteporzio	1.85 ± 0.04	0.99

3.2. Calibration curves from the field campaigns

The PS calibration curve for each of the 14 field campaigns was obtained by measuring ambient UV doses by means of YES radiometers or electronic dosemeters. Collected data for each campaign were best fitted using a cubic polynomial function with the same form of equation (1) but different values of the c coefficient. The dates and sites of the field experiments are listed in chronological order in table 1, while the calibration curves are plotted in figure 2 together with the Diffey curve. Values of c from the best fit procedure and its goodness (R) are also reported in table 1.

From figure 2 it can be seen that the calibration curves show a large variability, which is reflected in the values of the coefficient c, varying within a factor of more than 2. This effect cannot be due to differences among the PS dosemeters. Urban calibration curves have the smallest c values (average 0.94 ± 0.02 kJ m^{-2}), which increase in the semi-rural and rural sites (average 1.41 ± 0.04 kJ m^{-2} and 1.44 ± 0.03 kJ m^{-2} , respectively). Moreover, table 1 shows that there is variability among the calibration curves even within the same month.

4. Analysis of results and discussion

A mathematical interpretation of equation (1) is given in the appendix using a perturbative method, but it should be reminded that a complete justification of the coefficients in brackets is empirical.

Data collected from the field experiments indicate that the variability of the c coefficient could be attributed to the different environmental conditions during each field campaign. Keeping in mind that the polysulphone and the erythema have different responses beyond 300 nm (figure 1), special attention was focused on the total ozone amounts and solar zenith angle ranges. In order to investigate their effect on the calibration patterns, the STAR radiative transfer model (Ruggaber 1994) was used under clear sky conditions in an urban, a semi-rural and a rural scenario. The agreement between the UV measurements and the modelled values was already assessed in a field campaign in Rome (Meloni *et al* 2000). Here the model was used to calculate spectral irradiances from 280 to 400 nm with 0.5 nm wavelength steps, total ozone values O_3 ranging from 200 to 500 DU in steps of 50 DU and SZA ranging from 20 to 70° in steps of 10°. The sites were differentiated taking into account surface albedo, boundary layer height and tropospheric aerosol type, while the same standard values of stratospheric aerosol and vertical profiles of ozone, temperature and humidity, named US profiles were used. Modelled spectral irradiances were then convolved with the CIE erythema action spectrum and the PS action spectrum, and integrated over the entire wavelength range.

According to Krins *et al* (2001), the g factor was determined as follows:

$$g = \frac{\int I(\lambda) S_{\mathrm{ery}}(\lambda)\, \mathrm{d}\lambda}{\int I(\lambda) S_{\mathrm{PS}}(\lambda)\, \mathrm{d}\lambda}, \tag{2}$$

where $I(\lambda)$ is the solar spectral irradiance at the Earth's surface, $S_{\mathrm{ery}}(\lambda)$ the CIE erythema action spectrum and $S_{\mathrm{PS}}(\lambda)$ the polysulphone action spectrum. In the appendix we show that c can be expressed by dividing g by the constant $\alpha = 7.4 \times 10^{-5}$ m^2 J^{-1}. The behaviour of g follows the variability of $I(\lambda)$, which is affected by atmospheric and geometric parameters.

The model was used to find out which factors play a major role in the fluctuation of g. No significant discrepancies were found in g values owing to the characterization of the site in terms of typical aerosol loading and surface albedo.

The analysis showed that total ozone and SZA are the main parameters affecting the variability of g. Values of g as a function of O_3 amounts and SZA, summarized in table 2, show that significant variations of g are related to lower O_3 and SZA values, while at higher O_3 and SZA levels no changes occur. This indicates that g variability is mainly modulated by changes of solar UVB irradiance where the erythemal action spectrum is more effective. This is in agreement with the results shown by Krins *et al* (2001).

The values in table 2 allow us to estimate c (see table 3). In order to interpret the results, it is useful to distinguish two regions in table 3:

- the first region (dark grey) highlights that for $O_3 \leqslant 300$ DU and SZA $\leqslant 40°$ the c values show a great variability (from 1.06 to 1.56 kJ m^{-2});

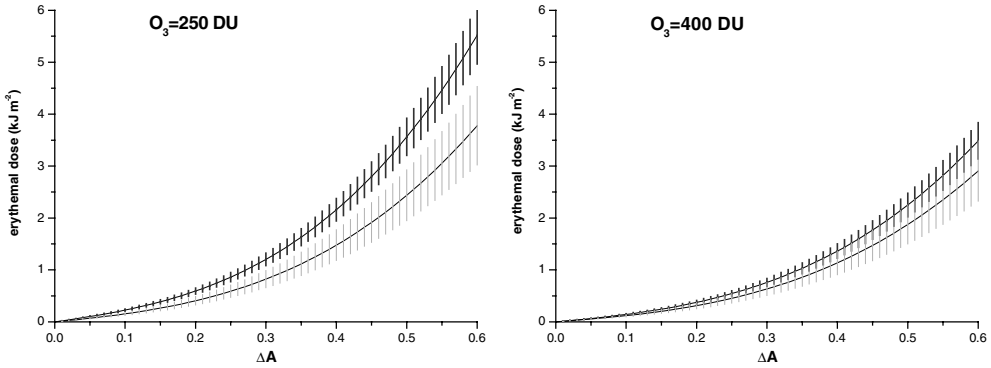

Figure 5. Measured (black) and modelled (grey) calibration curves for two different groups (left: $O_3 = 250$ DU, SZA $> 50^\circ$; right: $O_3 = 400$ DU, SZA $< 50^\circ$). The error bars are drawn as described in the text.

Table 2. Values of g as a function of total ozone (first column on the left, values in DU) and SZA (upper row, in degrees).

O_3/SZA	20	30	40	50	60	70
500	0.07	0.06	0.06	0.06	0.06	0.06
450	0.07	0.07	0.06	0.06	0.06	0.06
400	0.07	0.07	0.07	0.06	0.06	0.06
350	0.08	0.08	0.07	0.07	0.06	0.06
300	0.09	0.08	0.08	0.07	0.06	0.06
250	0.10	0.09	0.09	0.08	0.07	0.06
200	0.12	0.11	0.10	0.09	0.08	0.07

Table 3. Modelled values of c as a function of total O_3 (first column on the left, values in DU) and SZA (upper row, in degrees).

O_3/SZA	20	30	40	50	60	70
500	0.90	0.87	0.83	0.79	0.76	0.76
450	0.95	0.91	0.87	0.82	0.77	0.75
400	1.01	0.97	0.91	0.85	0.79	0.75
350	1.09	1.04	0.97	0.90	0.82	0.78
300	1.20	1.14	1.06	0.97	0.87	0.77
250	1.35	1.28	1.18	1.07	0.95	0.83
200	1.56	1.48	1.36	1.22	1.06	0.91

- the second (light grey) refers to $O_3 \geqslant 400$ DU and SZA $\geqslant 50^\circ$, where the c values are on average stable around 0.8 kJ m^{-2}.

A comparison between modelled (table 3) and measured (table 1) c values was performed taking into account four groups of total O_3 amounts (from 250 to 400 DU at 50 DU steps). Calibration curves, representative of each group, were then determined using the mean modelled and measured value of c in equation (1). The results for two different total ozone amounts (250 and 400 DU), representative of middle-latitude sites, are plotted in figure 5. The error bar assigned to each data point in figure 5 is 10% for the measured c and 20% for the modelled c (Schwander *et al* 1997). A comparison indicates that the calibration curves are

consistent for $O_3 = 400$ DU (measured $c = 1.22$, modelled $c = 0.96$) where the percentage difference, (measured − modelled)/measured, is 21%. In the case of $O_3 = 250$ DU (measured $c = 1.45$, modelled $c = 0.95$) the percentage difference is 34%.

The calibration curve is best fitted by a cubic expression with a multiplying coefficient c which is a function of g (see equation (2)). A mathematical interpretation is presented in the appendix, showing that the curve was obtained expanding the polysulphone response function to the limit of small doses and inverting the relation between the absorbance variation and the absorbed dose. It can be assessed that the multiplying coefficient is affected by the solar UV spectrum at the Earth's surface whilst the expression in brackets depends on the photoinduced reaction of polysulphone film dosemeters (Rivaton and Gardette 1999).

The mismatch between the polysulphone spectral curve and the CIE erythemal action spectrum is responsible for the variability among polysulphone calibration curves. Since the erythemally weighed irradiance is much more sensitive to the UVB radiation than the irradiance weighted by the polysulphone response function, c follows total ozone fluctuations and solar zenith angle changes. Similar results were shown by Krins *et al* (2001).

The solar zenith angle is involved in the radiation absorption law:

$$I(\mathrm{SZA}) = I(0)\,\mathrm{e}^{-\alpha/\cos(SZA)}, \tag{3}$$

where $I(\mathrm{SZA})$ is the direct beam radiation at a fixed wavelength reaching the Earth's surface at SZA, $I(0)$ is the irradiance at the top of the atmosphere and α is the atmospheric extinction coefficient.

For small angles, the following equation is obtained:

$$I(SZA) = I(0)\left[1 - \alpha\left(1 - \tfrac{1}{2}SZA^2 + \cdots\right)\right]. \tag{4}$$

Equation (4) yields that, for sufficiently small values of SZA, the dependence on the solar zenith angle is a second-order polynomial law. For increasing values of total ozone amount, the SZA dependence becomes negligible.

A best fitting procedure to describe the measured g values as functions of O_3 and SZA was performed by using the following relationship:

$$g(\mathrm{O_3}, \mathrm{SZA}) = g(200, 20) - a\mathrm{O_3} + b\mathrm{SZA} - \hat{b}(\mathrm{SZA})^2 \tag{5}$$

where g(200,20) is the g value at $O_3 = 200$ DU and SZA = 20°.

If g(200,20) = 0.12, the best fit ($R^2 = 0.93$) to the measured values of g, according to equation (5), gives

$$a = (1.3 \pm 0.2) \times 10^{-4}\ \mathrm{DU}^{-1}$$
$$b = (7.8 \pm 1.5) \times 10^{-4}\ \mathrm{deg}^{-1}$$
$$\hat{b} = (1.8 \pm 0.4) \times 10^{-5}\ \mathrm{deg}^{-2}.$$

5. Conclusions

The quantification of human UV exposure is a complex issue. A methodology for recording the level of exposure for different body postures is based on the use of polysulphone, a polymer which changes its optical properties (absorbance) when exposed to UV radiation. Any polysulphone dosimetry measurement programme requires specific procedures, in particular the determination of the calibration curve (ambient dose versus absorbance difference at 330 nm, ΔA). The calibration curve is best fitted by a cubic polynomial function having a multiplying coefficient c that is proportional to the ratio g between the erythemally weighted irradiance and the PS weighted irradiance.

The aim of the present work was to analyse the polysulphone dosemeter calibration curves obtained during 14 field campaigns carried out at three different middle latitude sites (urban, semi-rural and rural sites) and in any season of the year. Curves were obtained by measuring ambient UV doses both with broad-band radiometers and electronic dosemeters. No significant discrepancies were observed using two different UV detectors in the determination of the calibration curve (percentage difference is 9%). The observed variability among the 14 calibration curves was interpreted through a critical study of the c coefficient. It was noted that the c values ranged from 0.78 to 1.85 kJ m^{-2}. Calibration curves were characterized in urban sites by the smallest c values (average 0.94 kJ m^{-2}), which increase in the semi-rural and rural sites (average 1.41 and 1.44 kJ m^{-2}, respectively). Calibration curves change even if they are obtained in relatively short time periods within the same month. It was shown that such variability cannot be attributed to the different batch of the PS film since no significant discrepancies in ΔA at 330 nm were found.

In order to understand the factors affecting the calibration curve, a radiative transfer model was used, having as input the total ozone amount (from 200 to 500 DU) and the SZA (from 20 to 70°). It was found that when $O_3 \leqslant 300$ DU and SZA $\leqslant 40°$ the modelled c coefficient showed a rather large variability (from 1.06 to 1.56 kJ m^{-2}), while for $O_3 \geqslant 400$ DU and SZA $\geqslant 50°$ the values of c were approximately stable, around 0.8 kJ m^{-2}. A theoretical interpretation of the variability of the calibration curves was also provided, showing that the c coefficient depended linearly on the total ozone amount while it followed a quadratic law in the solar zenith angle.

In conclusion, in personal UV measurement programmes, a careful quantification of the polysulphone calibration curve is recommended under the same atmospheric conditions of exposure of population groups. This implies that in the PS measurement programme a proper number of dosemeters should be planned for the characterization of the most reliable dose-response curve *in situ* and not in a laboratory environment by means of artificial sources. Future investigations will aim at the assessment of polysulphone calibration curves obtained under the same total ozone amount and solar zenith angle interval at different altitudes.

Acknowledgments

The authors are grateful to M G Kimlin for providing calibration curves of the USA and Australia sites. The authors thank Julian Gröbner from the Physikalisch-Meteorologisches Observatorium Davos, World Radiation Center (PMOD/WRC) for his helpful comments.

Appendix

Starting from the best fit of the polysulphone calibration curves to a polynomial function of the type

$$D = c(\Delta A + a\Delta A^2 + b\Delta A^3), \tag{A.1}$$

in this work the variability of the polysulphone calibration curves is parameterized by varying the overall coefficient c and leaving the $(\Delta A + a\Delta A^2 + b\Delta A^3)$ term unchanged. This approach was suggested by Diffey (1987). Here we try to give a theoretical interpretation of equation (A.1).

The mismatch between the polysulphone action spectrum $S_{PS}(\lambda)$ and the CIE erythemal action spectrum $S_{ery}(\lambda)$ causes the dependence of the polysulphone absorbance variation on the UV radiation exposure and is responsible for the variability of the polysulphone calibration curves.

The polysulphone response function at 330 nm for a monochromatic radiation of 306 nm and a polysulphone film thickness of 26 μm was studied by Krins *et al* (1999), and is given by the following expression:

$$\Delta A = -\ln\left(A + B\exp\left(-\frac{D_{PS}}{D_1}\right) + C\exp\left(-\frac{D_{PS}}{D_2}\right)\right) \tag{A.2}$$

where D_{PS} is the dose weighted by the polysulphone action spectrum, D_1 and D_2 are threshold doses, A, B, C are dimensionless coefficients satisfying the condition

$$A + B + C = 1. \tag{A.3}$$

The polysulphone absorbance variation is strongly dependent on the film thickness (Parisi *et al* 1999), so the coefficients given for 26 μm thickness are not valid in the case of 40 μm thickness dosemeters. Anyway, here we assume that the functional dependence of ΔA on D_{PS} is always given by equation (A.2) and that the polysulphone thickness only affects the values of the coefficients.

In order to determine A, B, C, D_1 and D_2 in the case of 40 μm thickness polysulphone films, we use the values of absorbance variations found by Diffey (1989) irradiating the dosemeters with two different calibration lamps (helarium and fluorescent lamp), whose absolute power spectra are known. Equation (A.2) can be used if D_{PS} is known. We determine D_{PS} following the definition of g given by Krins *et al* (2001), where $H(\lambda)$ is the lamp spectral irradiance:

$$g = \frac{\int S_{ery}(\lambda)H(\lambda)\,d\lambda}{\int S_{PS}(\lambda)H(\lambda)\,d\lambda} = \frac{D_{ery}}{D_{PS}}. \tag{A.4}$$

By using the calibration lamps power spectra we calculate the ratio between the CIE dose, D_{ery} and the PS dose, D_{PS}. The g values obtained are $g = 0.20$ in the case of helarium lamp and $g = 0.60$ for the solar fluorescent lamp. Thus, they can be used to find the D_{PS} values helpful for best fitting to the function given by equation (A.2) leaving the five parameters free.

We find the following best fitted parameter values for the polysulphone response function in the case of 40 μm thickness:

$$\begin{aligned} A &= -0.017 \\ B &= 0.142 \\ C &= 0.875 \\ D_1 &= 2413\ \text{J m}^{-2} \\ D_2 &= 58759\ \text{J m}^{-2}. \end{aligned}$$

If we study equation (A.2) in the limit

$$\frac{D_{PS}}{D_1}, \frac{D_{PS}}{D_2} \ll 1, \tag{A.5}$$

we obtain

$$\begin{aligned} \Delta A &\cong -\ln\left(A + B\left(1 - \frac{D_{PS}}{D_1} + \frac{1}{2}\frac{D_{PS}^2}{D_1^2} - \frac{1}{3!}\frac{D_{PS}^3}{D_1^3}\right) + C\left(1 - \frac{D_{PS}}{D_2} + \frac{1}{2}\frac{D_{PS}^2}{D_2^2} - \frac{1}{3!}\frac{D_{PS}^3}{D_2^3}\right)\right) \\ &= \ln\left(1 - \left(\frac{B}{D_1} + \frac{C}{D_2}\right)D_{PS} + \frac{1}{2}\left(\frac{B}{D_1^2} + \frac{C}{D_2^2}\right)D_{PS}^2 - \frac{1}{3!}\left(\frac{B}{D_1^3} + \frac{C}{D_2^3}\right)D_{PS}^3\right). \end{aligned} \tag{A.6}$$

Then, defining

$$\alpha = \frac{B}{D_1} + \frac{C}{D_2}, \qquad \beta = \frac{1}{2}\left(\frac{B}{D_1^2} + \frac{C}{D_2^2}\right), \qquad \gamma = \frac{1}{3!}\left(\frac{B}{D_1^3} + \frac{C}{D_2^3}\right) \tag{A.7}$$

and taking into account that $\alpha \ll 1$, $\beta \sim o(\alpha^2)$, $\gamma \sim o(\alpha^3)$, we find

$$\begin{aligned}\Delta A &\cong -\ln\left(1-\alpha D_{\mathrm{PS}}+\beta D_{\mathrm{PS}}^2-\gamma D_{\mathrm{PS}}^3\right)\\ &\cong \alpha D_{\mathrm{PS}}-\beta D_{\mathrm{PS}}^2+\gamma D_{\mathrm{PS}}^3\\ &= \alpha D_{\mathrm{PS}}\left(1-\frac{\beta}{\alpha}D_{\mathrm{PS}}+\frac{\gamma}{\alpha}D_{\mathrm{PS}}^2\right).\end{aligned} \tag{A.8}$$

Inverting this relation the following equation holds:

$$D_{\mathrm{PS}} \cong \frac{\Delta A}{\alpha}\left(1+\frac{\beta}{\alpha}D_{\mathrm{PS}}-\frac{\gamma}{\alpha}D_{\mathrm{PS}}^2+\frac{\beta^2}{\alpha^2}D_{\mathrm{PS}}^2+\cdots\right). \tag{A.9}$$

Keeping the terms up to ΔA^3,

$$\begin{aligned}D_{\mathrm{PS}} &\cong \frac{\Delta A}{\alpha}\left(1+\frac{\beta}{\alpha}\frac{\Delta A}{\alpha}\left(1+\frac{\beta}{\alpha}\frac{\Delta A}{\alpha}\right)+\left(\frac{\beta^2}{\alpha^2}-\frac{\gamma}{\alpha}\right)\left(\frac{\Delta A}{\alpha}\right)^2+\cdots\right)\\ &= \frac{\Delta A}{\alpha}\left(1+\frac{\beta}{\alpha}\frac{\Delta A}{\alpha}+\left(\frac{2\beta^2}{\alpha^2}-\frac{\gamma}{\alpha}\right)\left(\frac{\Delta A}{\alpha}\right)^2+\cdots\right).\end{aligned} \tag{A.10}$$

Using the definition given by equation (A.4), the relationship between the radiant exposure weighted by the CIE erythemal spectrum D_{ery} and the polysulphone absorbance variation is obtained, valid in the limit of small doses:

$$D_{\mathrm{ery}} = g\frac{\Delta A}{\alpha}\left(1+\frac{\beta}{\alpha}\frac{\Delta A}{\alpha}+\left(\frac{2\beta^2}{\alpha^2}-\frac{\gamma}{\alpha}\right)\left(\frac{\Delta A}{\alpha}\right)^2\right). \tag{A.11}$$

The calibration curve obtained is a third-order polynomial law, without the constant term, with a multiplying coefficient that is a function of the ratio g between the radiant exposure weighted by the CIE erythemal curve and the radiant exposure weighted by the polysulphone spectral efficiency. All the dependence on the spectrum is in the multiplying coefficient whilst the expression in parentheses in equation (A.11) is independent of the measured spectrum, being an intrinsic characteristic of the photoinduced reaction of polysulphone film dosemeters. The g values can be estimated using equation (A.12):

$$g = 1000 \times c \times \alpha \tag{A.12}$$

Values found by equation (A.12) seem to agree well with experimental data. The average of the estimated and measured g values obtained in three different field experiments performed in Rome during 2004 and 2005, where spectral UV irradiance data were available, are respectively 0.07 and 0.08.

References

Bernhard G, Booth C R and Ehramjian J C 2003 Real-time UV and column ozone from multi-channel UV radiometers deployed in the National Science Foundation's UV monitoring network *Proc. SPIE, Ultraviolet Ground and Space-Based Measurements, Models and Effects III (San Diego, Aug.)* **5156** 167–78

Boldemann C, Dal H and Wester U 2004 Swedish pre-school children's UVR exposure—a comparison between two outdoor environments *Photodermatol. Photoimmunol. Photomed.* **20** 2–8

CIE (Commission Internationale d'Eclairage) 1987 Research note. A reference action spectrum for ultraviolet induced erythema in human skin *CIE J.* **6** 17–22

Casale G R, Meloni D, Miano S, Siani A M, Palmieri S and Cappellani F 2000 Solar UV-B irradiance and total ozone in Italy: fluctuations and trend *J. Geophys. Res.* **105** 4895–901

Cockell C S, Rettberg P, Horneck G, Wynn-Williams D D, Scherer K and Gugg-Helminger A 2002 Influence of ice and snow covers on the UV exposure of terrestrial microbial communities: dosimetric studies *J. Photochem. Photobiol. B* **68** 23–32

Cockell C S, Scherer K, Horneck G, Rettberg P, Facius R, Gugg-Helminger A, Driscoll C and Lee P 2001 Exposure of arctic field scientists to ultraviolet radiation evaluated using personal dosemeters *Photochem. Photobiol* **74** 570–8

Davis A, Deane G H W and Diffey B L 1976 Possible dosemeter for ultraviolet radiation *Nature* **261** 169–70

de Gruijl F R 1999 Skin cancer and solar UV radiation *Eur. J. Cancer* **35** 2003–9

Di Menno I, Moriconi M L, Di Menno M, Casale G R and Siani A M 2002 Spectral ultraviolet measurements by a multichannel filter instrument and a Brewer spectroradiometer: a field campaign *Radiat. Prot. Dosim.* **102** 259–63

Diffey B L 1984 Personal ultraviolet radiation dosimetry with polysulphone film badges *Photodermatol.* **1** 151–7

Diffey B L 1987 A comparison of dosemeters used for solar ultraviolet radiometry *Photochem. Photobiol.* **46** 55–70

Diffey B L 1989 Ultraviolet Radiation dosimetry with polysulhone film *Radiation Measurement in Photobiology* (New York: Academic) pp 135–59

Diffey B L 2004 Climate change, ozone depletion and the impact on ultraviolet exposure of human skin *Phys. Med. Biol.* **49** R1–11

Diffey B L and Davis A 1978 A new dosemeter for the measurement of natural ultraviolet radiation in the study of photodermatoses and drug photosensitivity *Phys. Med. Biol.* **23** 318–23

Diffey B L and McKinlay A F 1987 A reference action spectrum for ultraviolet induced erytema in human skin *Human Exposure to Ultraviolet radiation: Risks and Regulations* ed W R Passchler and B F M Bosnajokovic (Amsterdam: Elsevier)

Holick M F 2000 Sunlight and vitamin D: the bone and cancer connections *Radiat. Prot. Dosim.* **91** 65–71

Kerr J B 2003 Understanding the factors that affect surface UV radiation *Proc. SPIE, Ultraviolet Ground and Space-Based Measurements, Models and Effects III (San Diego, Aug.)* **5156** 1–14

Kimlin M G 2003 Techniques for assessing human UV exposures *Proc. SPIE, Ultraviolet Ground and Space-Based Measurements, Models and Effects III (San Diego, Aug)* **5156** 197–206

Kimlin M G 2005 personal communication

Kimlin M G, Parisi A V and Wong J C F 1998a Quantification of personal solar UV exposure of outdoor workers, indoor workers and adolescents at two locations in Southeast Queensland *Photodermatol. Photoimmunol. Photomed.* **14** 7–11

Kimlin M G, Parisi A V and Wong J C F 1998b The facial distribution of erythemal ultraviolet exposure in south-east Queensland *Phys. Med. Biol.* **43** 231–40

Kollias N, Baqer A, Sadiq I, Gillies R and Ou-Yag H 2003 Measurement of solar UVB variations by polysulphone film *Photochem. Photobiol.* **78** 220–4

Krins A, Dörschel B, Henniger J, Knuschke P and Bais A 1999 Reading of polysulphone film after fractionated and continuous exposures to UV radiation and consequences for the calculation of the reading resulting from polychromatic UV radiation, *Radiat. Prot. Dosim.* **83** 303–7

Krins A, Dörschel B, Knuschke P, Seidlitz H K and Thiel S 2001 Determination of the calibration factor of polysulphone film UV dosemeters for terrestrial solar radiation *Radiat. Prot. Dosim.* **95** 345–52

Mariutti G F, Bortolin E, Polichetti A, Anav A, Casale G R, Di Menno M and Rafanelli C 2003 UV dosimetry in Antarctica (Baia Terranova): analysis of data from polysulphone films and GUV 511 radiometer *Proc. SPIE, Ultraviolet Ground- and Space-Based Measurements, Models and Effects III (San Diego, Aug.)* **5156** 254–61

Meloni D, Casale G R, Siani A M, Palmieri S and Cappellani F 2000 Solar UV dose patterns in Italy *Photochem. Photobiol.* **71** 681–90

Parisi A V 2005 Physics concepts of solar ultraviolet radiation by distance education *Eur. J. Phys* **26** 313–20

Parisi A V, Meldrum L R and Kimlin M G 1999 Polysulphone film thickness and its effects in ultraviolet radiation dosimetry. Protection Against the Hazards of UVR: Virtual Conf. 18 Jan.–5 Feb., www.photobiology.com

Parisi A V, Wong J C F and Moore G I 1997 Assessment of the exposure to biologically effective UV radiation using a dosimetric technique to evaluate the solar spectrum *Phys. Med. Biol.* **42** 77–8

Quintern L E, Puskeppeleit M, Rainer P, Weber S, El Naggar S, Eschweiler U and Horneck G 1994 Continuous dosimetry of the biologically harmful UV-B radiation in Antarctica with the biofilm technique *J. Photochem. Photobiol.* B **22** 59–66

Rivaton A and Gardette J L 1999 Photodegradation of polyethersulfone and polysulphone *Polym. Degradation Stab.* **66** 385–403

Ruggaber A, Dlugi T and Nakajima T 1994 Modelling radiation quantities and photolysis frequencies in the troposphere *J. Atmos. Chem.* **18** 171–210

El Naggar S, Hans G, Magister H and Rochlitzer R 1995 An electronic personal UV-B dosemeter *J. Photochem. Photobiol.* B **31** 83–6

Schwander H, Koepke P and Ruggaber A 1997 Uncertainties in modelled UV irradiances due to limited accuracy and availability of input data. *J. Geophys. Res.* **102** 9419–29

Seckmeyer G 2000 Coordinated ultraviolet radiation measurements *Radiat. Prot. Dosim.* **91** 99–103

Siani A M, Benevento G and Casale G R 2003 Temperature dependence of Brewer UV measurements at Rome station *Proc. SPIE, Ultraviolet Ground- and Space-Based Measurements, Models and Effects III (San Diego, Aug.)* **5156** 355–66

Sisto R, Lega D and Militello A 2001 The calibration of personal dosemeters used for evaluating exposure to solar UV in the workplace *Radiat. Prot. Dosim.* **97** 419–22

van der Leun J C 2004 The ozone layer *Photodermatol. Photoimmunol. Photomed.* **20** 159–62

Webb A 1995 Measuring UV radiation: a discussion of dosemeter properties, uses and limitations *J. Photochem. Photobiol.* B **31** 9–13

Webb A 1998 *Solar UVB Instrumentation and Applications Amsterdam* (London: Gordon and Breach)

WMO (World Meteorological Organization) 2002 *Scientific Assessment of Ozone Depletion: WMO Ozone Report* vol 47 (Geneva)

RESPONSE OF POLYSULPHONE DOSIMETERS EXPOSED UNDER DIFFERENT ENVIRONMENTAL CONDITIONS

G.R. Casale[1], N. Bono[1], A.M. Siani[1], M.G. Kimlin[2]
[1]Department of Physics, University of Rome "La Sapienza"
Piazzale A. Moro 2, I-00185 Rome (Italy)
[2]Center for Health Research, School of Public Health, Queensland University of Technology
Kelvin Grove Campus, Brisbane, Queensland (Australia) 4001

INTRODUCTION

The importance of solar ultraviolet radiation UV and its impact on human heath is widely recognized in the scientific community. The only well-established beneficial effect of solar UV is the production of vitamin D_3 required for skeleton health, while the harmful effects (acute and chronic) of UV exposure mainly concern damage to the soft tissues of the eyes and skin.
Solar UV flux reaching the earth's surface is influenced by numerous atmospheric factors, such as the absorption and scattering by molecules (oxygen and ozone) and by aerosols and clouds. The Sun's activity, earth-sun distance, surface albedo, latitude and altitude above sea level affect the variability of UV radiation on the ground.
Currently there is still low spatial coverage of ground-based instruments measuring UV irradiance (spectral or on a wide wavelength range) and the length of time over which reliable UV observations have been made, is still only around 10 years. UV sensors can be classified as, spectroradiometers, broadband and narrowband multifilter radiometers. These instruments measure the irradiance on a horizontal surface (ambient UV radiation). Radiative transfer models and satellite instruments are further resources for studying ambient UV radiation typically over a broader (global) scale when compared to isolated instrument measurements.
The impact of UV radiation requires knowledge of the action spectra of biological systems, namely of functions expressing the effectiveness of electromagnetic radiation in causing a specific response in a biological system. The erythemal action spectra is a weighting function which simulates the damaging process occurring in the skin (Diffey and McKinley, 1987).
However, although the biological action spectra can help in understanding some biological effects, they do not contain information on the simultaneous effect of multiple wavelengths and feedback mechanisms.
An accurate methodology for recording level of exposure in different body postures is based on the use of polysulphone dosimeters, a polymer which changes its optical properties (absorbance) when exposed to UV radiation. Its response is close to the erythemal response of human skin (Kimlin, 2003).
This work aimed to define ambient UV radiation in terms of UV index at middle latitudes using well calibrated and maintained instruments and to quantify the exposure ratio (ER) of differently-oriented surfaces at sites having different environmental conditions.

1. CHARACTERIZATION OF AMBIENT UV RADIATION AT THE MID LATITUDE OF ROME

Solar spectral irradiance (from 290 to 325 nm at 0.5nm wavelength increments) and total irradiance has been measured at the Rome station by means of Brewer spectrophotometry (single monocromator) since 1992 and broad-band meter (model UVB-1, Yankee Environmental System, MA, USA) since 2000. Values of the erythemal dose rate using the C.I.E. action spectrum (McKinlay-Diffey, 1987), integrated up to 400 nm are obtained from Brewer UV measurements or alternatively from the YES radiometer which has a spectral response similar to that of skin erythema.
The solar radiometry station is located on the roof of the Physics Department building of the University of Rome "La Sapienza" (41.9°N, 12.5°E, 60m a.s.l.). This building is one of many on the extensive University campus, which itself is located very close to the center of the city and thus influenced by intense human activity. For this reason the site is classified as "urban" (Meloni et al., 2000). More details on the site and on data quality control can be found in Casale at al., 2000.
Rome is influenced by the European continental climate and the Mediterranean climate with precipitation in the cold and mid season and a dry, hot summer.

A characterization of this middle latitude site, in terms of UV index, UVI (COST -713, 2000) will now be provided. The UV Index is a measure of the intensity of harmful UV radiation at the Earth's surface and UVI is calculated by weighting the irradiance (280-400nm) using the erythemal action spectrum, and the dose rate obtained is divided by 25 mW/m^2 in order to produce a unit-less quantity.
Figure 1 shows daily means of the UV index values for Rome for the period 1992-2004 at approximately mid-day local time on clear-sky days. The seasonal variation is clearly evident, with higher values in summer (up to 8) and low ones (<3) during winter.

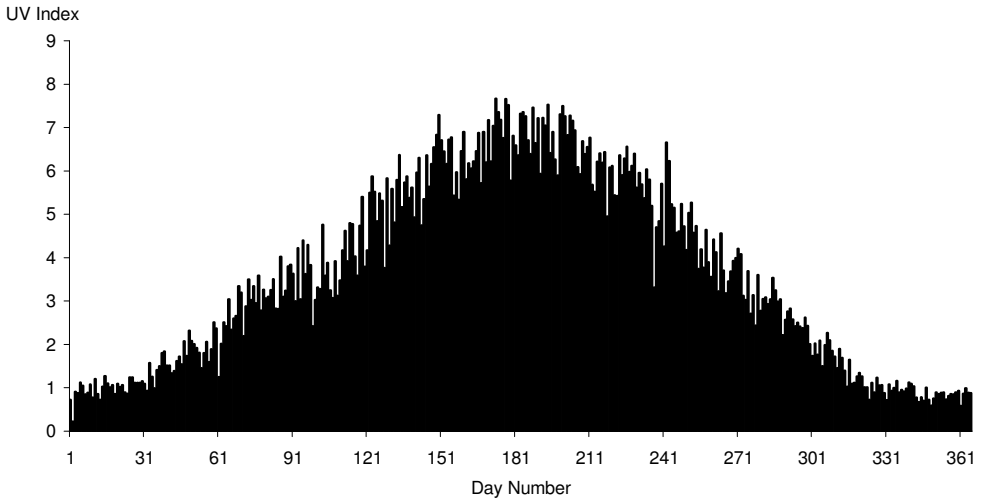

Figure 1: Daily means of UV index

Following the guidelines provided by COST-713, 2000) UVI values are grouped into exposure categories from low (0-2) to extreme (>11).
Seasonal distribution of frequency of UVI values within each category at Rome is given in Table 1

Table 1: Seasonal UVI frequency distribution at Rome

	Low UVI range: 0-2	Moderate UVI range: 3-5	High UVI range: 6-7	Very high: UVI range:8-10
Dec-Jan-Feb	99.0%	1.0%		
Mar-Apr-May	27.7%	52.5%	18.6%	1.2%
June-July-Aug	5.4%	20.7%	63.5%	10.4%
Sept-Oct-Nov	54.1%	43.9%	1.3%	0.7%

It can be seen in Figure 2 that in summer higher UV levels (UVI = 8-9) occur on only 10% of days, while the most frequent category is "High" (about 65%). The potentially harmful consequences of this situation for human skin cannot be ignored, especially when the time of exposure is prolonged. In the cold season levels of UV radiation are "Moderate

2. METHODOLOGY

Polysulphone dosimetry is a reliable and widely tested methodology to assess ultraviolet radiation exposure (Davis et al., 1976; Parisi et al., 1996, Kimlin 2003). Polysulphone is a polymer which changes its optical properties (absorbance) when exposed to UV radiation, and it has response matching closely the erythemal action spectrum. Following the procedure described in Kimlin (2003) polysulphone calibration curves were obtained by measuring doses and corresponding changes in absorbance (ΔA at 330nm), prior and post exposure. Doses were measured by the YES broad-band, detector calibrated at the European Reference Centre for Ultraviolet Radiation Measurements (Joint Research Centre, Ispra, Italy) in 2004 and they agree with those measured by Brewer at Rome "La Sapienza"(within 10% of uncertainty).
A pilot study using an exposure device capable to set the dosimeters at fixed different zenith angles (ZA) (Figure 3) under different environmental conditions is carried out to estimate the exposure ratio

(ER). This is defined as ratio between the dose received by a differently-inclined surface to the ambient UV dose (i.e that received by horizontal surface). The device is a holder capable to expose dosimeters placed from ZA= 0° (horizontal dosimeter) to ZA= 90° (vertical dosimeter) at every angle of 15°. Such device can provide an useful estimate of ER when data from experiments *in vivo* or with manikins are not available. When ER is known for each angle and in different sites then it could be possible to model exposure of different parts of the body on the basis on their orientation, on measurements of the ambient UV levels, and on activity index (Kimlin,2003).

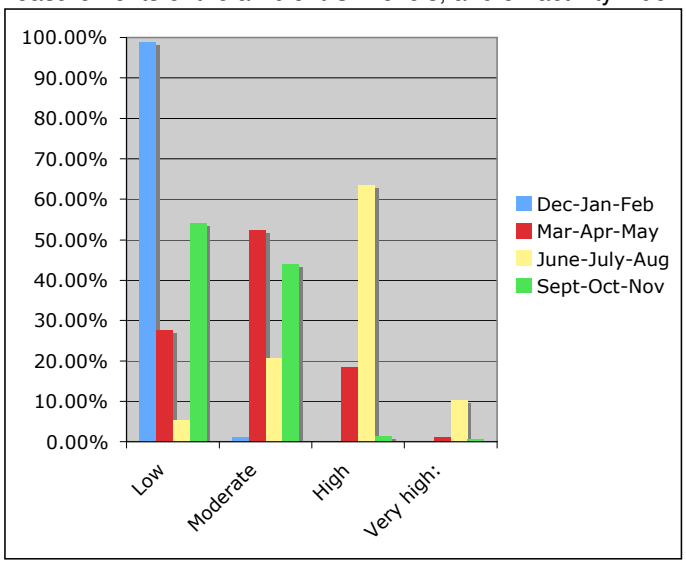

Figure 2 Seasonal UVI frequency distribution

Figure 3: The exposure device for estimating ER

In order to test the device and to assess the variability of exposure from local environment conditions, experiments took place at an urban site (Rome, city centre, Lat.41.9°, Long.12.5°), at a coastal site close to Rome (Fregene, Lat.42°, Long.12.2°), on the mountain site with snow cover (Roccaraso (AQ) on Apennine, Lat. 42°, Long.14°, 1680m a.s.l.), and at rural site (S. Felice (SI) in Tuscany, Lat.43.3°, Long.11.3°) during spring 2005 under clear sky conditions. All sites are located around the latitude of 42° and over the solar zenith angle (SZA) range of 21° to 61° during this season. During the field campaigns the device was faced at south, and the exposure time was chosen centred at local noon in order to have the same ambient dose in all sites (four hours at urban and mountain sites, five hours at rural site and three hours at the beach site.) In these field campaigns the YES radiometer was utilized as travelling instrument for measurements of the ambient exposure.

3. RESULTS

Measurements of ambient doses recorded by the radiometer located close to the exposure device were compared with doses incident on horizontal dosimeter (ZA=0° ER=1). Both values for each field campaign are reported in Table 2 and they show a reasonable agreement within the associated uncertainties.

Table 2: Ambient Exposure measured by the radiometer and derived from dosimeter at ZA=0°

Site	Ambient Exposure(Jm^{-2}) from the radiomter	Ambient Exposure (Jm^{-2}) Dosimeter at ZA=O°
S. Felice (on the 4th April,2005)	1900±100	2000±200
Roccaraso (on 20th March 2005)	1800±100	2100±200
Rome (on 2nd May 2005)	1900±100	1700±200
Fregene (on 27th May 2005)	2000±100	1900±200

In Figure 4 values of ER versus ZA of exposed dosimeters are plotted for the considered sites.

All curves decrease gradually approximately at ZA= 30° except the mountain site where the ER curve remains close to 0.9. This can be due to the contribution of the additional upwelling radiation to enhance the exposure of inclined surfaces. In presence of snow the effect of ground albedo becomes significant while it is not visible in other conditions.

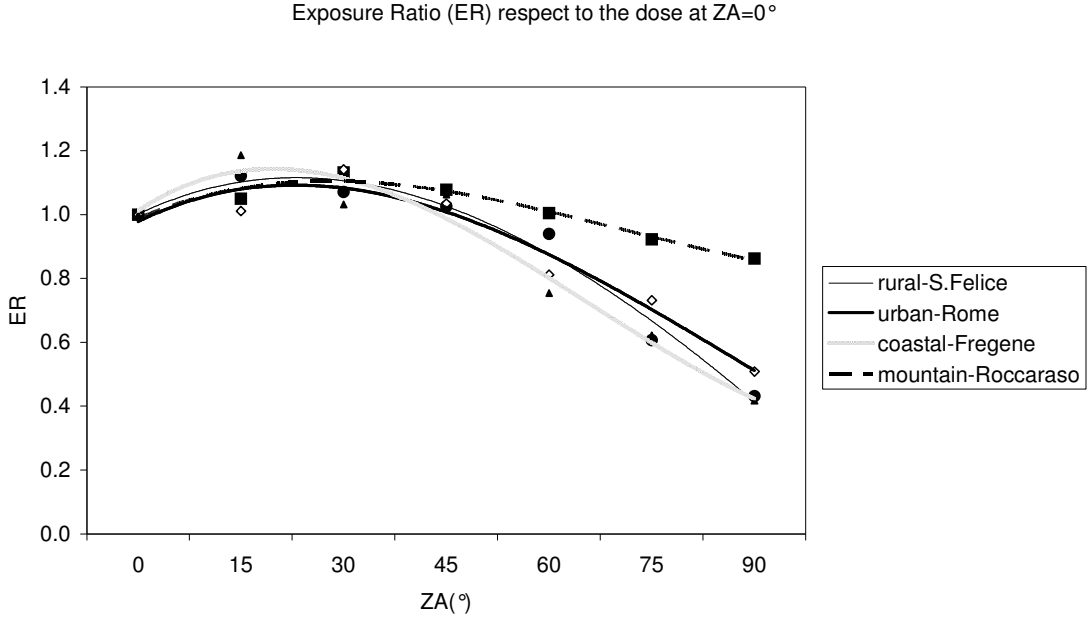

Figure 4 Exposure ratio respect to the dose at ZA=0°, the lines represent the best fit to the data.

4. CONCLUSIONS

In this preliminary study, results from pilot experiments, aiming at estimating the exposure ratio of inclined surface in different environment conditions were presented. An UV dosimeter exposure device capable to set the dosimeters at fixed different solar zenith angles (SZA) was used. It is interesting to note that when ground albedo is high (specifically snow) produce an enhancement of the exposure of inclined dosimeters due to the increasing ratio of direct to diffuse radiation. In fact the exposure ratio is only slightly smaller than the horizontal value. Such results from this high albedo site indicate that human exposures in this region are altered when compared to a low albedo site.
This study will be followed by other field campaigns in order to collect more data about ER and hence to better assess environmental factors affecting human exposure.

REFERENCES

Casale, G.R., Meloni, D., Miano, S., Siani, A.M., Palmieri, S., Cappellani, F., 2000: Solar UV-B irradiance and total ozone in Italy: fluctuations and trends. J. Geophys. Res., 105: 4895-4901.
COST -713 Action, 2000: UV Index for the Public, European Communities, Brussels, 27 pp.
Davis, A., Deane, G.H.W, Diffey, B.L., 1976: Possible dosimeter for ultraviolet radiation, Nature, 261:, 169-170.
Diffey, B. and McKinlay, A.F., 1987: A reference action spectrum for ultraviolet induced erytema in human skin. In Human Exposure to Ultraviolet radiation: Risks and Regulations (Edited by W. R. Passchler and B. F. M. Bosnajokovic), Elsevier Publishers, Amsterdam, NL.
Meloni D., Casale, G.R., Siani, A.M., Palmieri, S., Cappellani, F., 2000: Solar UV dose patterns in Italy. Photochem. Photobiol., 71(6): 681-690.
Kimlin M.G., 2003: Techniques for assessing human UV exposures, 48th SPIE MEETING, S.Diego (CA): 197-206.
Parisi, A.V., Kimlin, M.G., Wong, C.F. , Fleming, R.A., 1996: The efefcts of body size and orientation on ultraviolet radiation expsoure, Photodermatol. Phoimmunol.Photomed.: 12,66-72.

Short Communication

SOLAR ULTRAVIOLET RADIATION AT THE EARTH'S SURFACE: FACTORS AFFECTING ITS IMPACT ON HUMAN BEINGS

Giuseppe Rocco Casale (a), Anna Maria Siani (a), Alfredo Colosimo (b)
(a) Department of Physics - University of Rome "La Sapienza"
(b) Department of Human Physiology and Pharmacology - University of Rome "La Sapienza"

Introduction

The ultraviolet (UV) region spans the wavelength range from 200 to 400 nm and accounts for less than 9% of the solar output (around 120 Wm^{-2}). UV radiation reaching the earth's surface is controlled by many factors such as astrophysical (sun's activity), astronomical (earth-sun distance, solar elevation), atmospheric (absorption and scattering due to gases, such as ozone, aerosols and clouds) and geographical (altitude, albedo, surface orientation) (1).

Solar ultraviolet radiation is usually classified as UV-A (315-400 nm), as UV-B (280-315 nm) and as UV-C (200-280 nm) (2). The UV portion of spectrum relevant to environmental biology is restricted to the UV-B and UV-A ranges. Wavelengths shorter than 280 nm are completely absorbed before reaching the biosphere, UV-B radiation is efficiently but not completely blocked by atmospheric ozone while atmospheric constituents affect UV-A radiation less. The established effect of stratospheric ozone depletion has given rise to concern about its effect on the ecosystems and on human health (3).

The need to identify possible threats to the biosphere requires proper sensors capable to directly detect biological effects caused by ambient UV radiation and possess high sensitivity to small changes of UV-B (4). Polysulphone dosimeters are reliable, portable, and cost-effective, which makes them a suitable choice.

The study of the factors affecting UV impact on people is characterized by an inner complexity due to the need of combining the accurate determination of the ambient UV radiation with the analysis of its biological effects.

Ambient UV radiation

The evolution and growth of most aquatic and terrestrial life forms is influenced by several environmental variables including the intensity of UV radiation at the earth's surface or under water. The negative correlation between spectral UV-B radiation and total ozone has been properly documented (3). If all other variables (astrophysical, astronomical, atmospheric and geographical) were constant, the degree of UV attenuation would depend only on ozone variability. However, the understanding of all processes affecting surface UV radiation is rather more complicated. Therefore, to quantify the effect of all parameters at different times and space scales is a cumbersome procedure.

Figure 1 is an example of this aspect. The local noon erythemal UV irradiance (i.e. the solar UV irradiance weighted with a function, erythemal action spectra expressing the epidermis

response) on the global scale on June 21st 2003 is shown on the left panel: the latitudinal gradient is governed by the environmental parameters on regional scales. Limitation of the mapping region (right panel) does not decrease the complexity of the UV field (5).

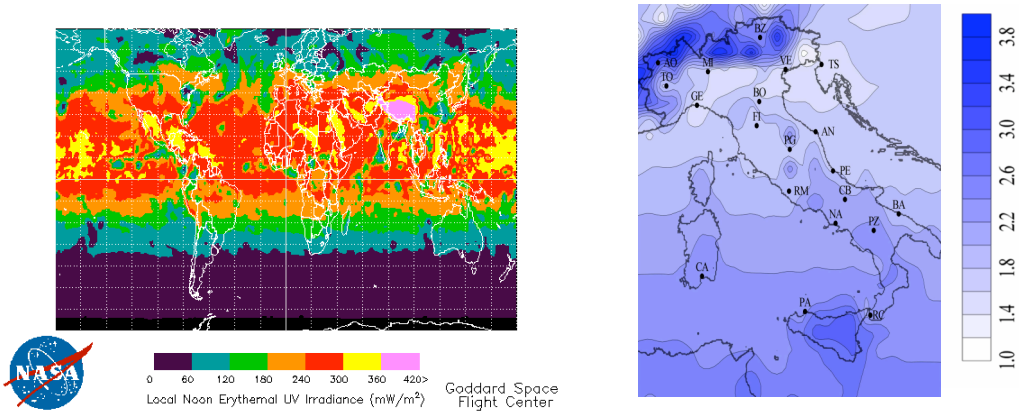

Figure 1. Left: local noon erythemal UV irradiance as measured by TOMS onboard Earth Probe satellite on June 21st 2003. Regional scale variability is superimposed on the latitudinal gradient determined by the differential sun illumination. Right: average erythemal UV daily dose in Italy as determined by a radiative transfer model. The latitudinal gradient is mainly modified by the different elevation of sites above sea level and the climatological atmospheric patterns

Measuring UV radiation

UV measurements are carried out via different independent instruments with various output formats and without standard calibration procedures (6). The classification of UV sensors is based on their spectral resolution: spectroradiometers (that measure the intensity of radiation every 1 nm or less), moderate and narrow-band radiometers (that measure in bands of ~10 nm) and broad-band radiometers (measuring in a specific range, usually UV-B, UV-A or a combination of both).

The accuracy of instruments, currently estimated at 5% for the best maintained spectroradiometers, is vital for the credibility of UV data. In spectral measurements the uncertainty increases at wavelengths below 300 nm, where the solar signal is weak and masked by instrumental noise (7). Broad-band instruments have higher uncertainty than spectroradiometers.

The impact of environmental UV radiation requires knowledge of action spectra of biological systems, namely of functions expressing the effectiveness of the electromagnetic radiation in causing a specific response of the biological system.

Action spectra have been used for several critical biological responses (Figure 2): DNA damage, inactivation of human fibroblast, keratinocytes and melanocytes, minimal erythema, squamous cell carcinoma in mice, malignant melanoma in fish and plant damage. However, even when measurements of UV radiation are highly accurate, the biologically effective irradiance can vary substantially as a result of experimental errors in the action spectra (such as

a too narrow waveband) and the underlying hypothesis of additive spectral effects, which is not always satisfied in nature (8).

In addition to the UV measurements, radiative transfer models are available to determine UV irradiances on the ground. Some of them are sophisticated multiple scattering codes based on a neural network approach and contribute to improve the understanding of complicated scattering and absorption processes in the atmosphere.

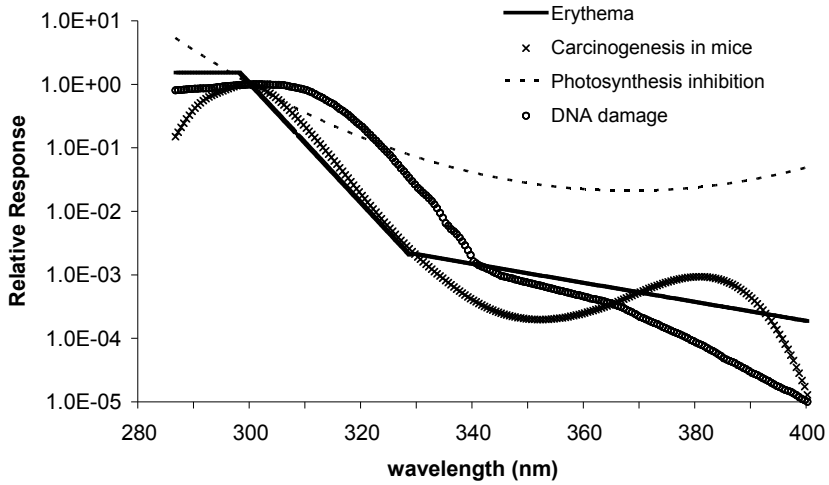

Figure 2. Action spectra for some selected UV-related effects (eryhtema, carcinogenesis in mice, photosynthesis inhibition and DNA damage). The relative response among different spectra is normalised to unity at 300 nm to allow an intercomparison

Human UV exposure

The relationship between UV radiation and its biological consequences has been studied already for several years (9). Interest in this subject increased as a result of recent findings on stratospheric ozone decrease and the consequential increase of solar UV at ground. When UV photons impinge on people, the difficulty of the problem further increases, because solar exposures vary according to the length of time spent outdoors, the time of day and the period of the year, type of activity undertaken, body posture, and the UV protective used [10]. Depending on the amount of available ambient UV radiation, the individual response is determined by: (a) the amount of absorbed UV dose (hourly, daily, monthly etc.); (b) the characteristics of the interface radiation-matter (epidermis); (c) the photoreactions occurring in the inner layers.

Polysulphone personal dosimetry

The documented worldwide increase in skin cancer cases in recent years has stimulated research on the acute and chronic effects of UV radiation on protected/unprotected skin and eyes.

Polysulphone (PS) dosimetry (11) is oriented towards the understanding of the role of (a), (b) and (c) on target groups. They have been widely used to quantify personal UV exposure of humans in different settings during ordinary daily activities (12).

PS dosimeters, small devices requiring no external power input, are made up of a thin film (usually 40 μm) with spectral sensitivity similar to the erythemal response (Figure 3). When the dosimeter is exposed to solar UV, the diphenyl sulphone group in polysulphone absorbs UV at wavelengths shorter than 330 nm and an increase of optical absorbancy occurs. Since the largest change in the optical absorbancy, before and after the UV exposure, is at 330 nm, measurements of optical absorbancy change at this wavelength can be related to the ambient UV dose through a calibration curve. By using measured ambient UV irradiances in combination with an understanding of the distribution of solar UV in the human body, estimates of long term exposures can be determined. PS dosimeters cannot be reused after exposure to the sun.

Figure 3. Polysulphone dosimetry device for the study of the distribution of UV radiation on the human body: a dosimeter (left) is made by attaching a PS film on a PVC holder (size 3 cm x 3 cm with a 1.6 cm x 1.2 cm aperture). It can be used on manikins, too (right)

Results and conclusions

Experiments carried out in Rome and vicinity during the summer of 2004, both with manikins and volunteer bathers, show that PS dosimeters targeting specific population groups, allow for quantitative measurements of personal UV exposures. The measured doses on different sites of the human body can be determined by a calibration curve (Figure 4).

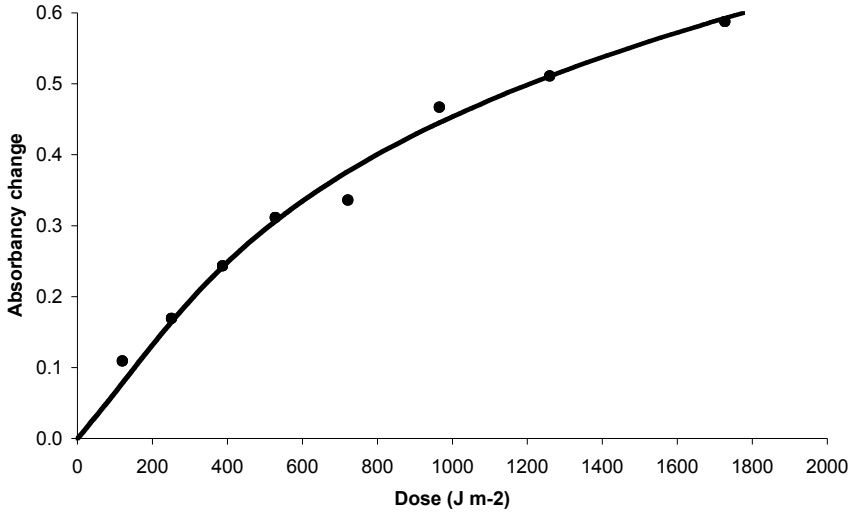

Figure 4. Calibration curve for evaluating personal exposures from changes of dosimeter absorbancy (Rome, July 2nd 2004). Each point refers to the change in absorbancy (vertical axis) recorded by a single dosimeter after a fixed exposure time. On the horizontal axis, the corresponding ambient dose as measured by a reference instrument is reported

Preliminary results obtained with manikins are presented in Table 1 for supine and sitting postures.

Table 1. Percentage of personal dose with respect to ambient dose for two different postures

Posture	shoulder	breast	cheek
Supine	21%	59%	63%
Sitting	83%	93%	102%

Doses affecting human beings are influenced mainly by the orientation of the body surface respect to the sun. UV dose tends to increase when the portion of body is exposed towards the incoming direct radiation. The albedo effect of the ground increases the percentage of personal dose more in the sitting than in the supine posture. In the sitting posture the dose is 1.6 (breast and cheeks) and 4 (shoulders) greater than the supine. Note also that the albedo effect, in combination with local atmospheric parameters, can enhance personal exposure beyond ambient level (102% for cheeks). Results are congruent with those obtained on volunteer bathers with a single dosimeter on the breast. Doses on individuals are modulated not only by the orientation of the body respect to the sun but also by the length of time spent in the shade. The values of volunteers exposure doses are up to 60% of ambient dose.

A proper methodology for measuring the level of UV radiation on different parts of the body, based on polysulphone dosimetry, has been discussed and tested. Results can be interpreted only if the local characterization of ambient UV radiation is taken into account. Future efforts will be addressed at the search for biological markers whose modification is a direct or indirect effect of UV radiation. Moreover, possible correlations between markers and personal absorbed doses will be studied.

References

1. Kerr JB . Understanding the factors that affect surface UV radiation. 48th SPIE MEETING, S.Diego (CA); 2003
2. Diffey BL What is light?, Photodermatol. Photoimmunol. Photomed., 2002; 18:68-74
3. WMO (World Meteorological Organization) *Scientific assessment of ozone depletion*: 2002 Global Ozone Research and Monitoring Project - Geneva, 2003; Report No. 47, 498
4. Webb A. Measuring UV radiation: a discussion of dosimeter properties, uses and limitations. *J. Photochem. Photobiol. B: Biol.*, 1995; 31: 9-13
5. Meloni D, Casale GR, Siani AM, Calmieri S, Cappellani F. *Solar UV dose patterns in Italy, Photochem. Photobiol.*, 2000; 71 (6): 681-690
6. WMO (World Meteorological Organization) *Guidelines for Site Quality Control of UV Monitoring* (lead author A.R. Webb) - Global Atmosphere Watch - Geneva, 1998, Report No. 126, 35.
7. WMO (World Meteorological Organization) *Instruments to measure solar ultraviolet radiation, part 1: spectral instrument* - Global Atmosphere Watch - Geneva, 2001,.Report No. 125, 30
8. Horneck G. Quantification of the biological effectiveness of environmental UV radiation. *J. Photochem. Photobiol. B: Biol.*, 1995; 31: 43-49
9. Diffey BL . Solar ultraviolet radiation effects on biological systems, *Phys. Med. Biol.*, 1991; 36 (3): 299-328
10. Diffey BL. Ultraviolet radiation and human health. *Clinics in Dermatology*, 1998;16: 83-89
11. Davis A, Deane GHW, Diffey BL . Possible dosimeter for ultraviolet radiation. *Nature*, 1976; 261: 169-170
12. Kimlin MG. *Techniques for assessing human UV exposures*, 48th SPIE MEETING, S.Diego (CA) 2003